NASA Contractor Report 175066

Characterization of Real Gas Properties for Space Shuttle Main Engine Fuel Turbine and Performance Calculations

Gary J. Harloff

Sverdrup Technology, Inc.
Lewis Research Center
Cleveland, Ohio

June 1986

NASA

National Aeronautics and
Space Administration

TABLE OF CONTENTS

CHARACTERIZATION OF REAL GAS PROPERTIES FOR SPACE SHUTTLE MAIN ENGINE

FUEL TURBINE AND PERFORMANCE CALCULATIONS

Gary J. Harloff
Sverdrup Technology, Inc.
Lewis Research Center
Cleveland, Ohio 44135

SUMMARY

Real thermodynamic and transport properties of hydrogen, steam, the SSME mixture, and air are developed. The SSME mixture properties are needed for the analysis of the space shuttle main engine fuel turbine. The mixture conditions for the gases, except air, are presented graphically over a temperature range from 800 to 1200 K, and a pressure range from 1 to 500 atm. Air properties are given over a temperature range of 320 to 500 K, which are within the bounds of the thermodynamics programs used, in order to provide mixture data which is more easily checked (than H_2/H_2O). The real gas property variation of the SSME mixture is quantified.

Polynomial expressions, needed for future computer analysis, for viscosity, Prandtl number, and thermal conductivity are given for the H_2/H_2O SSME fuel turbine mixture at a pressure of 305 atm over a range of temperatures from 950 to 1140 K. These conditions are representative of the SSME turbine operation.

Performance calculations are presented for the space shuttle main engine (SSME) fuel turbine. The calculations use the air equivalent concept. Progress towards obtaining the capability to evaluate the performance of the SSME fuel turbine, with the H_2/H_2O mixture, is described.

INTRODUCTION

The SSME fuel turbopump operates with a mixture of H_2 and H_2O at about 330 atm and 1105 K. These conditions are such that actual gas dynamic measurements in the turbine are difficult to obtain. One computational tool at NASA Lewis for analyzing turbomachinery is the combined computer programs of Katsanis and McNally (refs. 1 to 4). The program accepts constant thermodynamic and transport gas property data for each blade row. A current limitation of the analysis is that the boundary layer program (ref. 2) requires the temperature dependence of the transport properties to be input as a polynomial function. The program has thus far been limited to air properties.

The goals of the present study were:

(1) Determine the H_2/H_2O mixture thermodynamic and transport properties variation

(2) Calculate the air equivalent performance

(3) Curve fit the variation of μ, C_p, and Pr with temperature at the appropriate pressure

(4) Calculate the H_2/H_2O mixture performance accounting for property varations from blade row to blade row

(5) Modify the Katsanis and McNally computer programs to account for real gas effects.

The first three goals are addressed herein.

NOMENCLATURE

a	sound speed
c_{act}^2	actual sound speed squared, cm^2/s^2
c_{Id}^2/c_{act}^2	ideal/actual sound speed squared
C_p	specific heat at constant pressure, J/g-K
C_v	specific heat at constant volume, J/g-K
H,h	enthalpy, J/g
k	thermal conductivity, J/cm-s-K
M	molecular weight
n	mole fraction
Pr	Prandtl number
P_t	total pressure, atm
P	pressure, atm
R_{Id}/R_{act}	ideal/actual gas constant ratio
R_p	total pressure ratio
R	gas constant
S	entropy, J/g-K
T_{sl}	sea level temperature
T_t	total temperature, K
T	temperature, K
W/Wcr	relative velocity/relative velocity at sonic condition
Z	compressibility

$(\partial p/\partial \rho)_T$	partial derivative of pressure with respect to density at constant temperature, atm-cc/g
$(\partial p/\partial T)_\rho$	partial derivative of pressure with respect to temperature at constant density, atm/K
β	relative flow angle, deg
γ	ratio of specific heats
ξ	degrees of freedom
η	efficiency
λ	transport property
μ	molecular viscosity, g/cm-s
ρ	density, g/cc
ϕ_{ij}	mixture property

THERMODYNAMIC PROPERTIES

Real gas properties for H_2 and H_2O at elevated temperature and pressure are reported by Hendricks et al. (refs. 5 and 6), Goldberg and Haferd (ref. 7), and McCarty (ref. 8). All of the literature reviewed for hydrogen and steam present empirical relationships; theoretical relationships apparently do not exist. In contrast, a good theoretical real gas basis exists for air, see for example Hilsenrath and Klein (ref. 9). Perfect gas properties are available for hydrogen, Svehla (ref. 10) or the JANNAF tables (ref. 11). The JANNAF tables do cover real gas properties for H_2O. Raznjevic (ref. 12) presents a comprehensive collection of thermodynamic properties.

The Roder (ref. 13) 1975 parahydrogen report covers temperatures from the triple point to 700 K for pressures up to 3000 atm. The valid range of temperature and pressure for the NASA computer programs GASP (ref. 5) and WASP (ref. 6) are given in table I. 'GASP' and 'WASP' stand for gas properties and water and steam properties respectively. The temperature of interest, 1100 K, is higher than the limit of 1000 K, but the programs are believed to be appropriate for the current study. The computer programs GASP and WASP were modified such that mixture properties could be easily calculated.

MIXING RULE

It was assumed that the gas components occupy the entire space at the mixture temperature and pressure. For each gas, the mass dependent properties were divided by molecular weight and, except for viscosity and conductivity, the mass independent properties were mole fraction weighted, e.g.,

$$H_m = n\bar{h} = \sum n_i \bar{h}_i$$

3

$$S_m = n\bar{S} = \sum n_i \bar{S}_i$$

$$C_{p_m} = \sum n_i \bar{C}_{pi}$$

$$n_{mix} = \sum n_i = 1$$

$$p_{mix} = \sum p_i n_i$$

where the overbar represents mole basis properties. The other properties are:

$$\gamma = \frac{C_p}{C_v} = \frac{\left(\frac{\partial p}{\partial v}\right)_S}{\left(\frac{\partial p}{\partial v}\right)_T}$$

$$\frac{a^2}{\frac{\gamma p}{\rho}} = \frac{T\left(\frac{\partial Z}{\partial T}\right)_\rho + Z}{Z + T\left(\frac{\partial Z}{\partial T}\right)_p}$$

$$\left(\frac{\partial Z}{\partial T}\right)_\rho = \frac{Z}{p}\left(\frac{\partial p}{\partial T}\right)_\rho - \frac{Z}{T}$$

$$R \equiv C_p - C_v = \frac{T}{\rho^2} \frac{\left(\frac{\partial \rho}{\partial T}\right)_p^2}{\left(\frac{\partial \rho}{\partial p}\right)_T}$$

$$\left(\frac{\partial Z}{\partial T}\right)_p = -\frac{Z}{\rho}\left(\frac{\partial \rho}{\partial T}\right)_p - \frac{Z}{T}$$

where

$$\left(\frac{\partial \rho}{\partial T}\right)_p = -\frac{\left(\frac{\partial p}{\partial T}\right)_\rho}{\left(\frac{\partial p}{\partial \rho}\right)_T}$$

and

$$Z = \left(\frac{p}{\rho \frac{RT}{\bar{M}}}\right)_{mixture}$$

The GASP and WASP computer programs compute the partial derivatives $\partial p/\partial T|_\rho$ and $\partial p/\partial \rho|_T$. Other partial derivatives are obtained by Maxwell's equations.

4

For viscosity, and thermal conductivity, the mixing rule of Wilke (ref. 14) was used. The mixing rule is:

$$\varphi_{ij} = \frac{\left(1 + \left(\frac{\mu_i}{\mu_j}\right)^{1/2}\left(\frac{M_j}{M_i}\right)^{1/4}\right)^2}{(2)^{1.5}\left(1 + \left(\frac{M_i}{M_j}\right)\right)^{1/2}}$$

$$\lambda_{mix} = \frac{\sum\limits_{i=1}^{n} x_i \lambda_i}{\sum\limits_{j=1}^{n} x_j \varphi_{ij}}$$

where λ_i is either viscosity or thermal conductivity of gas i.

H_2 THERMODYNAMIC AND TRANSPORT PROPERTIES

Thermodynamic and transport properties for H_2 are presented in figures 1 to 20 for a range of temperatures from 800 to 1200 K and pressures from 1 to 500 atm. The real to perfect sound speed squared ratio varies from 1.0 to 1.13, the perfect to real gas constant ratio varies from 1.0 to 1.027, and compressibility varies from 1.0 to 1.13. The enthalpy and entropy are not zero at their respective reference temperatures e.g., 298 and 0 K due to the empirical nature of GASP and WASP. The shift is not important in the use of the enthalpy and entropy as only differences are of interest. The quantities of C_p/R and C_v/R approach their theoretical limits of $(\xi + 2)/2 = 3.5$ and $\xi/2 = 2.5$ where $\xi = 5$ is the molecular degrees of freedom.

H_2O THERMODYNAMIC AND TRANSPORT PROPERTIES

Thermodynamic and transport properties for H_2O are presented in figures 21 to 40 for a range of temperatures from 800 to 1200 K and pressures from 1 to 500 atm. The real to perfect sound speed squared ratio varies from 0.65 to 1.0, the perfect to real gas constant ratio varies from 1.0 to 7.4, and compressibility varies from 0.61 to 1.0. As previously mentioned the enthalpy and entropy are not zero at their respective reference temperatures. The quantities of C_p/R and C_v/R approach their theoretical limits of $(\xi + 2)/2 = 4.5$ and $\xi/2 = 3.5$ where $\xi = 7$ is the molecular degrees of freedom.

H_2/H_2O THERMODYNAMIC AND TRANSPORT PROPERTIES

Thermodynamic and transport properties for H_2/H_2O are presented in figures 41 to 60 for a range of temperatures from 800 to 1200 K and pressures from 1 to 500 atm. The H_2 and H_2O mole functions of 0.8687 and 0.1313 were determined by a computational analysis of the combustion process (ref. 15).

5

The real to perfect sound speed squared ratio varies from 1.0 to 1.19, the perfect to real gas constant ratio varies from 1.0 to 1.39, and compressibility varies from 1.0 to 1.075. Again, the enthalpy and entropy are not zero at their respective reference temperatures. The ratios of C_p/R and C_v/R approach their theoretical limits of $(\xi + 2)/2 = 3.5$ and $\xi/2 = 2.5$ where $\xi = 5$ is the molecular degrees of freedom.

The boundary layer code requires that μ, Pr, and k be known polynominals in temperature. Obtaining these polynominals removes the limitation of using air equivalent conditions. Thus, these transport properties for the hydrogen/steam mixture were fit using polynomial relationships for future turbine performance use. The polynomials were initially assumed to be up to 4th order in the temperature to sea level temperature ratio (T/T_{s1}) as the boundary layer computer program (ref. 2) needs this form. The pressure is for 305 atm and temperatures vary from 950 to 1140 K. The functional dependence of the transport properties on T/T_{s1} follows:

molecular viscosity

$$\frac{\mu(T)}{\mu(T_{s1})} = 0.2171 + 0.17677 \left(\frac{T}{T_{s1}}\right)$$

Prandtl number

$$Pr = 0.62366 - 0.015834 \left(\frac{T}{T_{s1}}\right) - 0.61071E\text{-}04 \left(\frac{T}{T_{s1}}\right)^2$$

thermal conductivity

$$\frac{k(T)}{k(T_{s1})} = 1.1879 + 0.032504 \left(\frac{T}{T_{s1}}\right) + 0.063622 \left(\frac{T}{T_{s1}}\right)^2$$

where:

$$T_{s1} = 288.16 \text{ K},$$

$$\mu(T_{s1}) = 0.3345E\text{-}03, \quad \sim \frac{g}{cm\text{-}s},$$

$$k(T_{s1}) = 0.19E\text{-}02 \quad \sim \frac{J}{cm\text{-}s\text{-}K}$$

An obvious problem with this approach is that the transport properties are a strong function of pressure which is not accounted for by this form of the equations.

For eventual use in TSONIC (ref. 1), MERIDL (ref. 3), and BLAYER (ref. 2) the options to account for real gas effects in the thermodynamic and transport properties include: (1) using GASP and WASP and calling these subroutines as needed, or (2) curve fitting these data as functions of T and P and calling the empirical representation of the computer programs. The forms of GASP and

WASP computer programs are such that they can be use as (1) above with no additional work.

AIR THERMODYNAMIC AND TRANSPORT PROPERTIES

Thermodynamic and transport properties for air are presented in figures 61 to 80 for a range of temperatures from 340 to 500 K and pressures from 1 to 500 atm. Real to perfect sound speed squared ratio varies from 1.0 to 1.65, the perfect to real gas constant ratio varies from 1.0 to 1.85, and compressibility varies from 1.0 to 1.31. As previously discussed, the enthalpy and entropy are not zero at their respective reference temperatures e.g., 298 and 0 K. The quantities of C_p/R and C_v/R approach their theoretical limits of $\xi + 2/2 = 3.5$ and $\xi/2 = 2.5$ respectively, where $\xi = 5$ is the number of molecular degrees of freedom. Real gas properties are given by Hansen (ref. 16) and Hansen and Heims (ref. 17).

MIXTURE PROPERTIES

For real gases, most of the thermodynamic and transport properties are functions of temperature and pressure. Using the static properties given by Jackson (ref. 18) see table II, the following property variation was calculated in this study:

$$8.00 \le C_p \le 8.08 \sim \frac{J}{g\text{-}K}$$

$$1.375 \le \gamma \le 1.378$$

$$1.073 \le \frac{R_{id}}{R_{act}} \le 1.076$$

$$1.04 \le \frac{c_{id}^2}{c_{act}^2} \le 1.05$$

$$0.278 \times 10^{-3} \le \mu \le 0.293 \times 10^{-3} \sim \frac{g}{cm\text{-}s}$$

$$0.563 \le P_r \le 0.565$$

$$0.396 \times 10^{-2} \le k \le 0.419 \times 10^{-2} \sim \frac{J}{cm\text{-}s\text{-}K}$$

From the above, the variation in the gas properties are: the gas constant is about 7.5 percent lower than the ideal gas constant, the actual speed of sound is about 2 percent lower than the ideal, viscosity decreases by about 5 percent, and thermal conductivity decreases by 5 percent through the turbine.

AIR EQUIVALENT CONDITIONS

Air equivalent conditions can be used as a performance reference, (ref. 19). Air equivalent conditions of the H_2/H_2O mixture were obtained for the inlet conditions. The Reynolds number and total temperature were held fixed between the gas mixture and the air equivalent case. The total pressure and hence mass flow are thus changed. The air equivalent calculation is necessitated by the boundary layer program requirement that polynomials of μ, Pr, and k be supplied. (These polynominals for the H_2/H_2O mixture were previously unknown.) Further, perfect gas assumptions are extensively used in the three computer programs of interest (refs. 1 to 3).

Equivalent conditions are obtained when (see also refs. 18 and 19).

$$\frac{W\sqrt{RT_{tin}}}{P_{tin}} = \left[\frac{W\sqrt{RT_{tin}}}{P_{tin}}\right]_{equivalent}$$

$$\frac{N}{\sqrt{RT_{tin}}} = \left[\frac{N}{\sqrt{RT_{tin}}}\right]_{equivalent}$$

The air equivalent conditions are listed in table III and the definitions are given below for reference:

$$W_{eq} = W\frac{\sqrt{\theta}}{\delta}\varepsilon$$

$$N_{eq} = \frac{N}{\sqrt{\theta}}$$

where

$$\theta \approx \left[\frac{V_a}{V_{a,std}}\right]^2 = \frac{2\gamma RZT_t}{(\gamma + 1)c^2}$$

$$\delta = \frac{P_{tin}}{P_{tstd}}$$

$$V_{cr}^2 = \frac{2\gamma}{\gamma + 1}gRT_t$$

$$\varepsilon = \frac{\gamma_{std}\left(\frac{2}{\gamma_{std} + 1}\right)^{\gamma_{std}/(\gamma_{std}-1)}}{\gamma\left(\frac{2}{\gamma + 1}\right)^{\gamma/(\gamma-1)}}$$

8

Table III lists the Rocketdyne mixture values, the previous study air equivalent values (ref. 20), and the present study mixture values and air equivalent values.

The equivalent conditions DO NOT account for real gas effects. They account for different (constant property) gases. Real gas affects can only be quantified by accounting for real property changes in the thermodynamic process. This has not yet been accomplished.

The use of GASP and WASP provides, for the first time, a capability to determine real gas mixture thermodynamics and transport properties. The air equivalent performance limitation has been removed.

SSME FUEL TURBINE PERFORMANCE CALCULATION

The computer programs TSONIC, MERIDL, and BLAYER have been used to compute the air equivalent performance of the SSME turbine (see refs. 20 and 21). The TSONIC computer program solves for the inviscid flow in the blade to blade frame, the MERIDL computer program calculates the flow in the hub to tip mid-channel frame, and the BLAYER computer program computes the boundary layer on the blades and the endwall friction losses and the mixing losses. The solution is quasi-three-dimensional. The downstream whirl distribution and total pressure losses were adjusted, outside the programs by manual intervention, to match the (suction and pressure) boundary layer edge velocity at the trailing edge. The TSONIC and MERIDL programs assume the gas to be ideal and perfect, inviscid, and irrotational.

The SSME fuel turbine first stage stator has 41 blades, the first stage rotor has 63 blades, the second stage stator has 39 blades and the second stage rotor has 59 blades. The SSME fuel turbine mid channel blade geometry is represented schematically in figure 81. The computed relative velocities at the hub, mean, and tip are shown in figure 82. The flow stagnates at the leading edge. At the trailing edge the suction and pressure side edge of boundary layer velocities meet at the trailing edge. There are no known experimental data for comparison.

The loss analysis is given in table IV for previous calculations (ref. 20) and the current study. The loss analysis methodology is given in reference 4. As shown in table IV the largest losses for the stators is the profile and mixing loss. The tip clearance loss is the largest loss for the rotors. As shown in table V the first stage efficiency calculated here is 0.902 versus 0.893 from reference 20, and for the second stage the calculated efficiency is 0.915 versus 0.900 from reference 20. The aerodynamic performance information is presented in table V. Computed pressure, temperatures, flow angles, and velocity ratios are given for hub, mid, and shroud locations for the air equivalent case.

SUMMARY OF RESULTS

The study has developed thermodynamic and transport real gas data for the SSME mixture of H_2 and H_2O. The GASP and WASP computer programs were modified and run together to determine mixture properties. The programs are general in that they can handle several gases over a range of pressure and temperature.

9

The current SSME capability at NASA Lewis is limited to running equivalent air, quasi-three-dimensional turbomachinery performance. An air equivalent case was calculated using constant real gas thermodynamic properties. This study has provided the tools to calculate the performance for the SSME mixture of H_2/H_2O.

Future studies are recommended to include variable real gas thermodynamic and transport properties in the TSONIC, MERIDL, and BLAYER computer programs.

REFERENCES

1. Katsanis, T.: FORTRAN Program for Calculating Transonic Velocities on a Blade-to-Blade Stream Surface of a Turbomachine. NASA TN D-5427, 1969.

2. McNally, W.D.: FORTRAN Program for Calculating Compressible Laminar and Turbulent Boundary Layers in Arbitrary Pressure Gradients," NASA TN D-5681, 1970.

3. Katsanis, T.; and McNally, W.D.: Revised FORTRAN Program for Calculating Velocities and Streamlines on the Hub-Shroud, Mid-Channel Stream Surface of an Axial-, Radial-, or Mixed-Flow Turbomachine or Annual Duct, I-Users Manual. NASA TN D-8430, 1977.

4. Boyle, R.J.; Haas, J.E.; and Katsanis, T.: Comparison Between Measured Turbine Stage Performance and the Predicted Performance using Quasi-3-D Flow and Boundary Layer Analyses. AIAA Paper 84-1299, June 1984.

5. Hendricks, R.C.; Baron, A.K.; and Peller, I.C.: Gasp: A Computer Code for Calculating the Thermodynamic and Transport Properties for Ten Fluids: Parahydrogen, Helium, Neon, Methane, Nitrogen, Carbon Monoxide, Oxygen, Fluorine, Argon, and Carbon Dioxide. NASA TN D-7808, 1975.

6. Hendricks, R.C.; Peller, I.C.; and Baron, A.K.: WASP: A Flexible Fortran IV Computer Code for Calculating Water and Steam Properties. NASA TN D-7391, 1973.

7. Goldberg, F.N.; and Haferd, A.M.: Numerical Procedures for Cal- culating Real Fluid Properties of Normal and Parahydrogen. NASA TN D-4341, 1968.

8. McCarty, R.D.; and Hord, J.; and Roder, H.M.: Selected Properties of Hydrogen. NBS Monograph 168, Feb. 1981.

9. Hilsenrath, J.; and Klein, M.: Tables of Thermodynamic Properties of Air in Chemical Equilibrium Including Second Virial Corrections from 1500° to 15,000* K. AEDC TR-65-58, Mar. 1965. (AD-612301)

10. Svehla, R.A.: Thermodynamic and Transport Properties for the Hydrogen-Oxygen System. NASA SP-3011, 1964.

11. JANAF Thermochemical Data, Compiled and Calculated by Dow Chemical, Midland, MI.

12. Raznjevic, Kuzman: Handbook of Thermodynamic Tables and Charts. Hemisphere Publishing Co., 1976.

13. Roder, H.M.; and McCarty, R.D.: A Modified Benedict-Webb-Rubin Equation of State for Parahydrogen-II. NBSIR 75-814, June 1975.

14. Wilke, C.R.: A Viscosity Equation for Gas Mixtures. J. Chem. Phys., vol. 18, no. 4, Apr. 1950, pp. 517-519.

15. VanOverbeke, T.: Private Discussions, 1985.

16. Hansen, C.F., "Approximations for the Thermodynamic and Transport Properties of High-Temperature Air," NASA TR-50, 1959.

17. Hansen, C.F.; and Helms, S.P., "A Review of the Thermodynamic, Transport, and Chemical Reaction Rate Propreties of High Temperature Air," NACA TN 4359, July 1958.

18. Jackson, E.O.: Rockwell International Letter to L. Povinelli of NASA Lewis, Feb. 16, 1984 (84RC01708).

19. Glassman, A.J., ed.: Turbine Design and Application, Vol. 1. NASA SP-290-VOL-1, 1972, pp. 45-62.

20. Haas, J.E.: Fuel and Oxidizer Turbine Loss Analysis. Advanced High Pressure O_2/H_2 Technology, S.F. Morea and S.T. Wu, eds., NASA CP-2372, 1984, pp. 560-570.

21. Haas, J.E., "Unpublished SSME notes," Feb. 1984.

TABLE I. - RANGES OF TEMPERATURE
AND PRESSURE FOR GASP AND WASP
COMPUTER PROGRAMS
(ref., Hendricks 5 and 6)

	P_{low}, atm	P_{high}, atm	T_{low}, K	T_{high}, K
N_2	0.1	500	64	1000
O_2	.1	1000	54	500
AR	.1	500	87	1000
CO_2	.1	500	216	1000
H_2	.001	1000	13.8	3000
Air	.1	500	54	500
H_2O	1.0	1000	273	1750

TABLE II. - COMPUTED BLADE ENTRANCE SSME TURBINE THERMODYNAMIC PROPERTIES, H_2/H_2O MIXTURE

				u, g/cm-s	u, lbm/ft sec	Pr	$\frac{k,J}{cm\ s\ k}$	$\frac{k,Btu}{ft\ sec\ °R}$	c^2_{Id}/c^2_{act}	Z	γ	$\frac{R_I}{R_{act}}$	Cp, $\frac{J}{g-k}$	Cp, $\frac{Btu}{lbm\ R}$
Total	T	a1105 K	1989.9 °R	0.302x10⁻³	0.203x10⁻⁴	0.566	0.433x10⁻²	0.695x10⁻⁴	1.060	1.057	1.373	1.076	8.117	1.940 (1.879)ᵃ
	p	a376 atm	5525.8 $\frac{lbf}{ft^2}$											
Stator 1	T	a1071	1928.4	.293x10⁻³	.197x10⁻⁴	.565	.419x10⁻²	.674x10⁻⁴	1.054	1.050	1.375	1.076	8.080	1.931 (1.869)
	p	a330	4855.5											
Rotor 1	T	a1053	1896.2	.289x10⁻³	.194x10⁻⁴	.564	.412x10⁻²	.662x10⁻⁴	1.050	1.047	1.376	1.075	8.057	1.926 (1.864)
	p	a305.2	4487.1											
Stator 2	T	a1026	1846.1	.282x10⁻³	.190x10⁻⁴	.563	.402x10⁻²	.645x10⁻⁴	1.045	1.042	1.377	1.073	8.024	1.918 (1.857)
	p	a272	3997.9											
Rotor 2	T	a1011	1819.2	.278x10⁻³	.187x10⁻⁴	.563	.396x10⁻²	.636x10⁻⁴	1.042	1.039	1.378	1.073	8.005	1.913 (1.853)
	p	a254.1	3736											

ᵃRocketdyne values, letter to Povinelli (ref. 18).

n H_2 = 0.8687   n H_2O = 0.1313   R = 376.5 ft-lbf/lbm R   M = 4.1164
O/F = 1.0364

TABLE III. - SSME INLET CONDITIONS AND PROPERTIES, BALANCE AT
FULL POWER LEVEL

	H_2/H_2O (Rocketdyneᵃ)	Air equivalentᵃ (ref. 19)	H_2/H_2O (This study)	Air equivalentᵇ (This study)
T_t, °R	1990	1990	1990	1990
P_t, atm	376	220	376	224
θ	28.2	4.0	24.9	4.0
ω, lbm/sec	177.7	274.3	177.7	259.5
Ω, rpm	13 890	14 541	13 890	1 548
ε	1.022	1.022	1.01	1.025
Re	2.18x10⁷	2.183x10⁷	2.06x10⁷	2.06x10⁷
W_{eq}, lbm/sec	2.565	2.565	2.384	2.384
N, rpm	36 742	36 742	36 742	36 742
Neq, rpm	6918	6918	7363	7363
γ	1.34	1.34	1.373	1.34
C_p, BTU/lbm R	1.879	.27	1.940	.27
Z	1.0587	1.07	1.057	1.07
u, lbm/ft-hr	.069	.106	.07297	.106
R ft-lbf / lbm R	376.5	53.35	349.1	53.35

ᵃRocketdyne, Feb. 1984 (ref. 18).
ᵇSame Reynolds number and total temperature as SSME.

TABLE IV. – SSME FUEL TURBINE LOSS ANALYSIS

Losses	1st stage, stator	1st stage, rotor	2nd stage, stator	2nd stage, rotor
This study				
Profile and mixing	0.012	0.014	0.013	0.014
Endwall friction	.006	.001	.007	.002
Secondary flow	.0050	.008	.003	.008
Incidence	.001	.003	.001	.004
Tip clearance	0	.050	0	.034
Δn blade row	0.024	0.076	0.024	0.062
P_{tinlet}/P_{sexit}	1.17	1.18	1.21	1.15
Previous study, reference 20				
Profile and mixing	0.014	0.016	0.013	0.017
Endwall friction	.007	.002	.007	.002
Secondary flow	.005	.009	.004	.009
Incidence	.001	.007	.001	.013
Tip clearance	0	.046	0	.034
Δn blade row	0.027	0.080	0.025	0.075
P_{tinlet}/P_{sexit}	1.19	1.17	1.24	1.19

TABLE V. – AERODYNAMIC PERFORMANCE INFORMATION, AIR EQUIVALENT

		Hub			Mid			Shroud		
		β, deg[b]	W, ft/sec	W/Wcr	β, deg[b]	W, ft/sec	W/Wcr	β, deg[b]	W, ft/sec	W/Wcr
Stator 1	In	0	286	0.15	0	298	0.15	0	310	0.16
	Out	-72.9	1082	.55	-70.5	991	.50	-68.3	924	.47
Rotor 1	In	-52.2	549	.28	-36.7	453	.23	-20.7	407	.21
	Out	+65.1	926	.48	+65.9	954	.49	+66.7	1004	.51
Stator 2	In	34.6	426	.22	33.7	398	.21	33.2	377	.20
	Out	-70.9	1172	.61	-69.5	1063	.55	-68.2	988	.51
Rotor 2	In	-53.8	637	.34	-42.1	499	.26	-28.3	414	.22
	Out	+61.9	821	.44	+61.9	867	.46	+63.5	908	.48

		P_t, lbf/ft^2	T_t, R	R_p	T_{tout}/T_{tin}	η_{stage}	$\Delta P_t/P_t$	Exit swirl, ft^2/sec
Stator 1	In	474041	1990					
	Out	471155	1990	0.994			0.0061	-401
Rotor 1	In	471120	1990					
	Out	367041	1877	.779	0.943	0.902	.0197	-93
Stator 2	In	367038	1877					
	Out	364694	1877	.994			.0064	-425
Rotor 2	In	364353	1877					
	Out	284188	1769	.779	.942	.915	.0101	-50

$\dfrac{Btu}{lbm}\,1 = Cp\,\Delta T_t = 54.8$; $\dfrac{Btu}{lbm}\,2 = Cp\,\Delta T_t = 52.39$ Btu; Total $= 107.2\ \dfrac{Btu}{lbm}$[a]

Blade row	Blade angle, deg	Incidence, deg	Exit design relative angles[b]	Deviation, deg[b]
S_1	0	0	-67.5	-3.0
R_1	-36.6	.1	64.5	1.4
S_2	21.0	12.7	-66.5	3.0
R_2	-35.6	6.5	60.5	1.4

[a]Rocketdyne value of work (with H_2/H_2O mixture) $= 314.6\ \dfrac{Btu}{lbm}$

[b]Positive angles are center-clockwise, see figure 81.
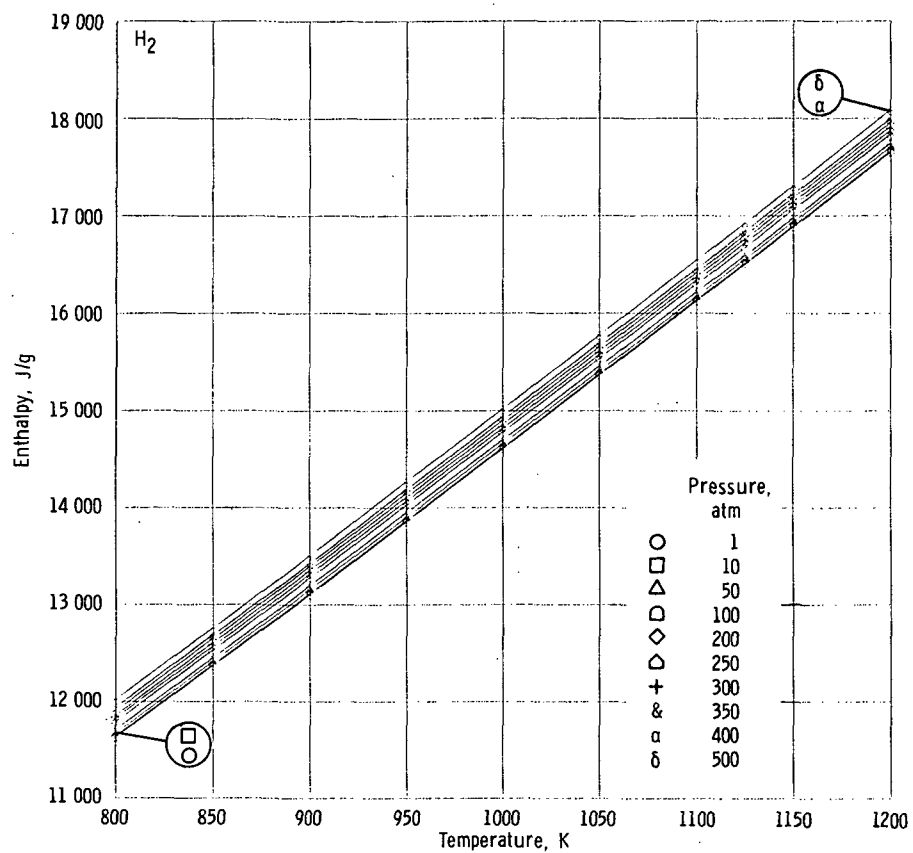
Figure 1. - Enthalpy versus temperature.
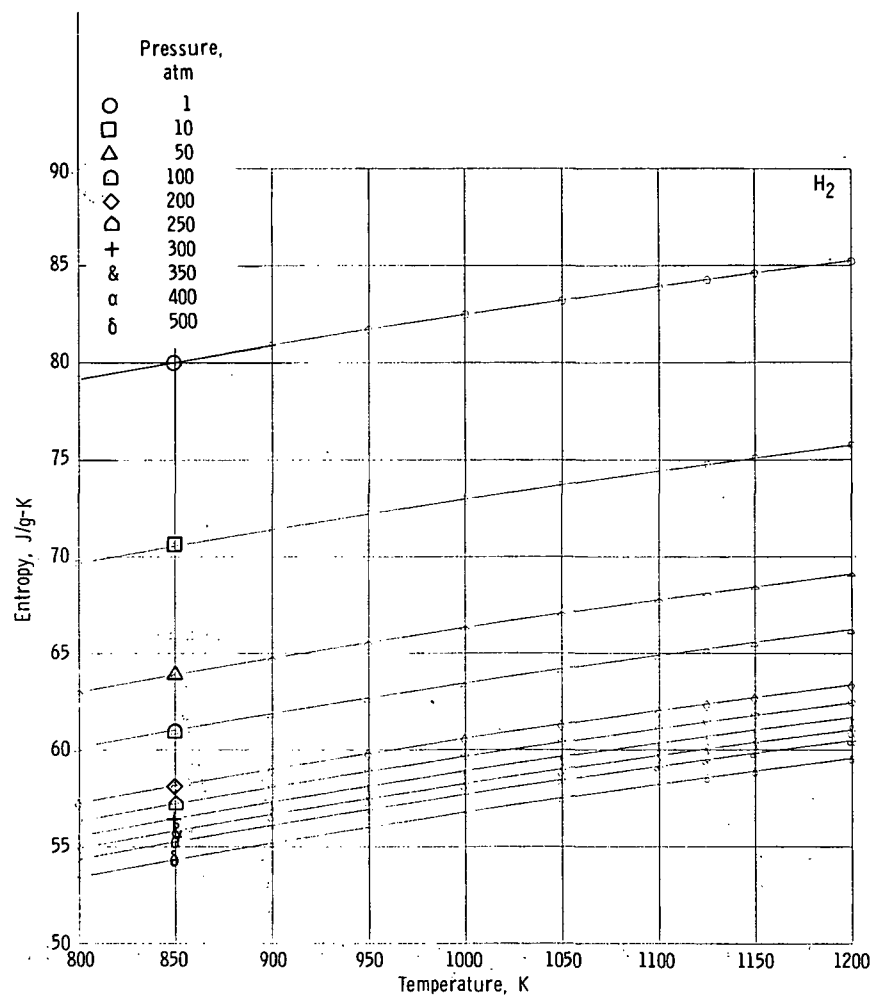
Figure 2. – Entropy versus temperature.
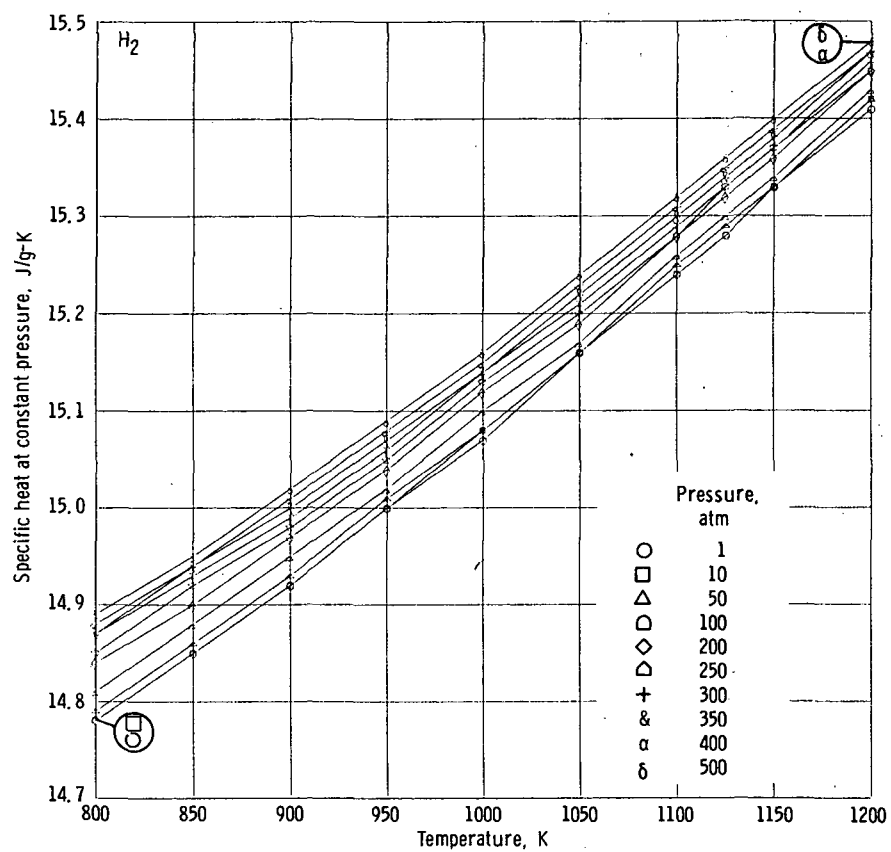
Figure 3. - Specific heat at constant pressure versus temperature.
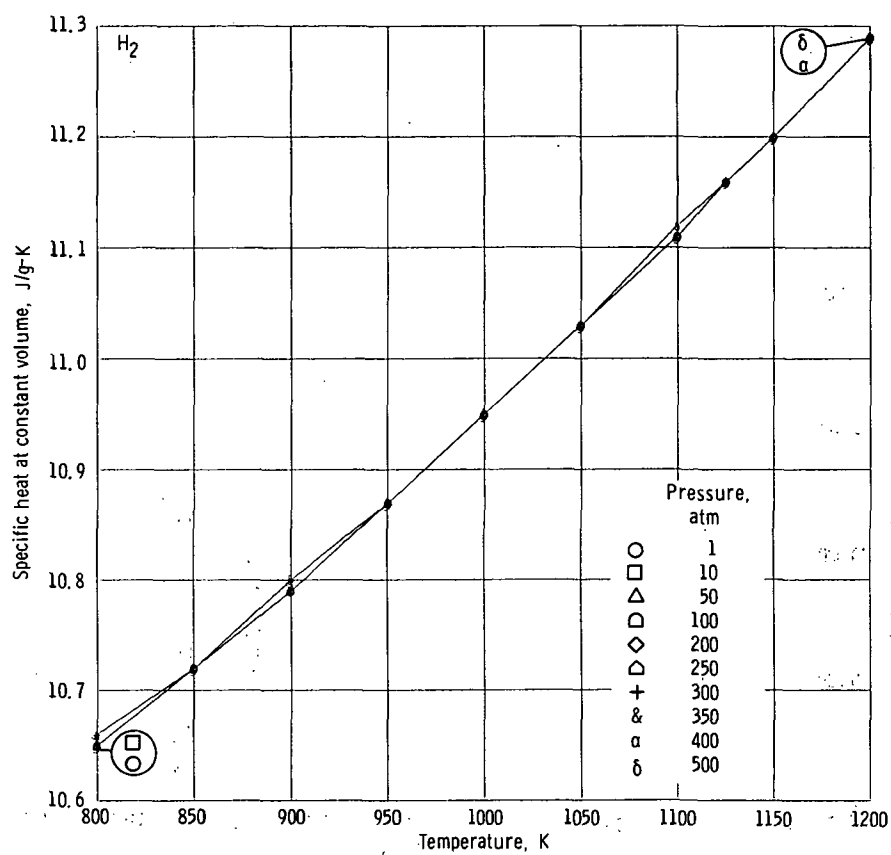
Figure 4. - Specific heat at constant volume versus temperature.
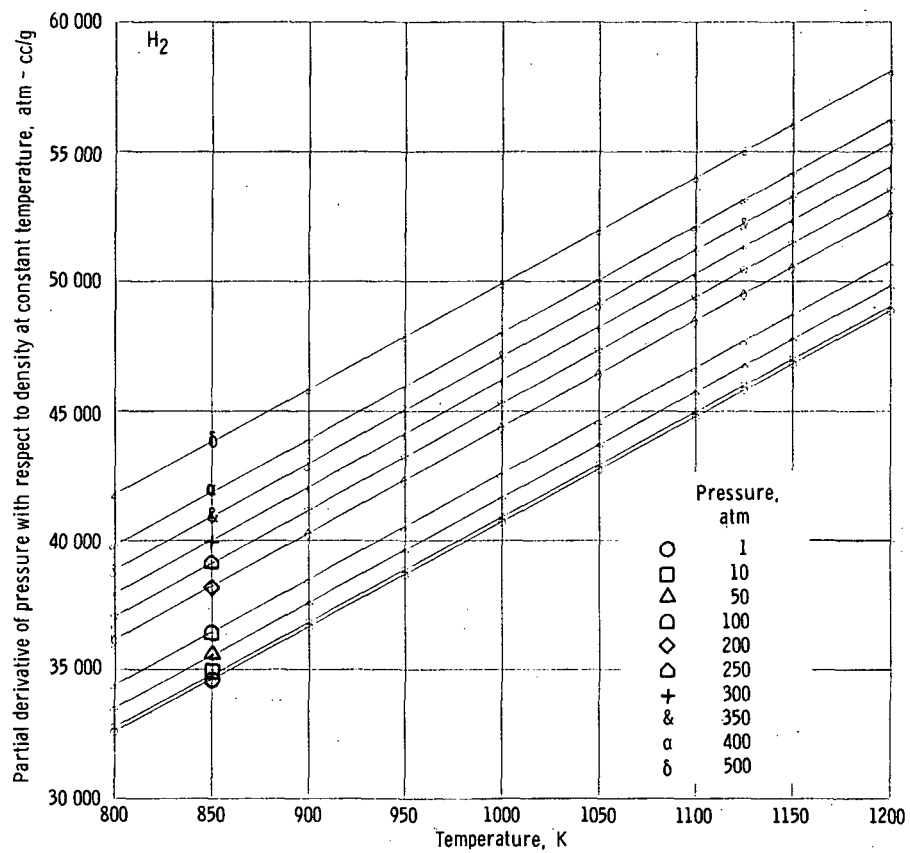
Figure 5. - Partial derivative of pressure with respect to density at constant temperature versus temperature.
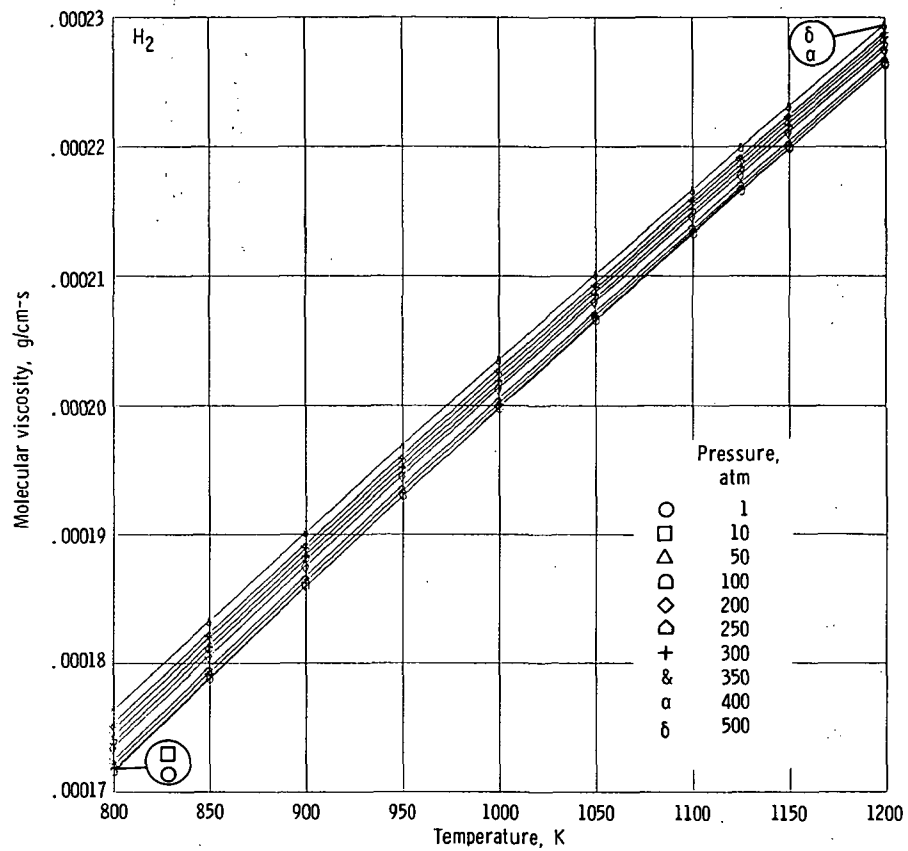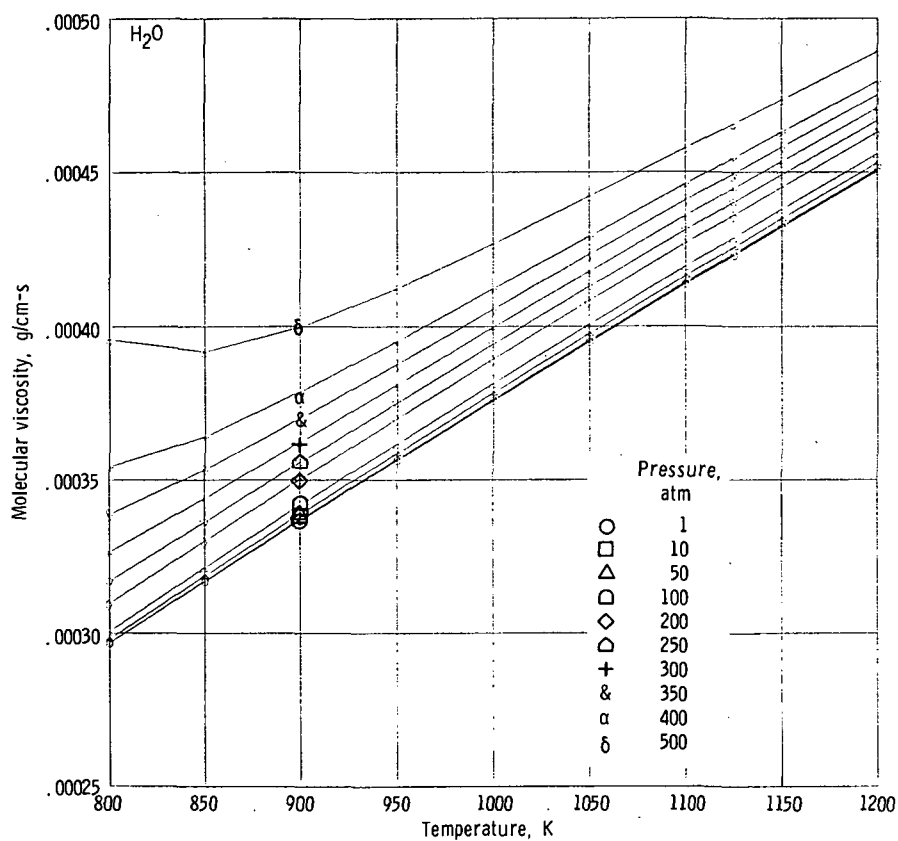
Figure 6. - Molecular viscosity versus temperature.
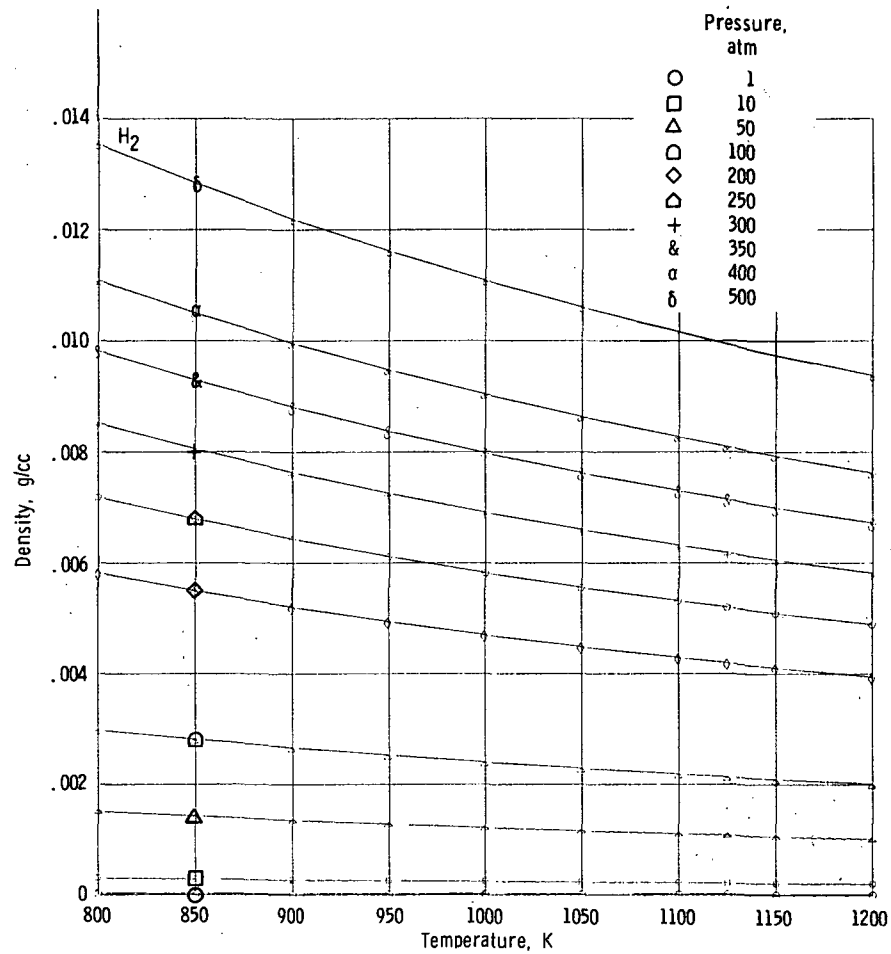
Figure 7. – Density versus temperature.
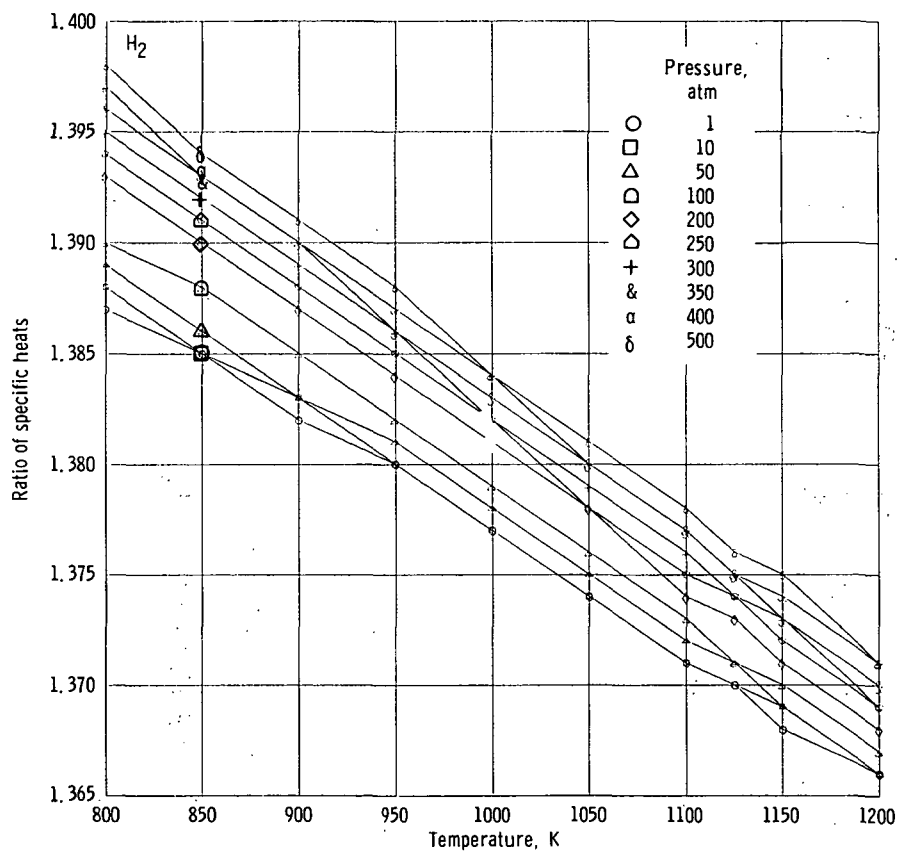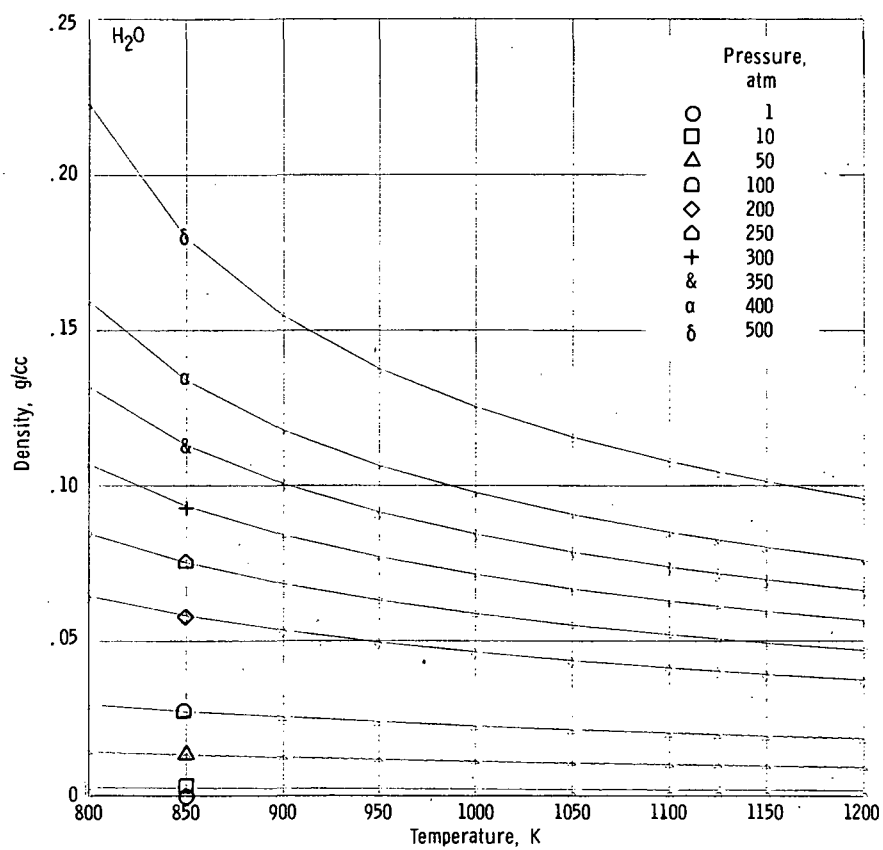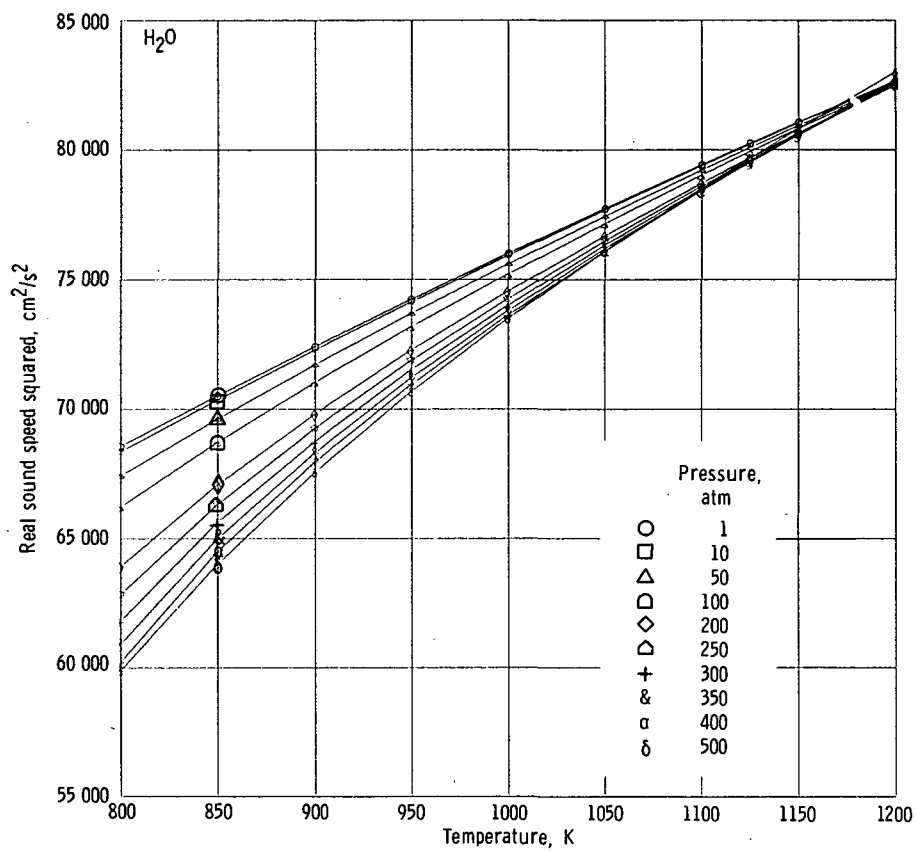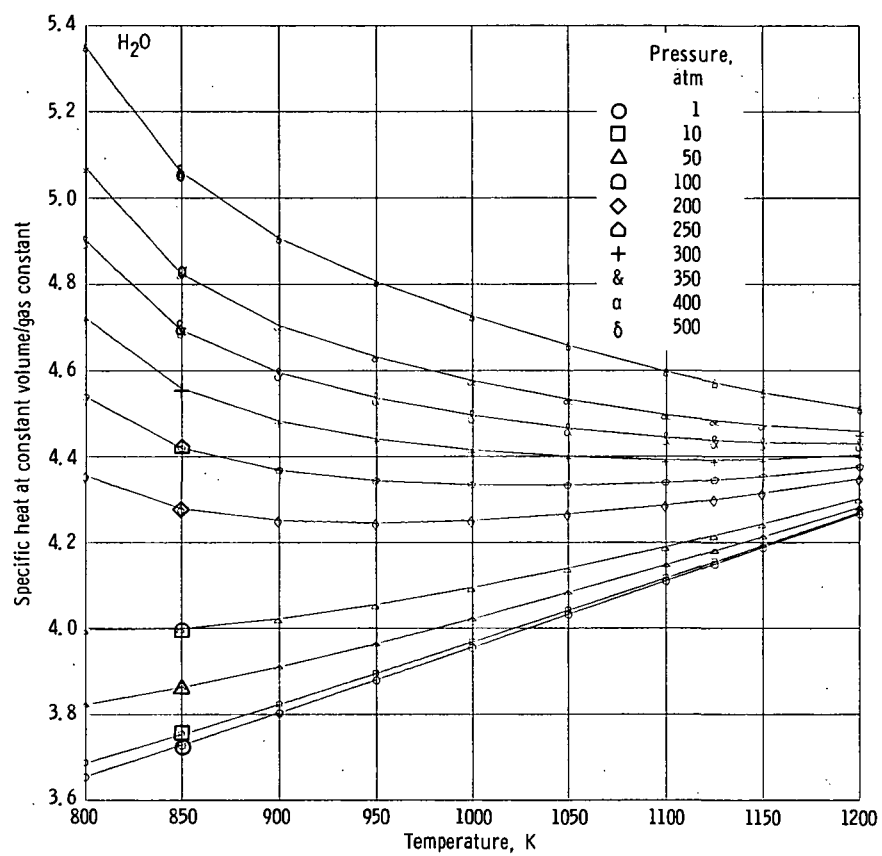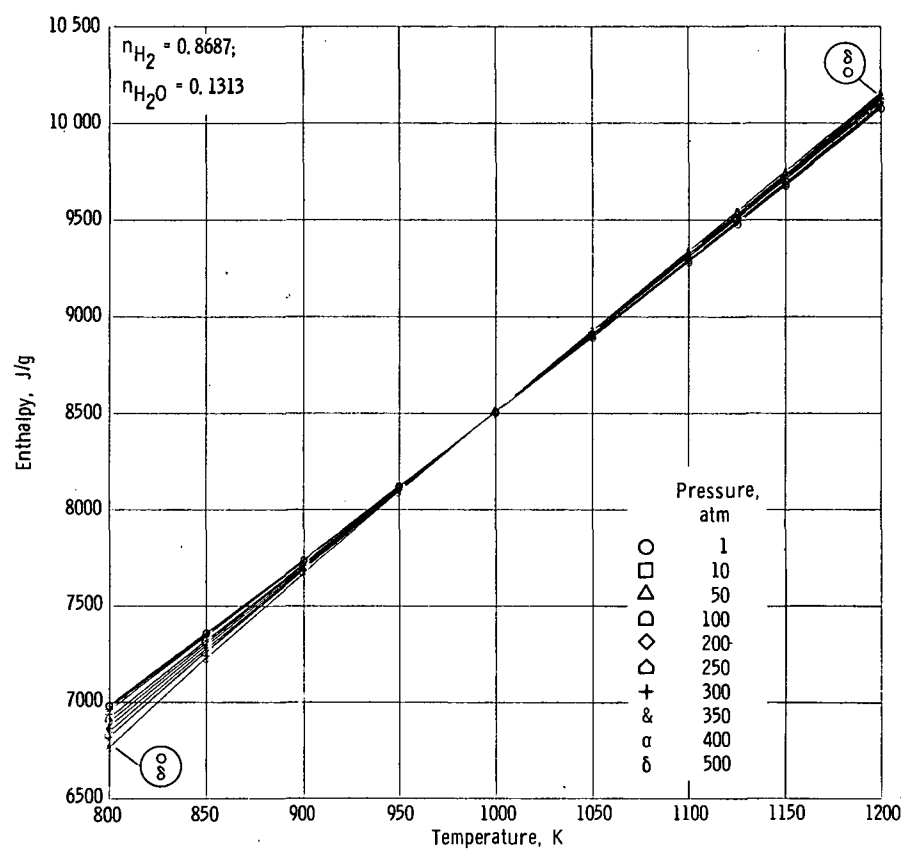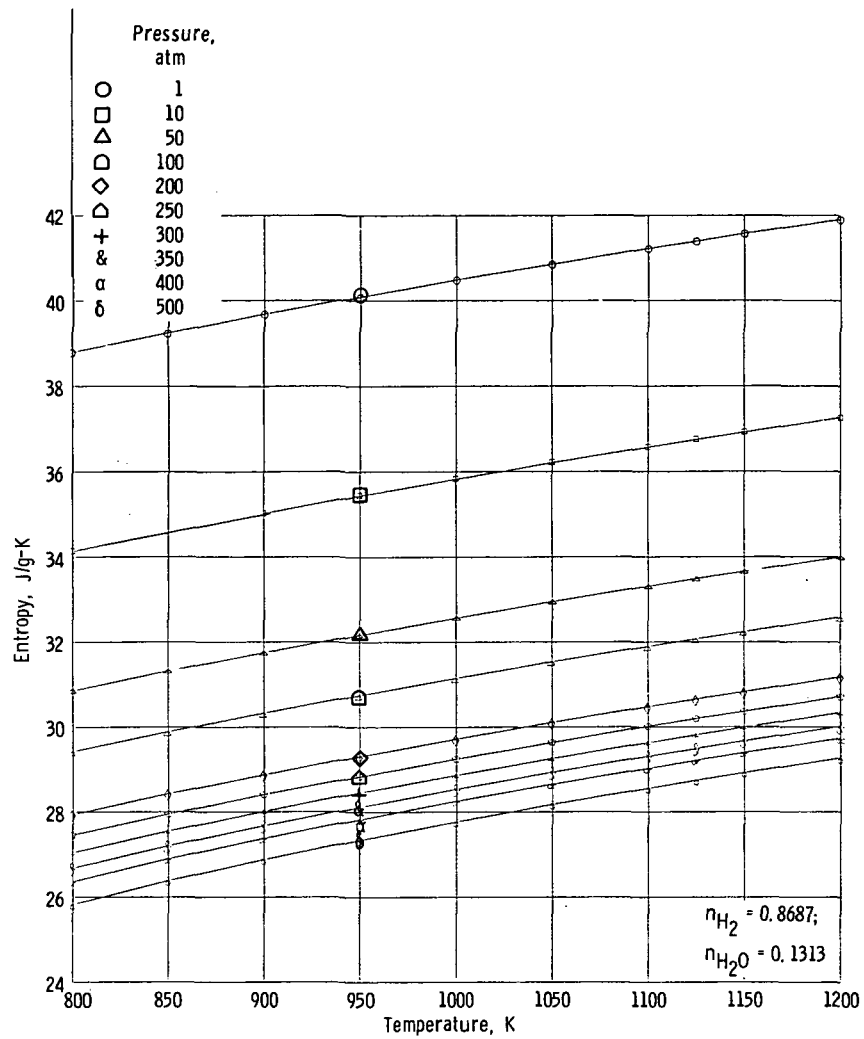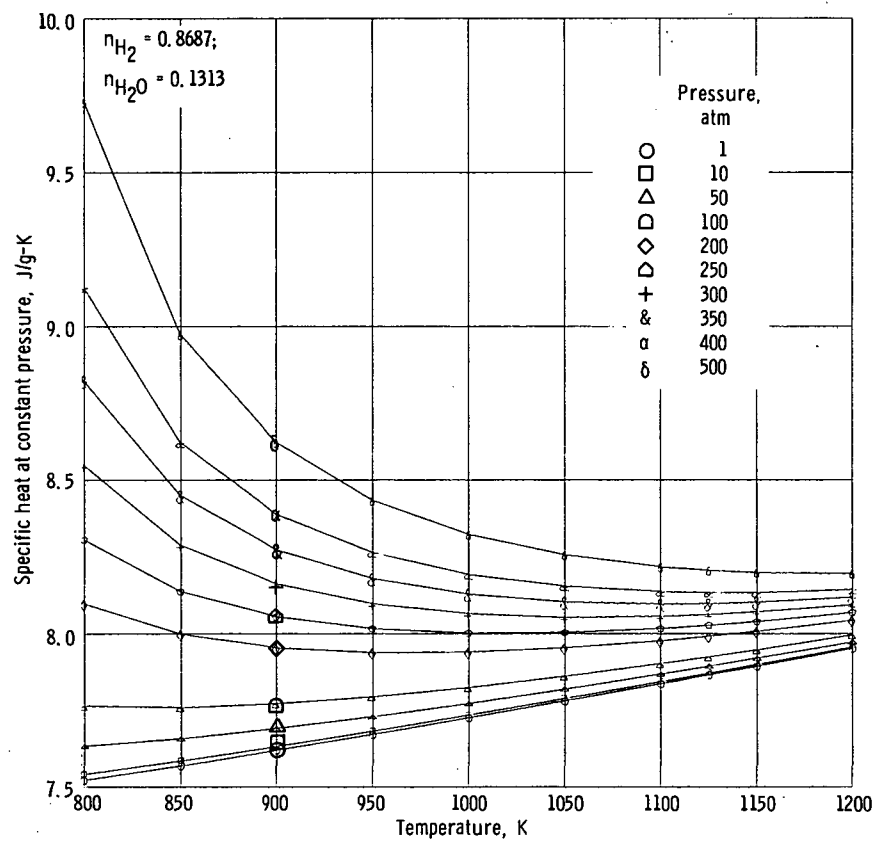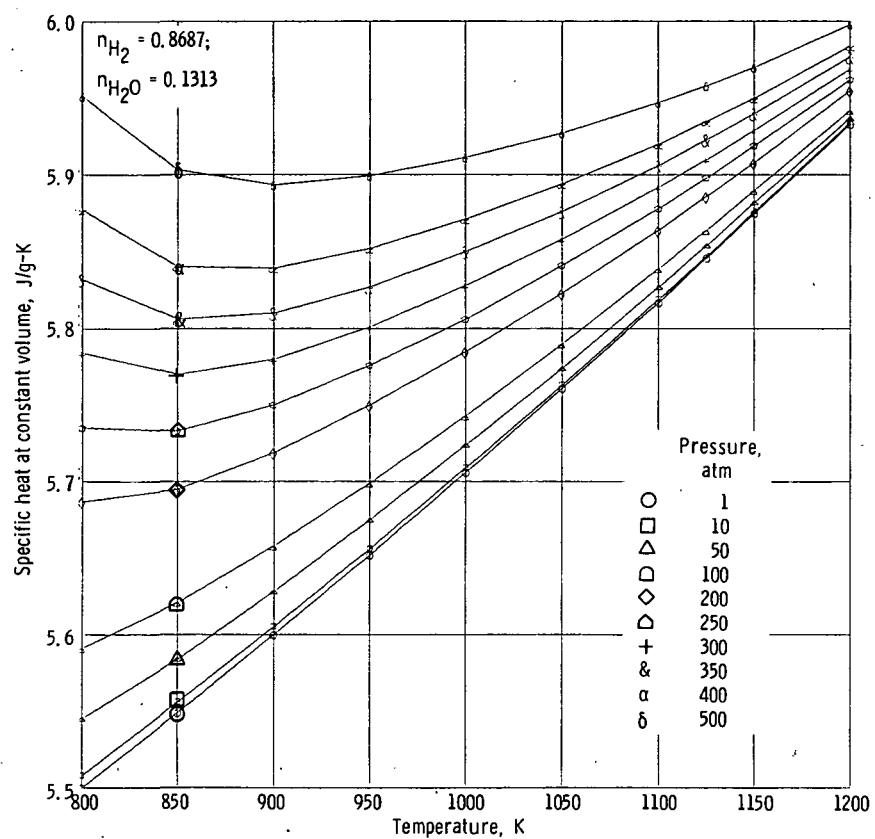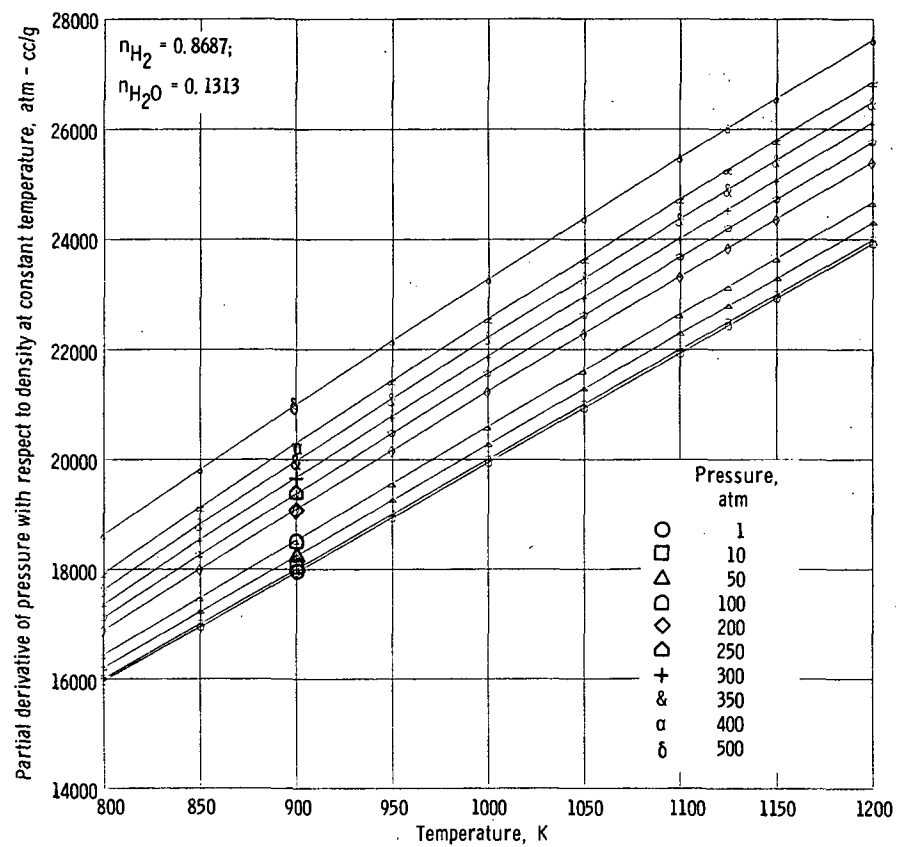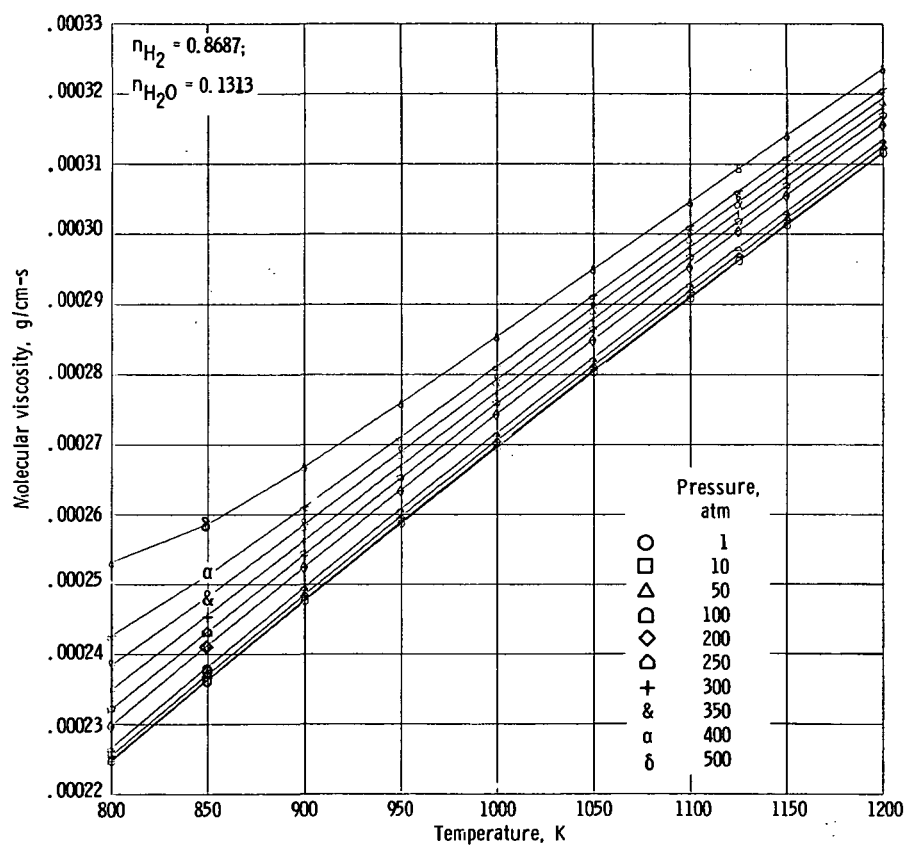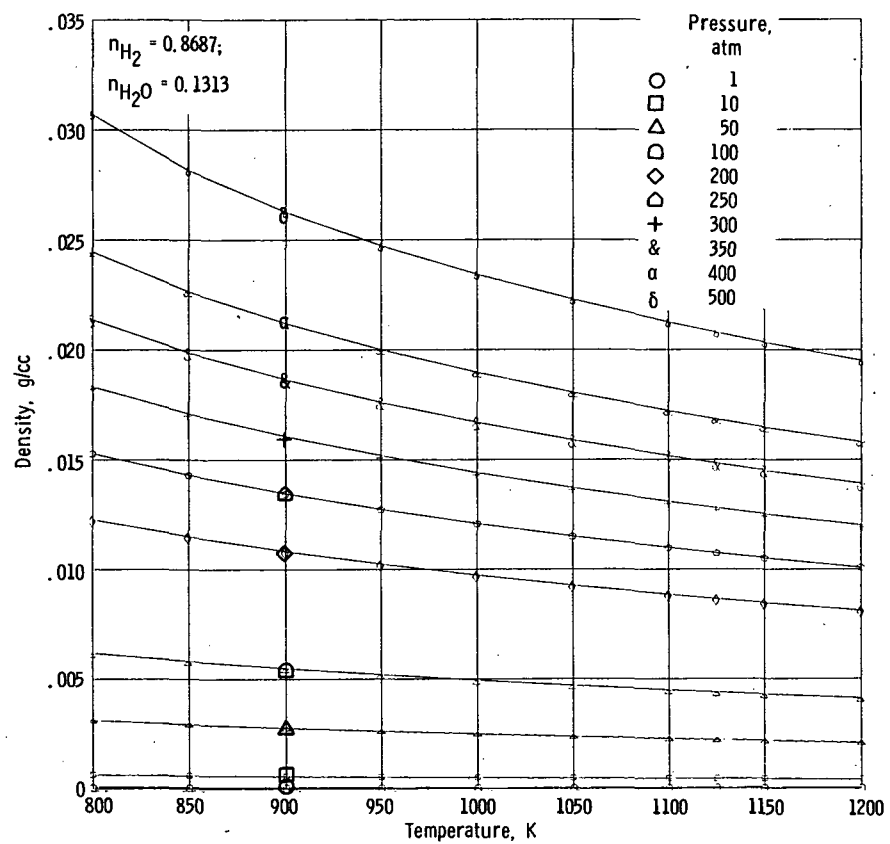
Figure 8. - Ratio of specific heats versus temperature.
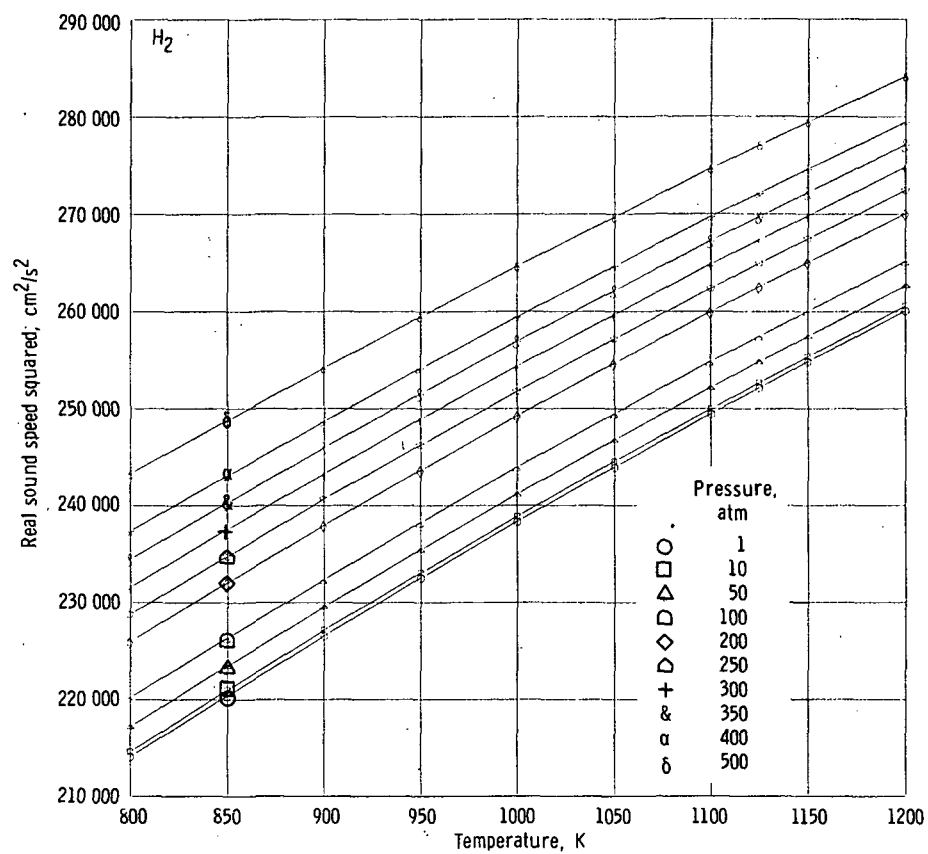
Figure 9. - Real sound speed squared versus temperature.
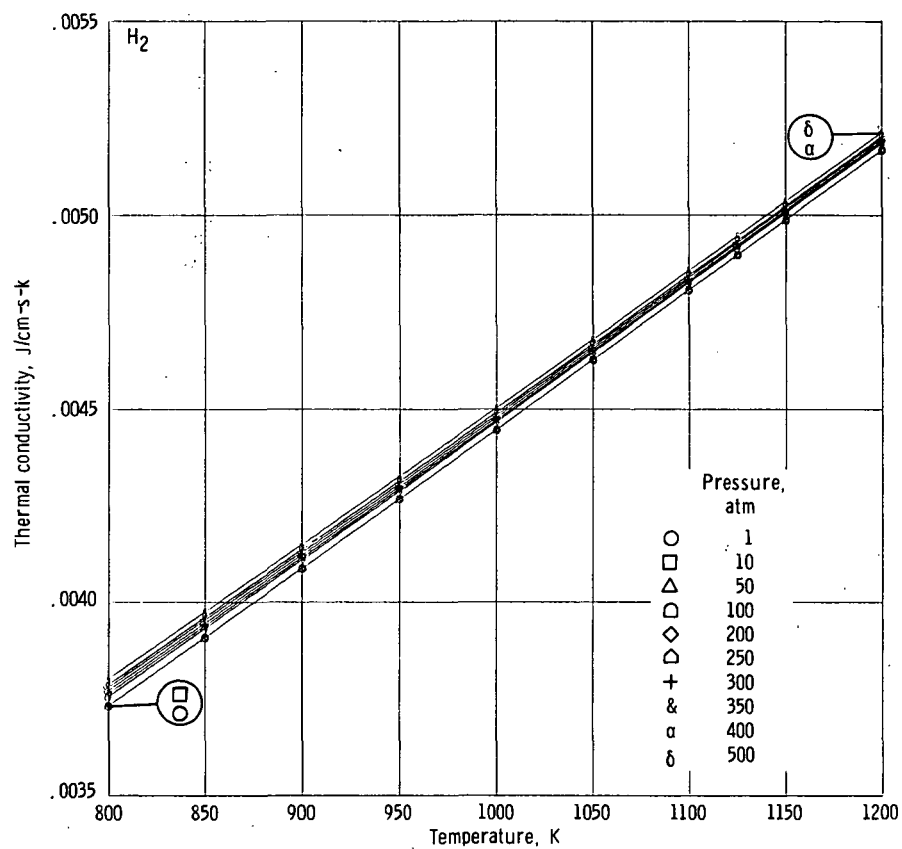
Figure 10. - Thermal conductivity versus temperature.
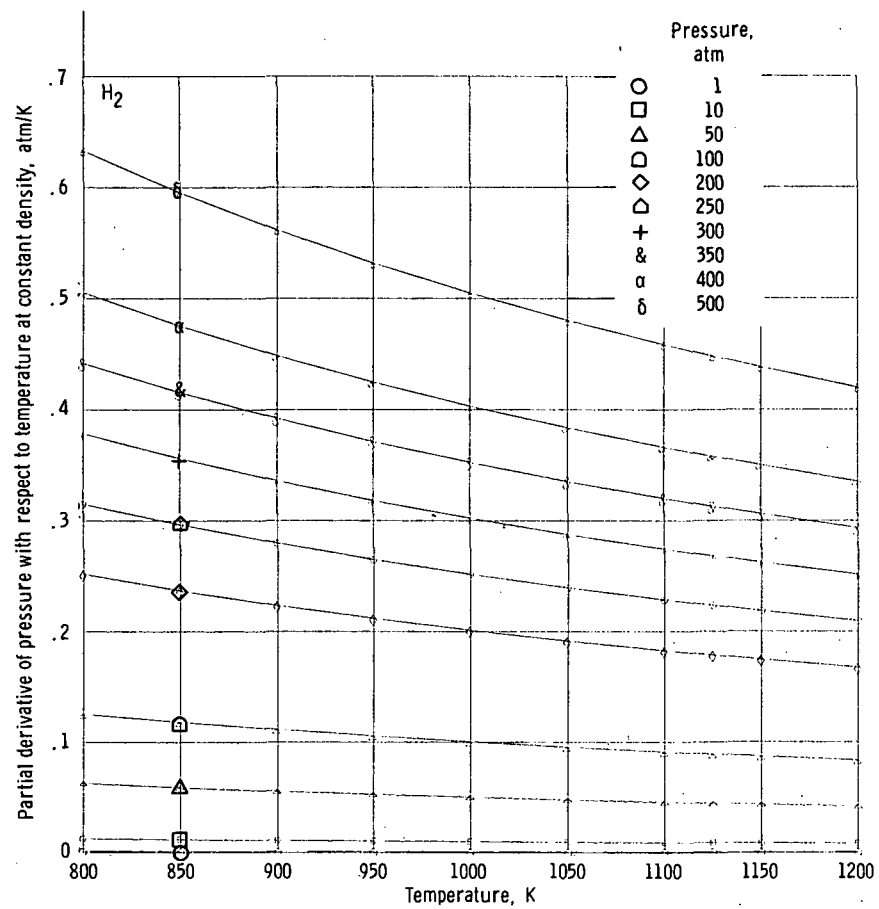
Figure 11. - Partial derivative of pressure with respect to temperature at constant density versus temperature.
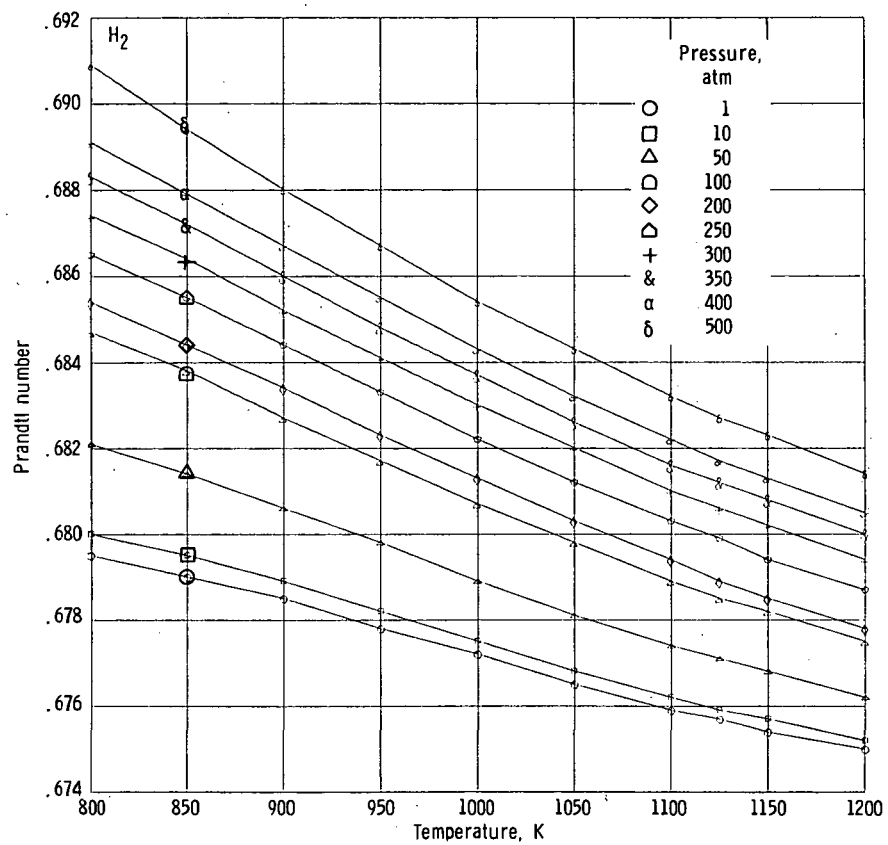
Figure 12. - Prandtl number versus temperature.
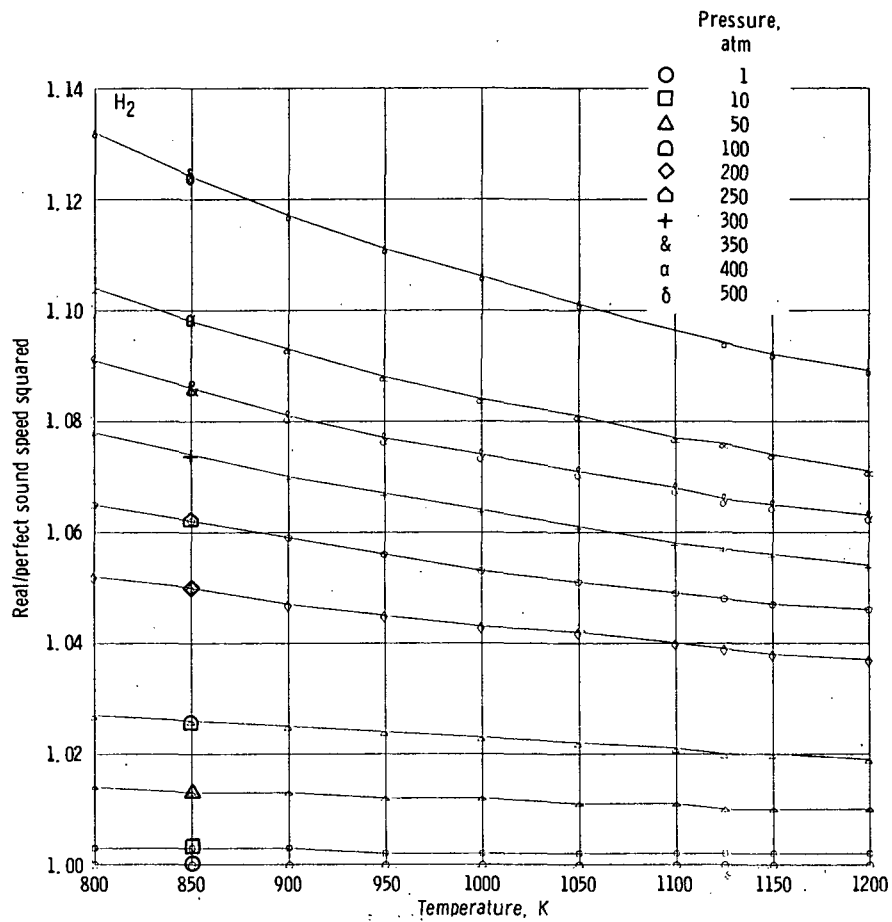
Figure 13. - Real/perfect sound speed squared versus temperature.
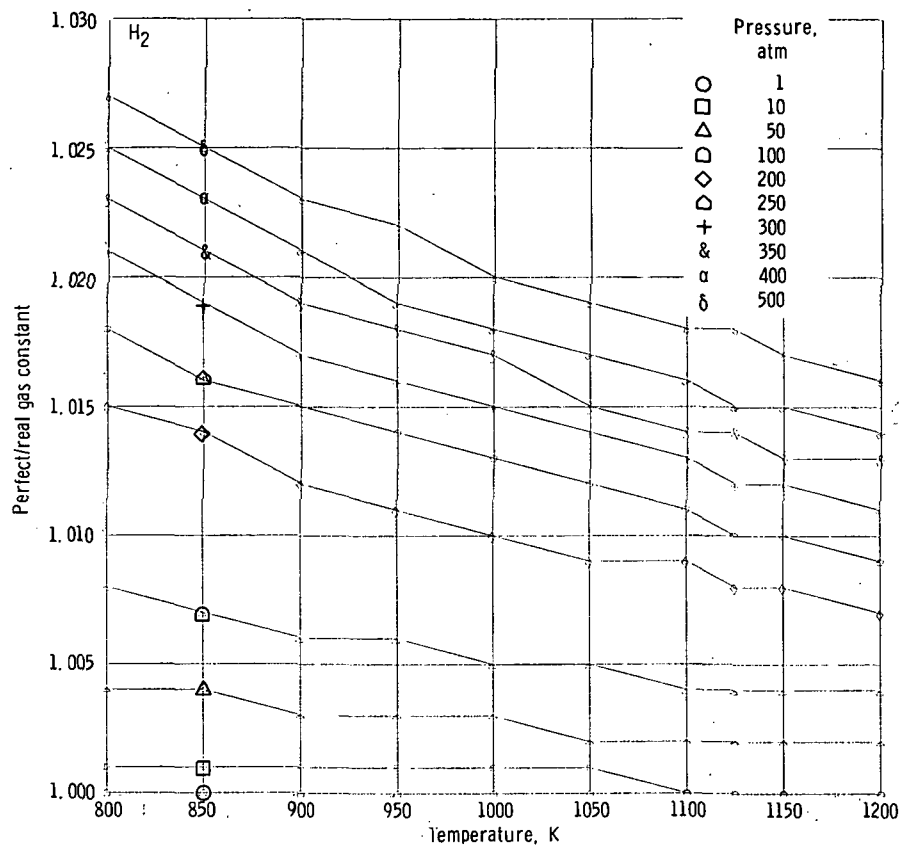
Figure 14. – Perfect/real gas constant versus temperature.
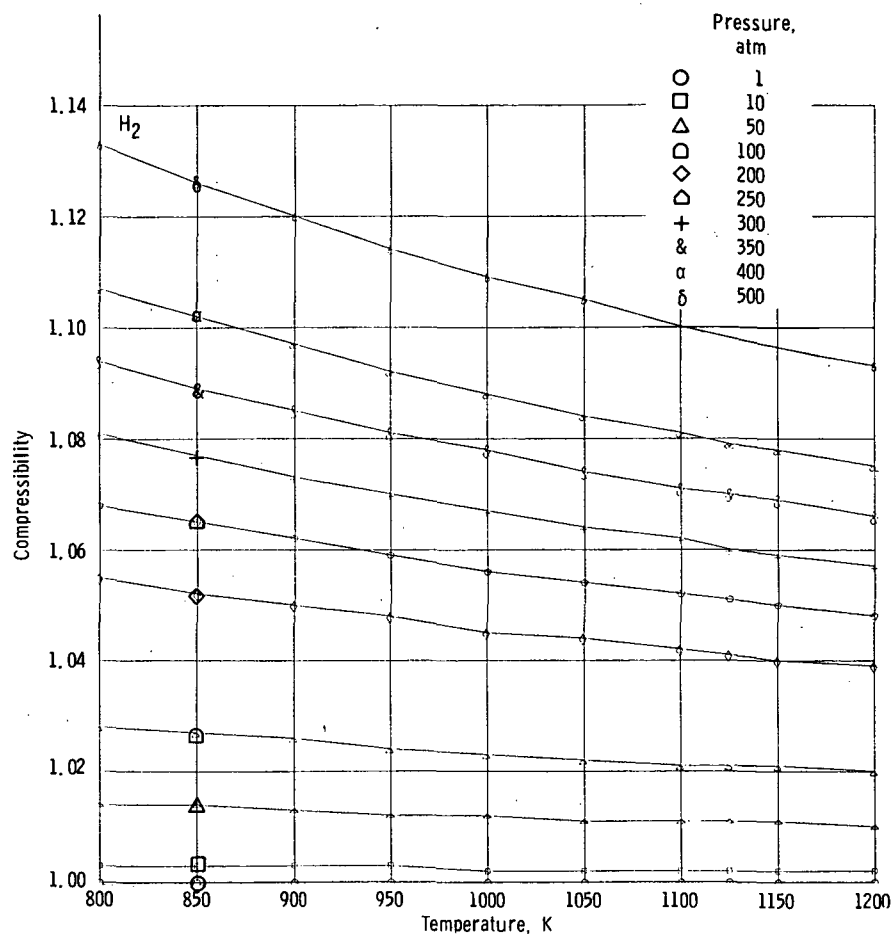
Figure 15. - Compressibility versus temperature.
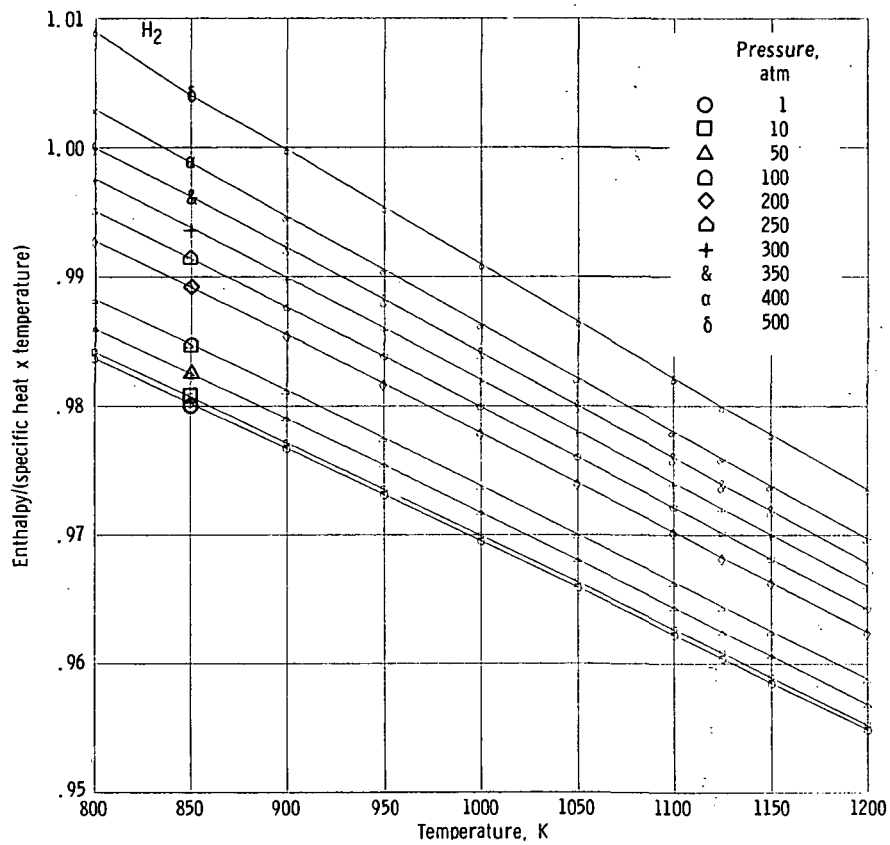
Figure 16. – Enthalpy/(specific heat x temperature) versus temperature.
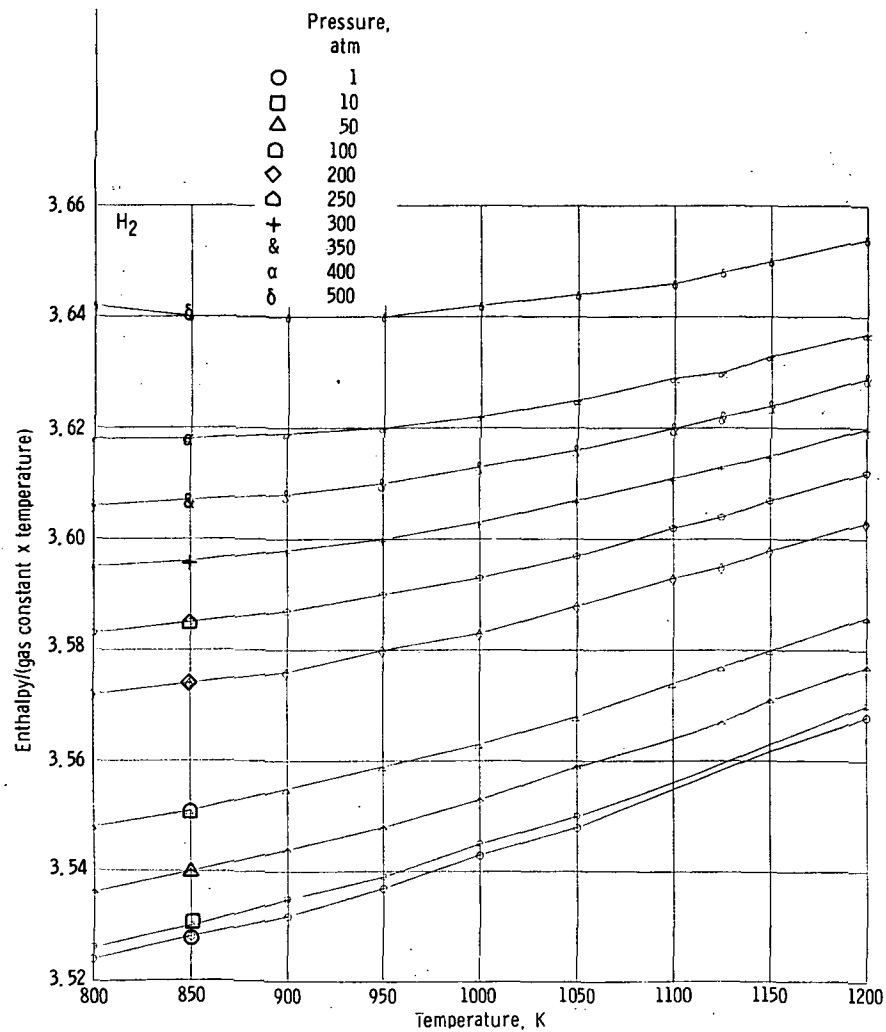
Figure 17. - Enthalpy/(gas constant x temperature) versus temperature.
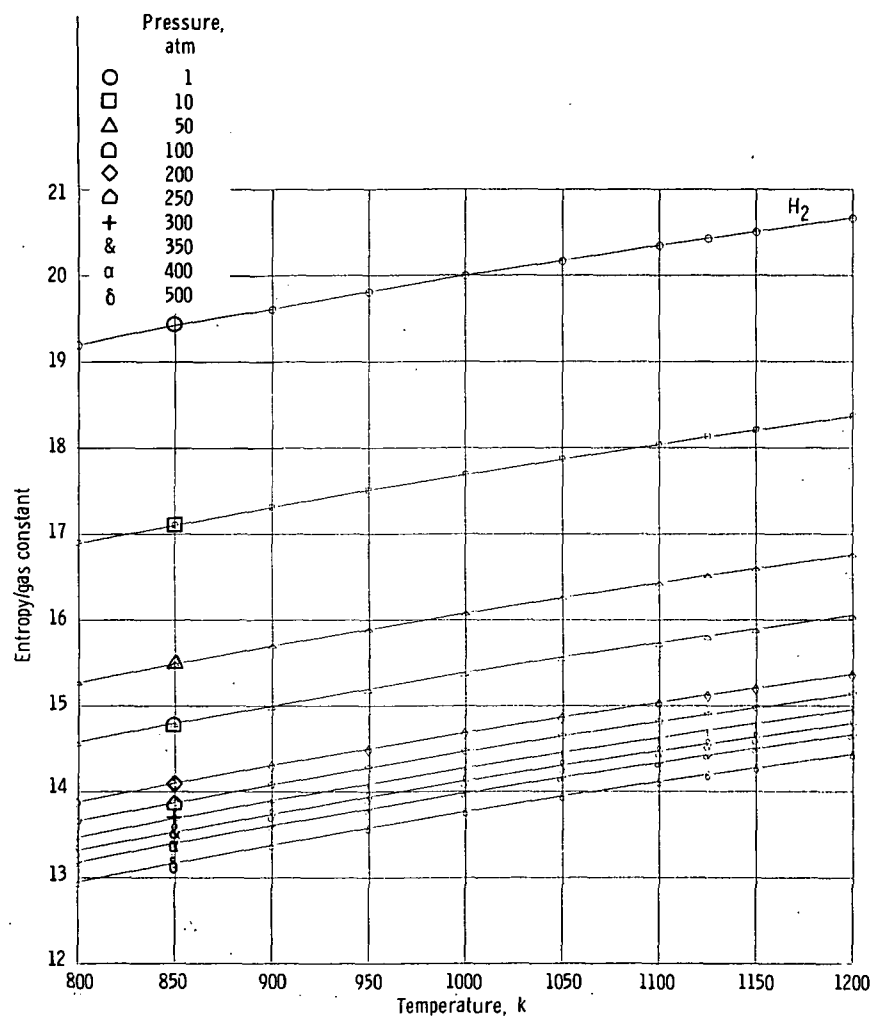
Figure 18. - Entropy/gas constant versus temperature.
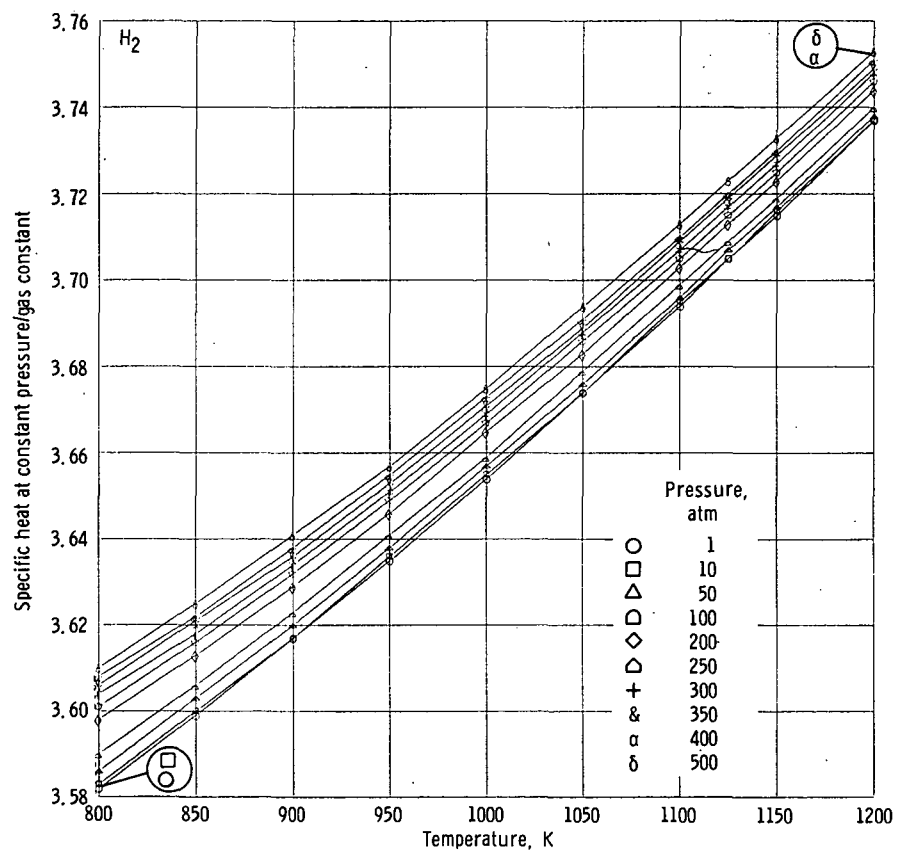
Figure 19. - Specific heat at constant pressure/gas constant versus temperature.
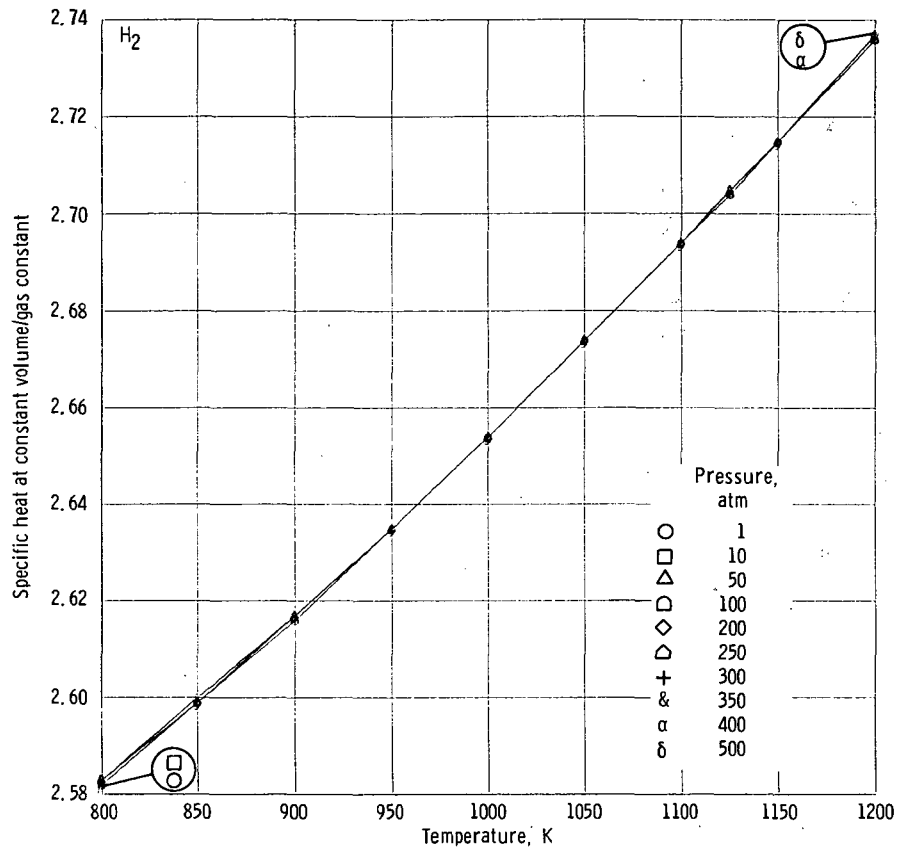
Figure 20. - Specific heat at constant volume/gas constant versus temperature.
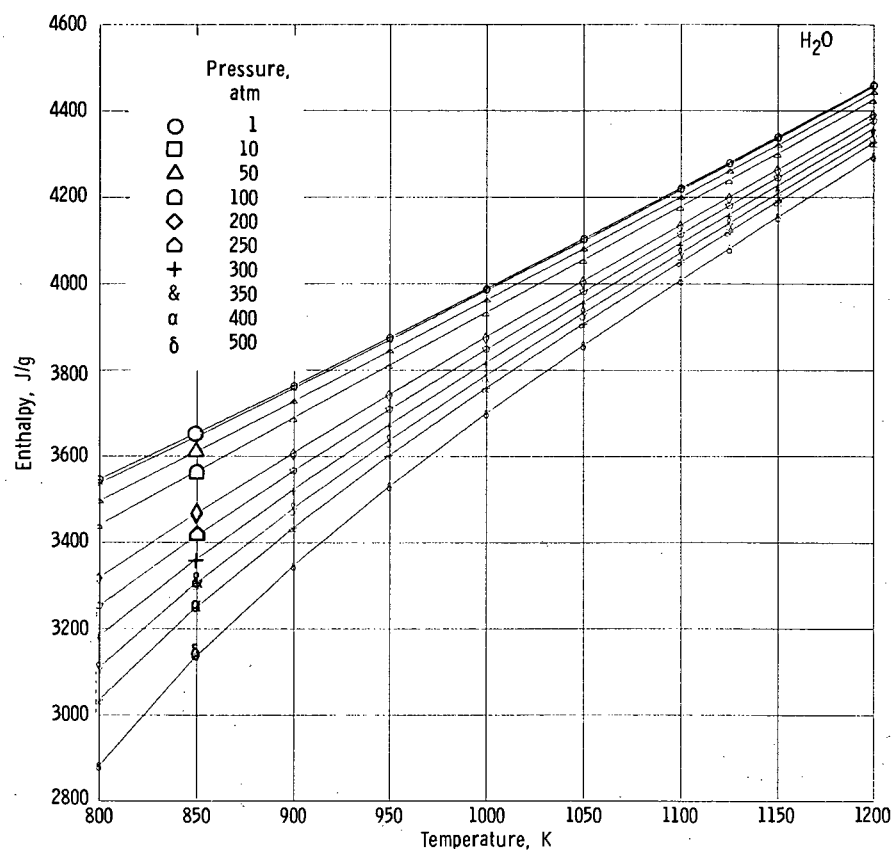
Figure 21. - Enthalpy versus temperature.
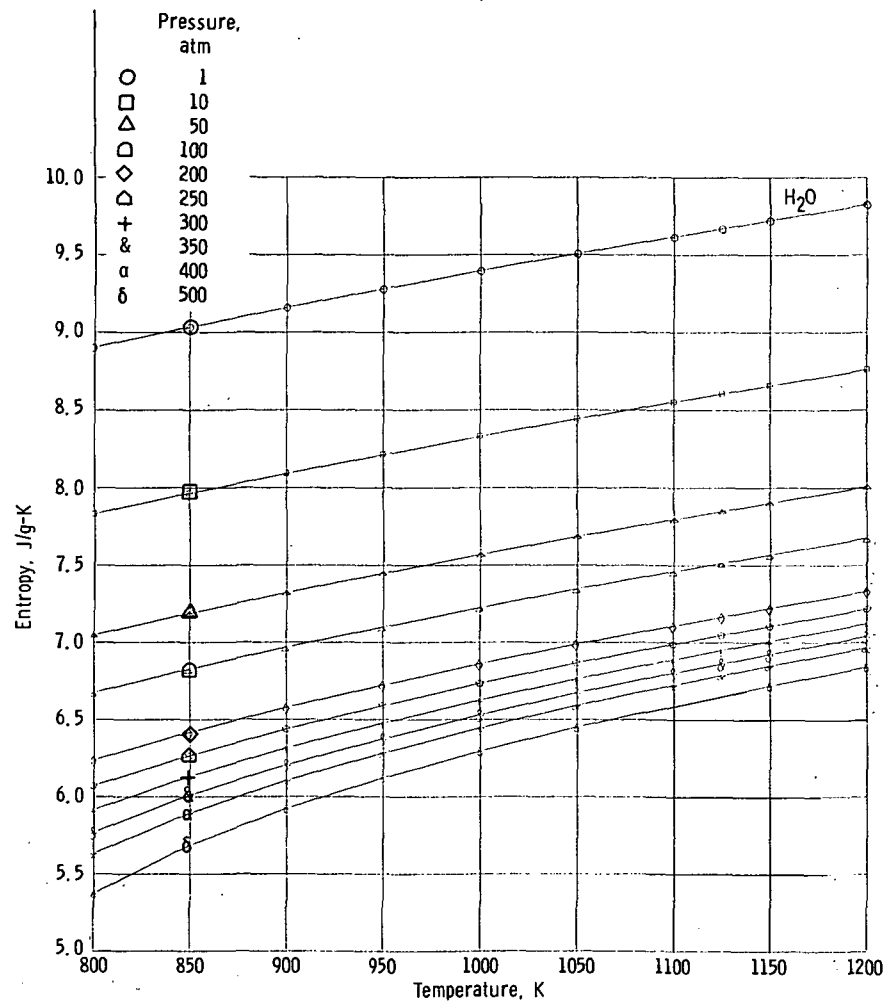
Figure 22. - Entropy versus temperature
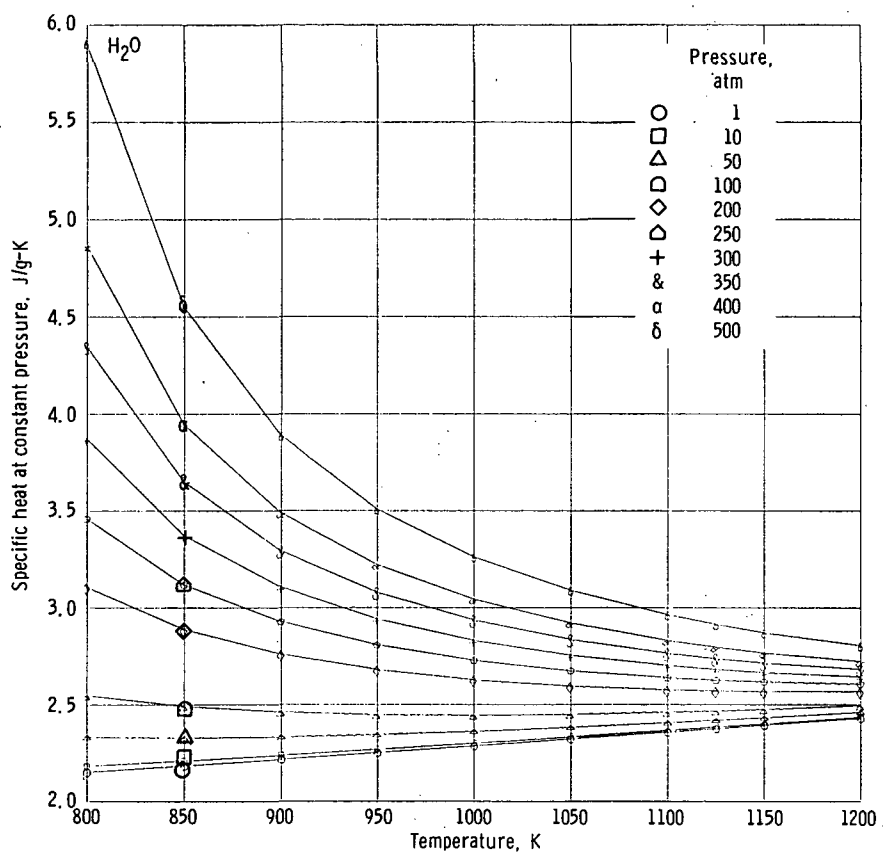
Figure 23. – Specific heat at constant pressure versus temperature.
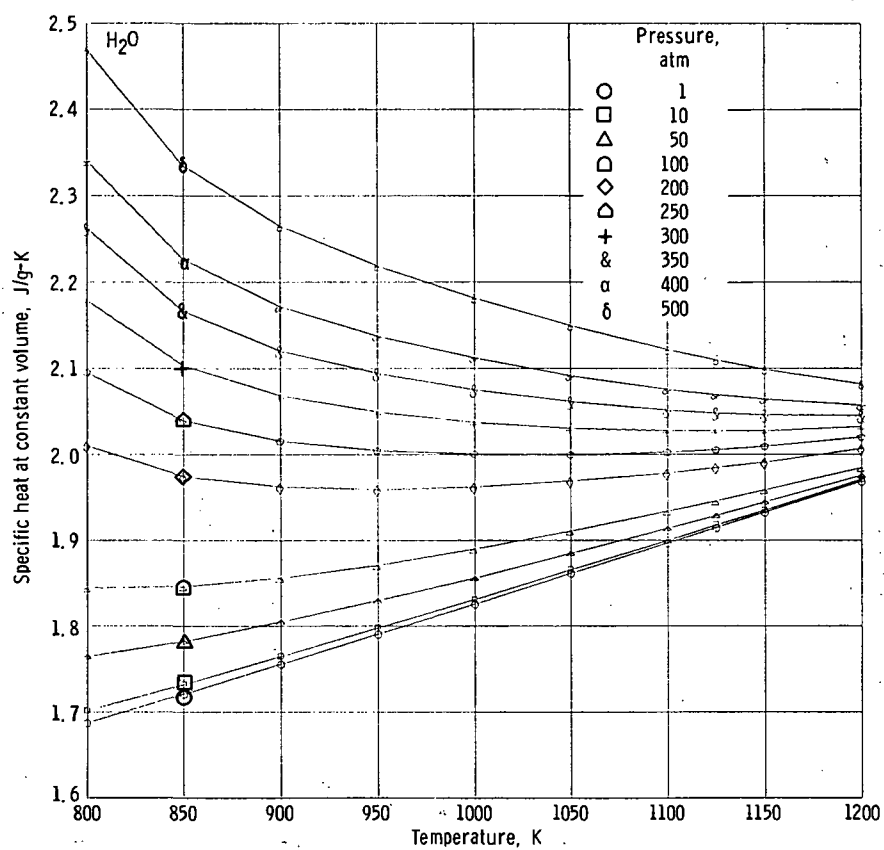
Figure 24. - Specific heat at constant volume versus temperature.

Partial derivative of pressure with respect to density at constant temperature, atm - cc/g

H₂O — H_2O

5500

5000

4500

4000

3500

3000

2500

2000

1500

1000

800   850   900   950   1000   1000   1050   1100   1150

Temperature, K

Pressure,
atm

○	1
□	10
△	50
◠	100
◇	200
△	250
+	300
&	350
α	400
δ	500
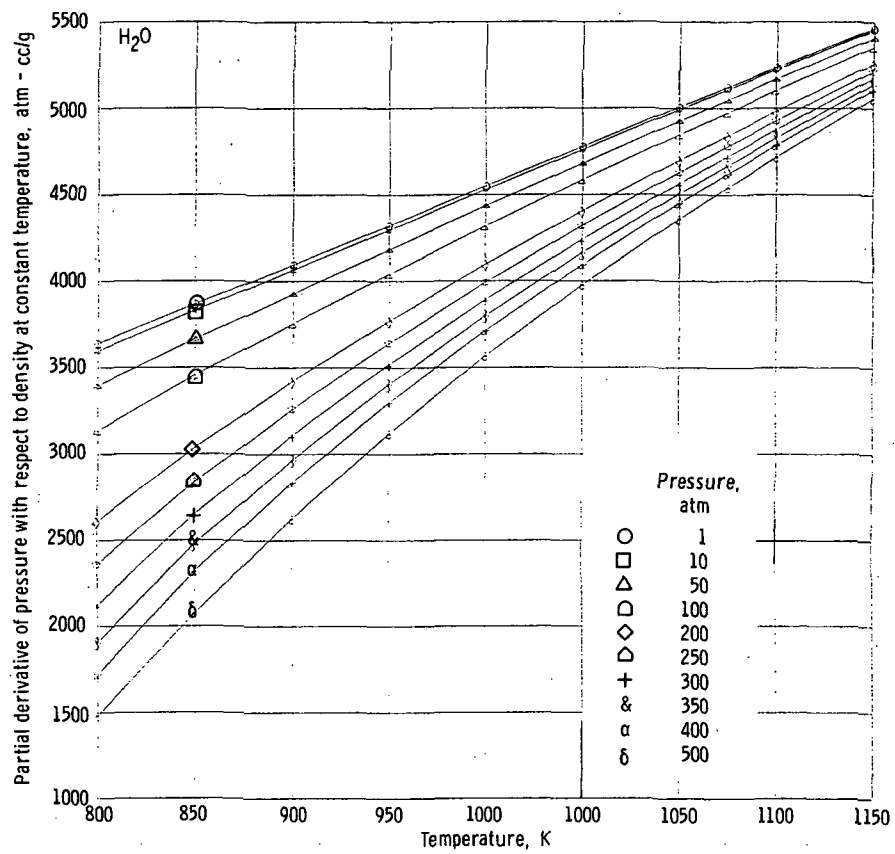
Figure 25. – Partial derivative of pressure with respect to density at constant temperature versus temperature.

Figure 26. - Molecular viscosity versus temperature.

Figure 27. – Density versus temperature.
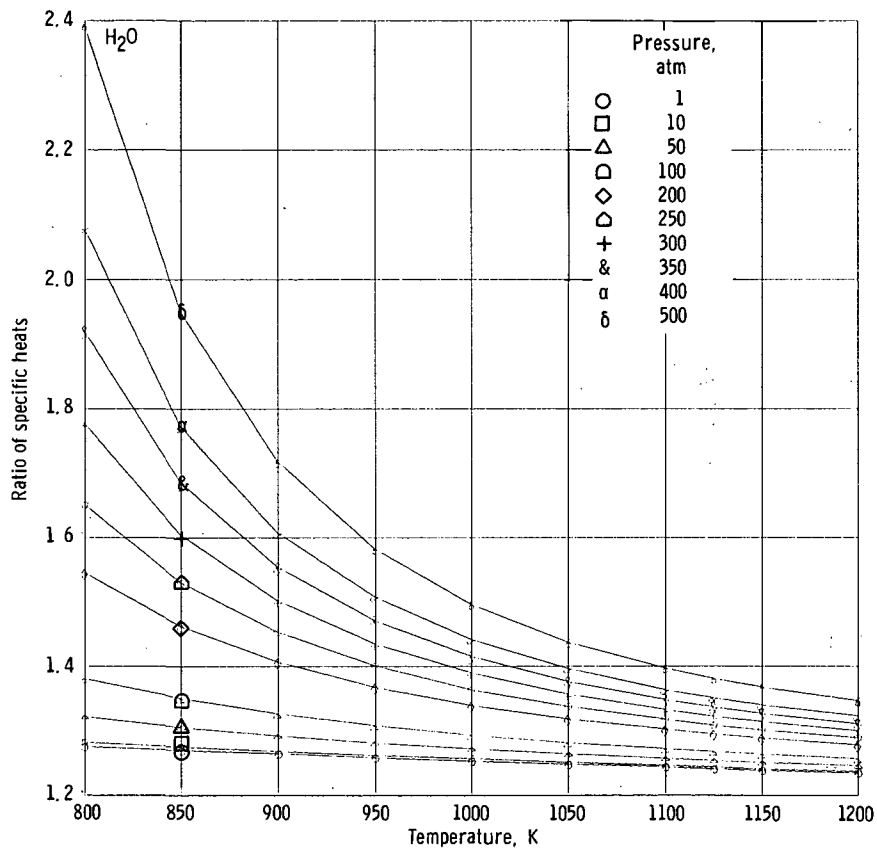
Figure 28. – Ratio of specific heats versus temperature.

Figure 29. - Real sound speed squared versus temperature.
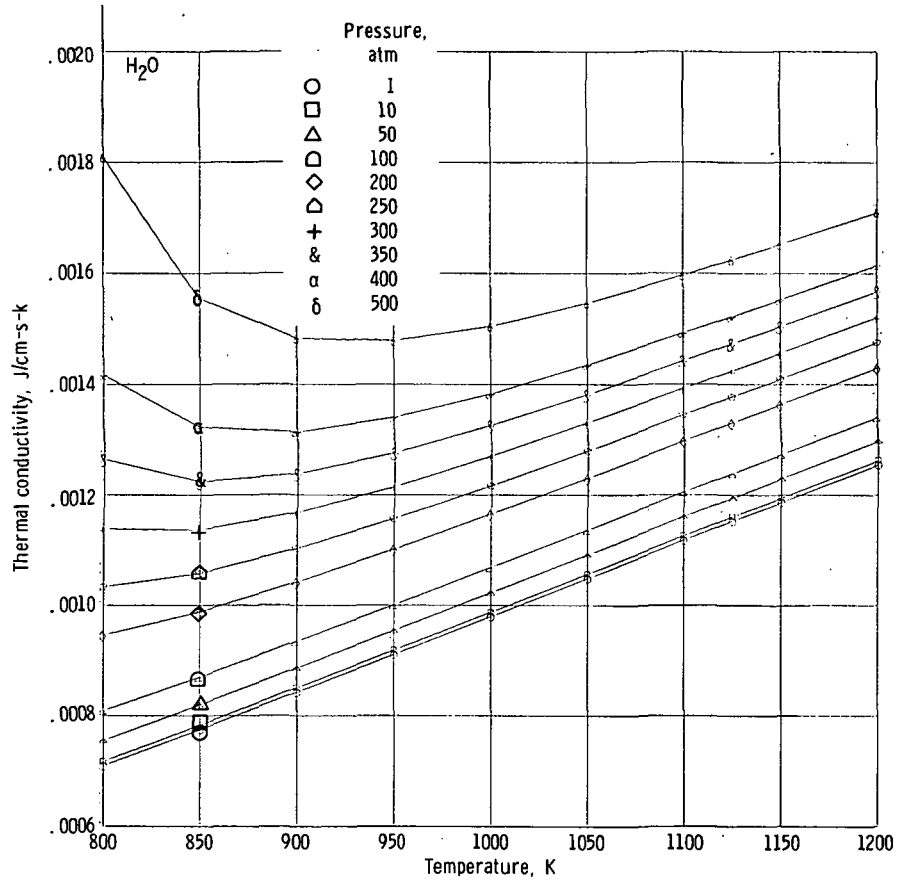
Figure 30. - Thermal conductivity versus temperature.
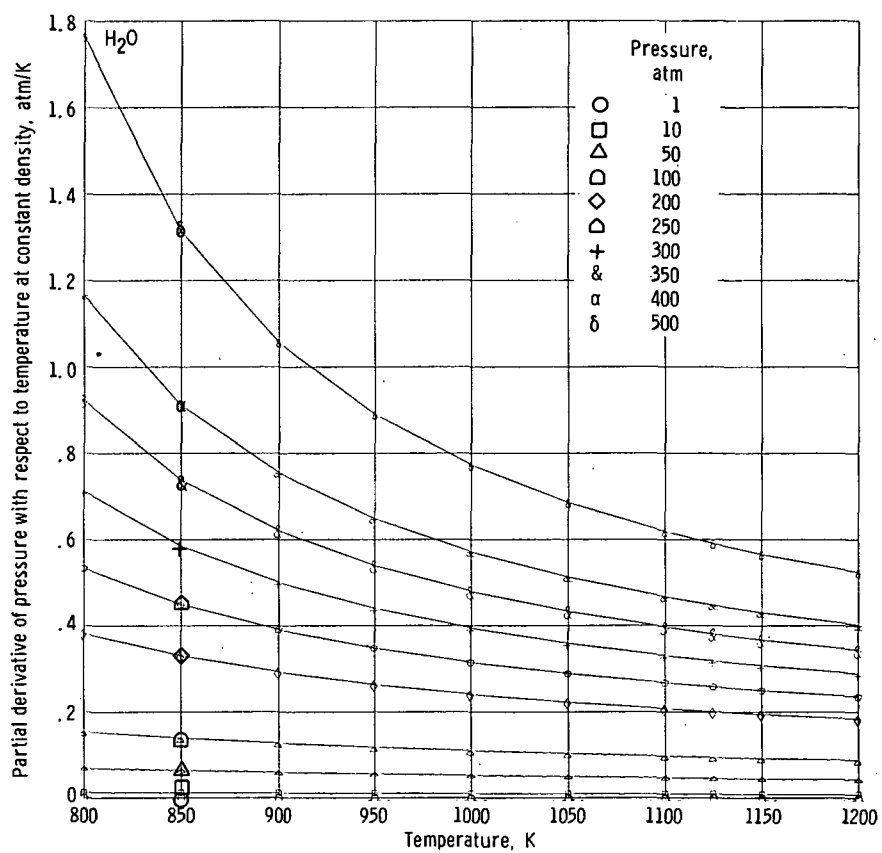
Figure 31. – Partial derivative of pressure with respect to temperature at constant density versus temperature.
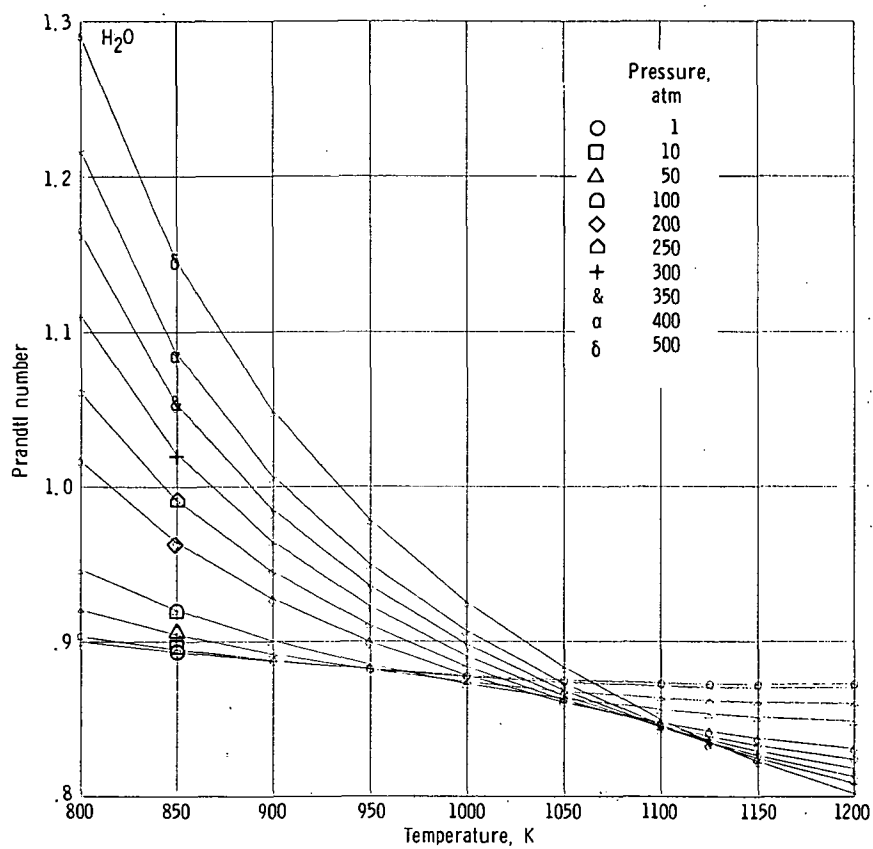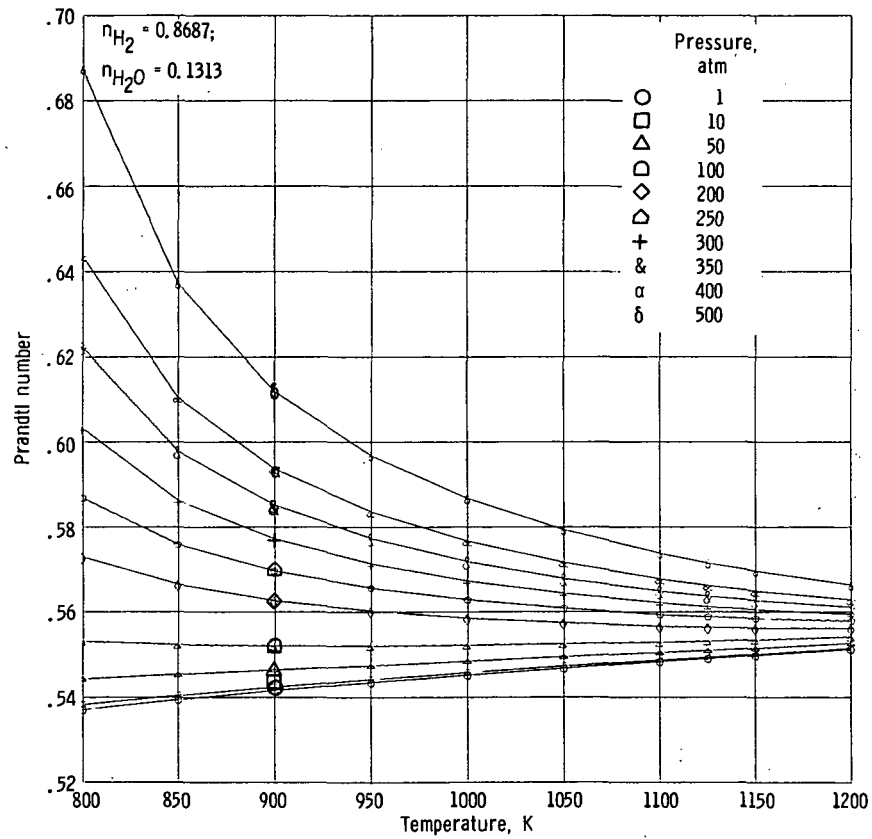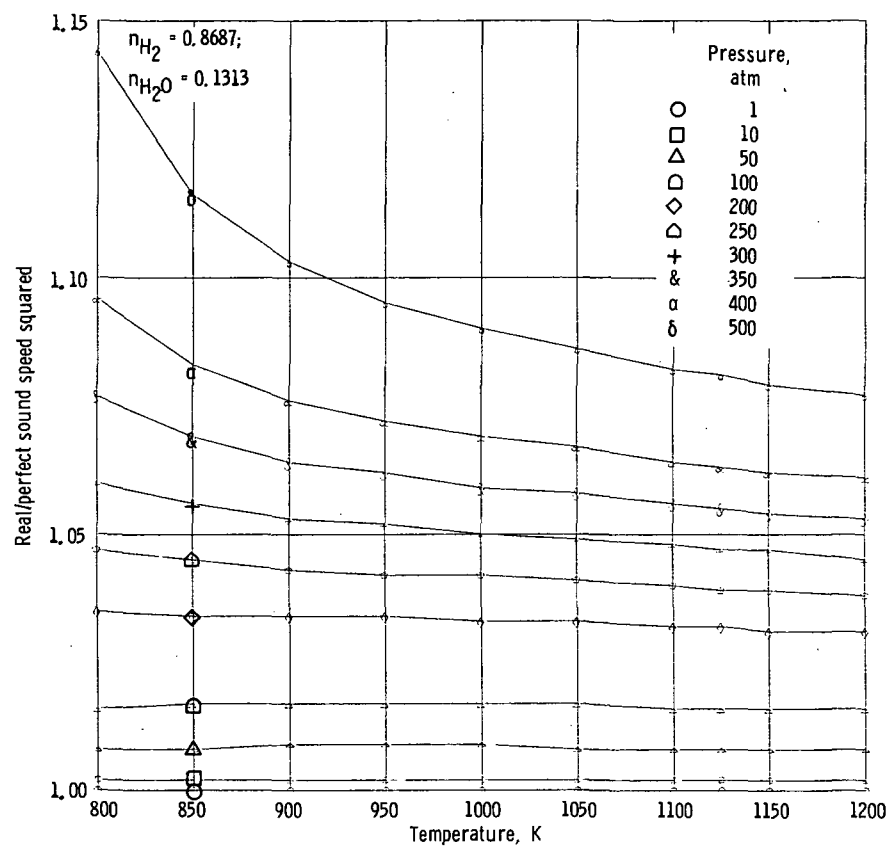
Figure 32. - Prandtl number versus temperature.
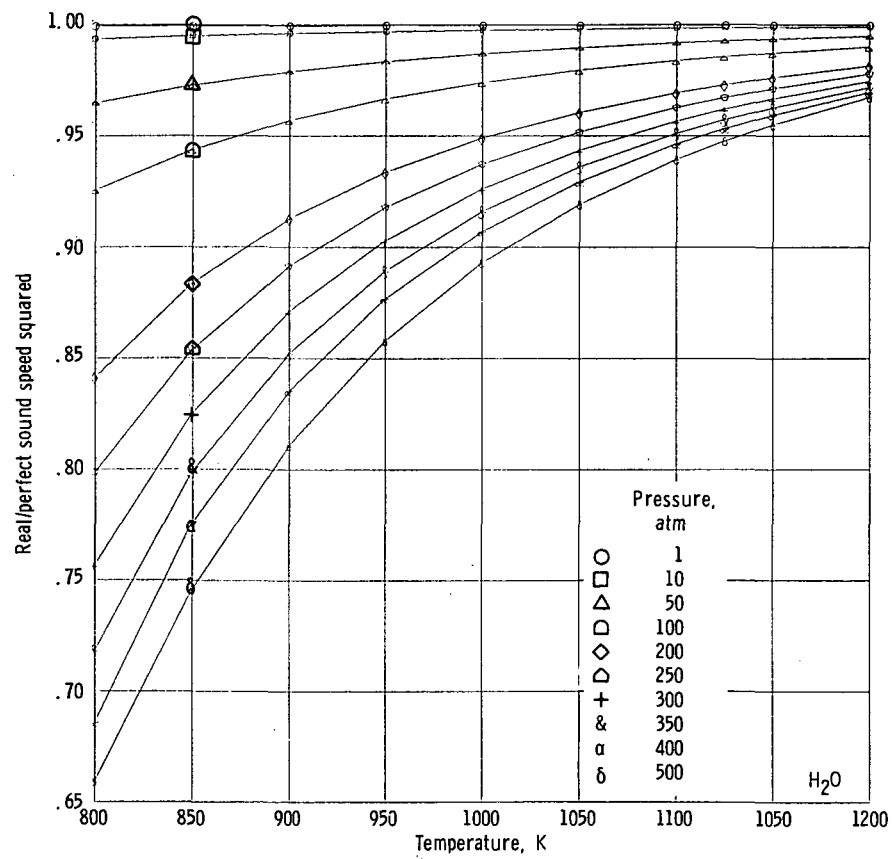
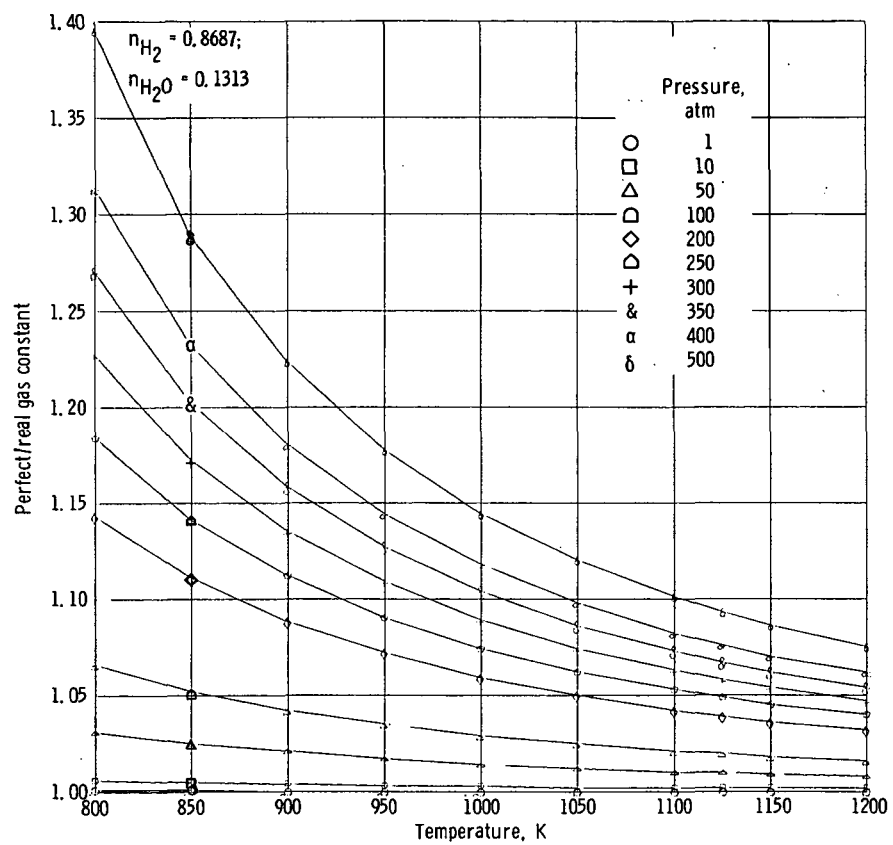Figure 33. - Real/perfect sound speed squared versus temperature.
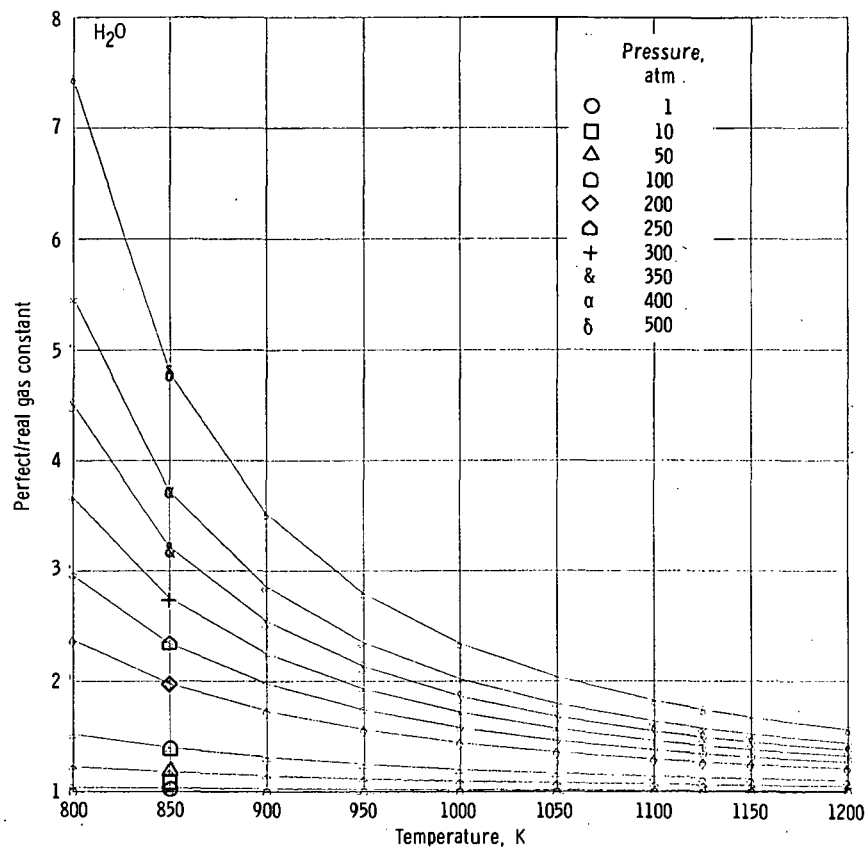
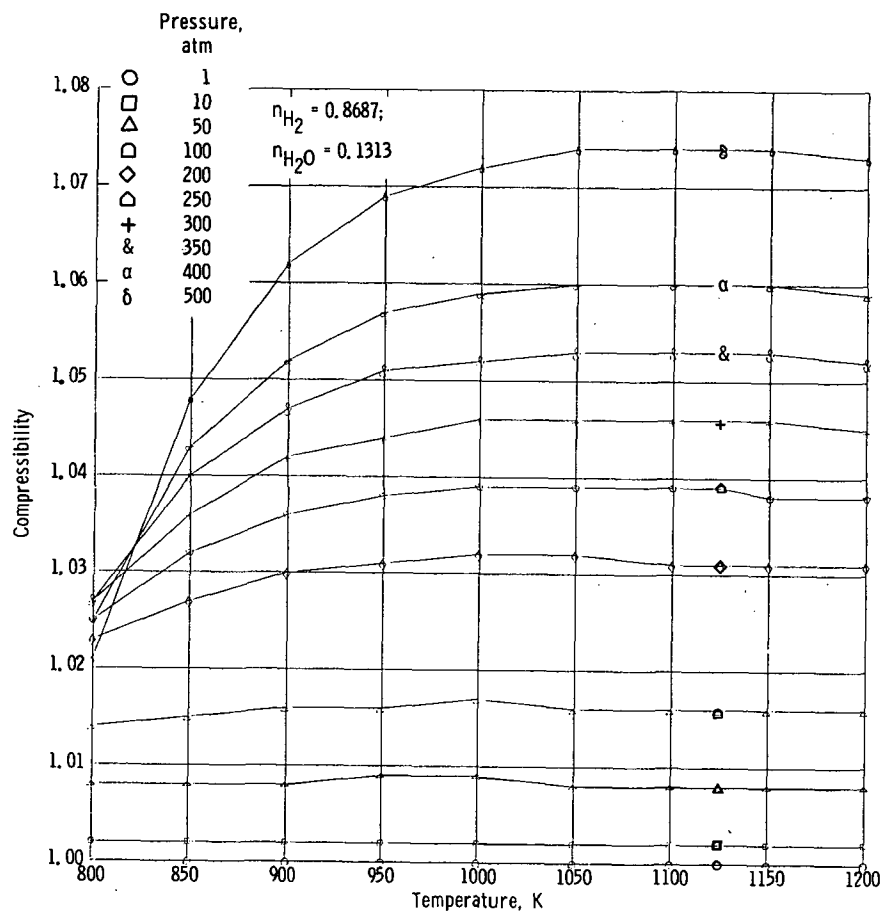Figure 34. - Perfect/real gas constant versus temperature.
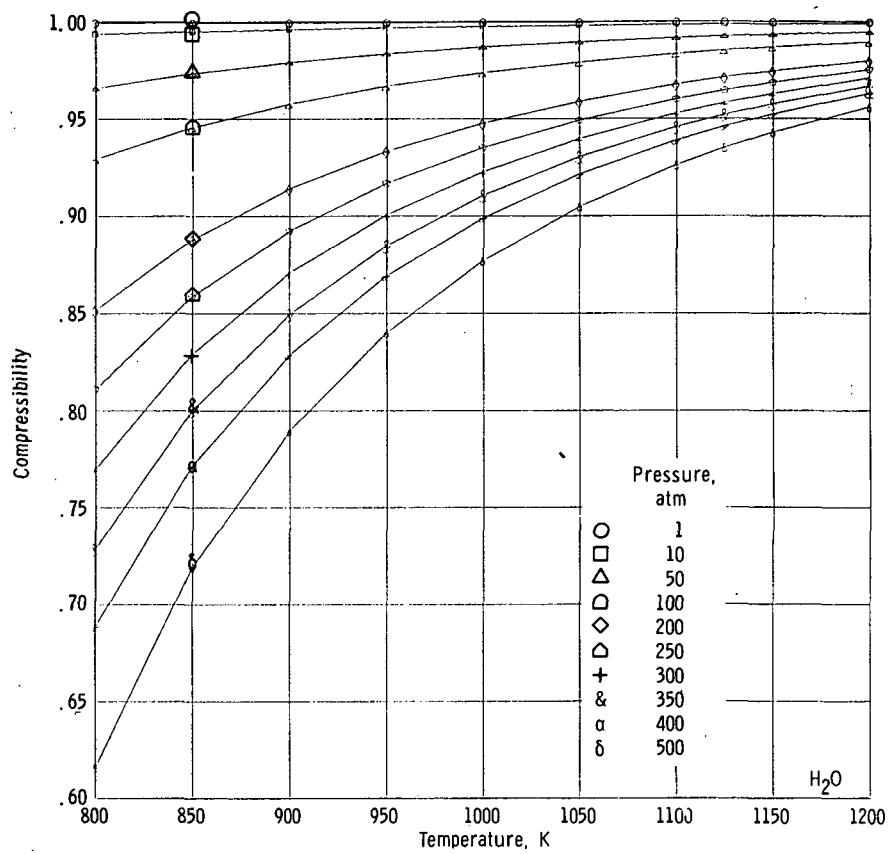
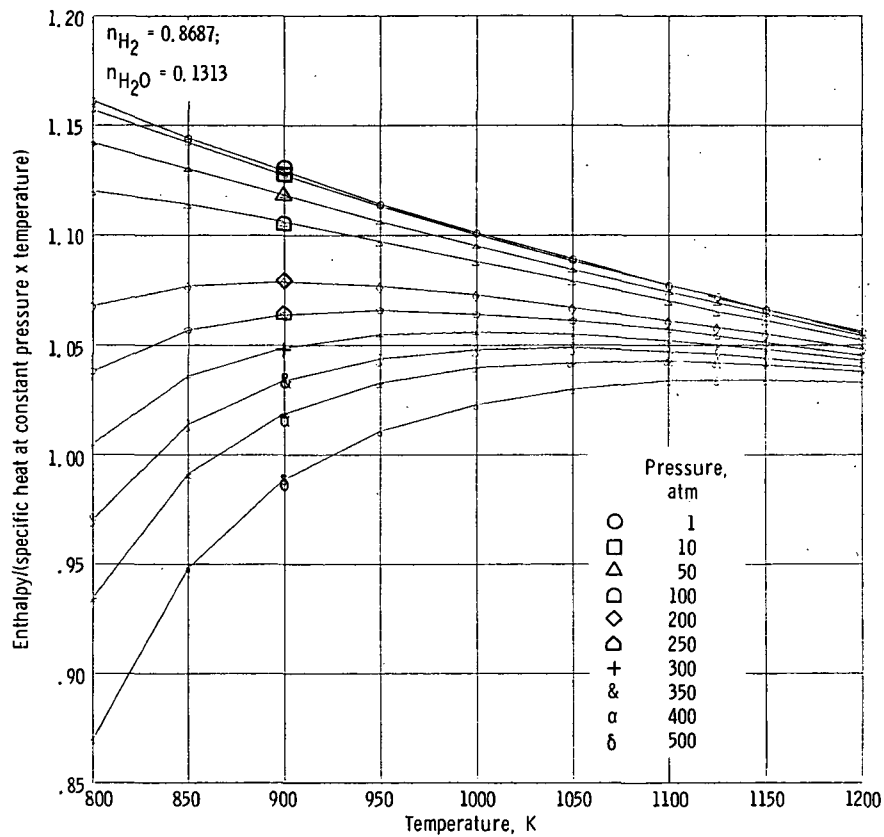Figure 35. – Compressibility versus temperature.
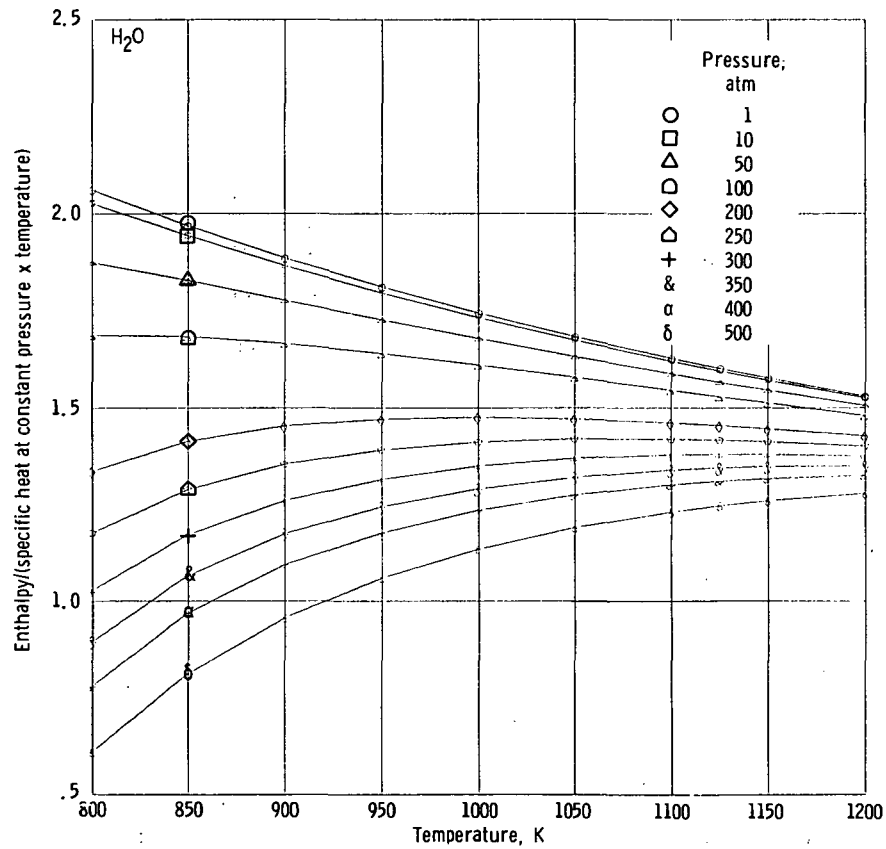
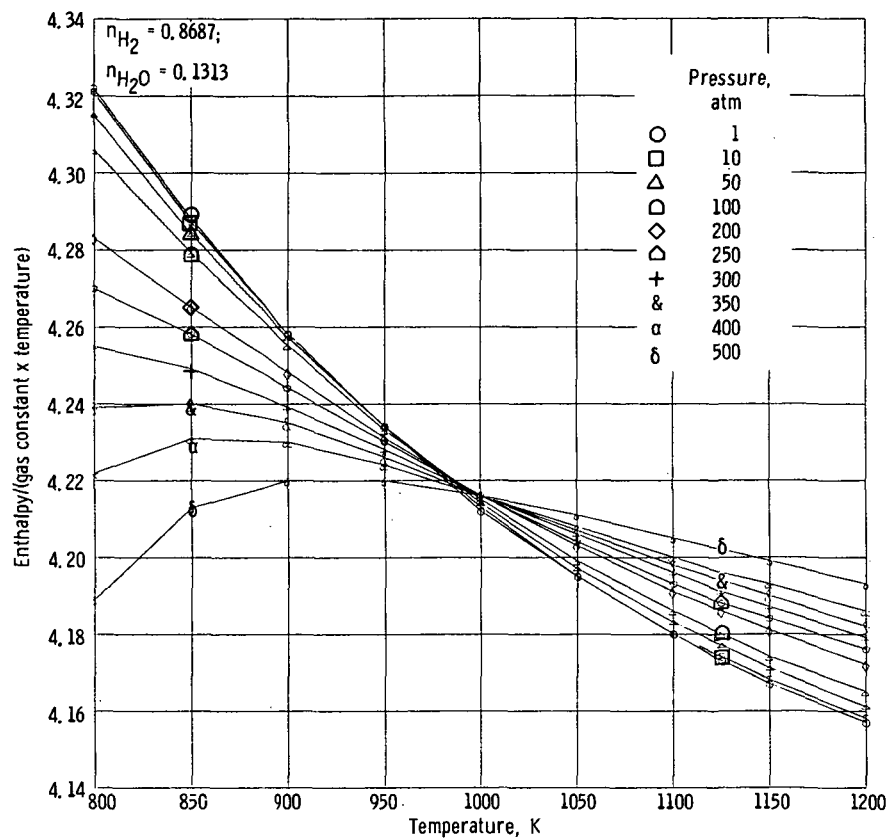Figure 36. — Enthalpy/(specific heat at constant pressure x temperature) versus temperature.
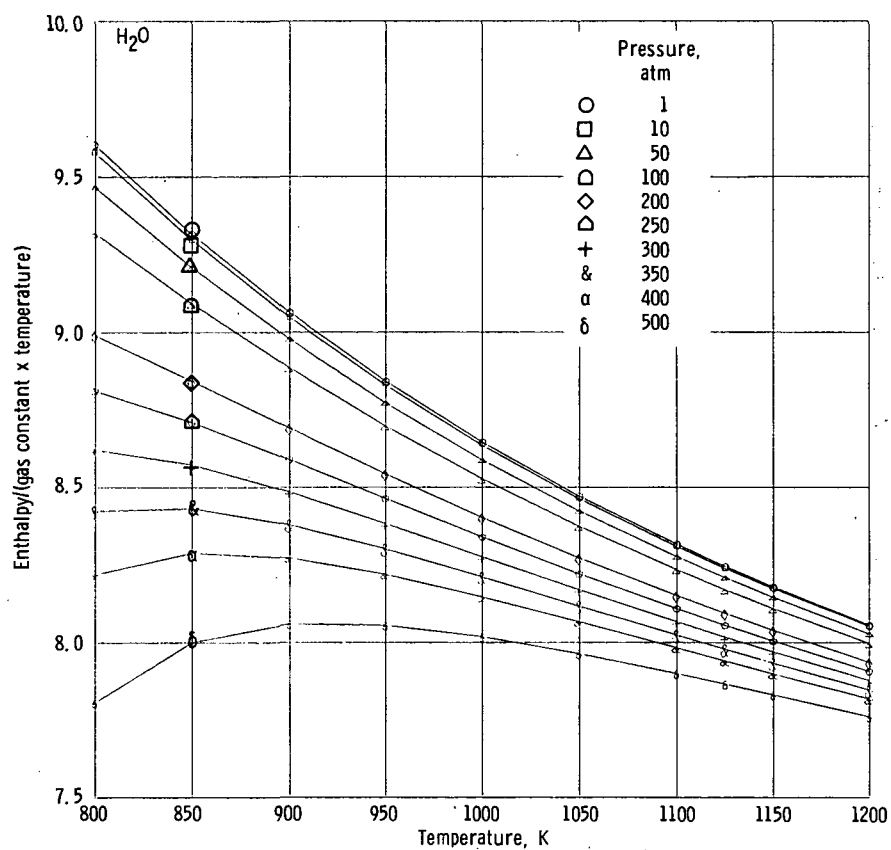
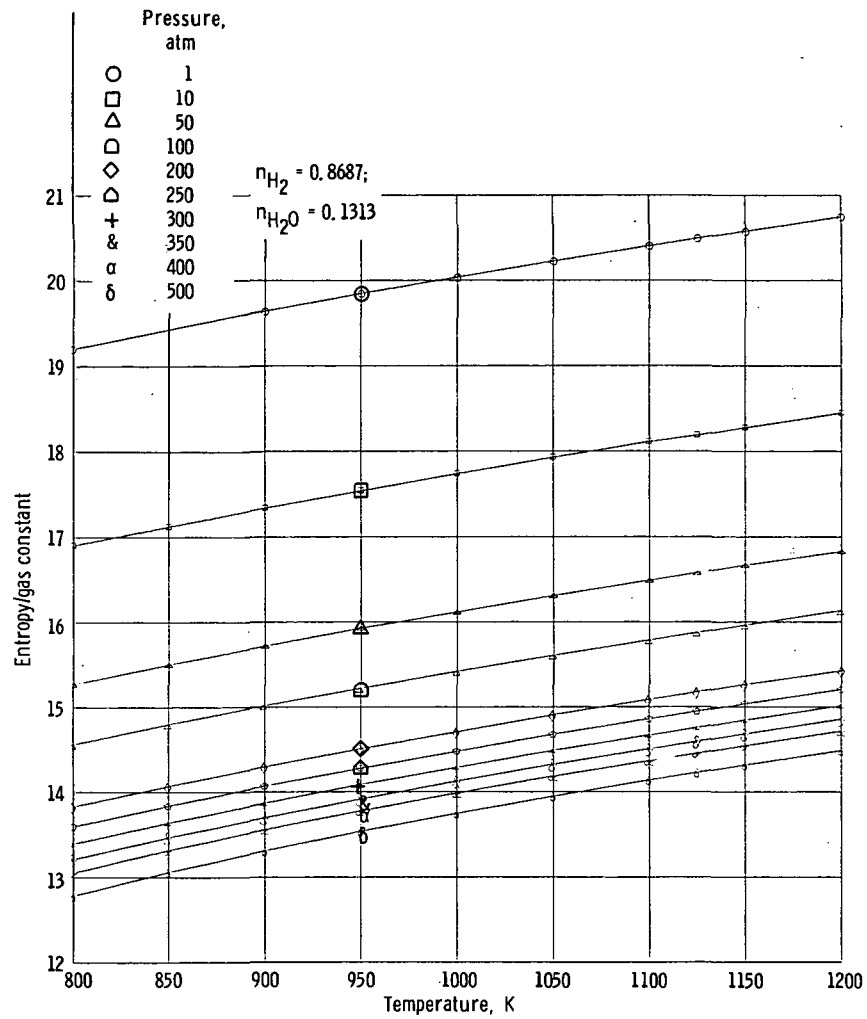Figure 37. – Enthalpy/(gas constant x temperature) versus temperature.
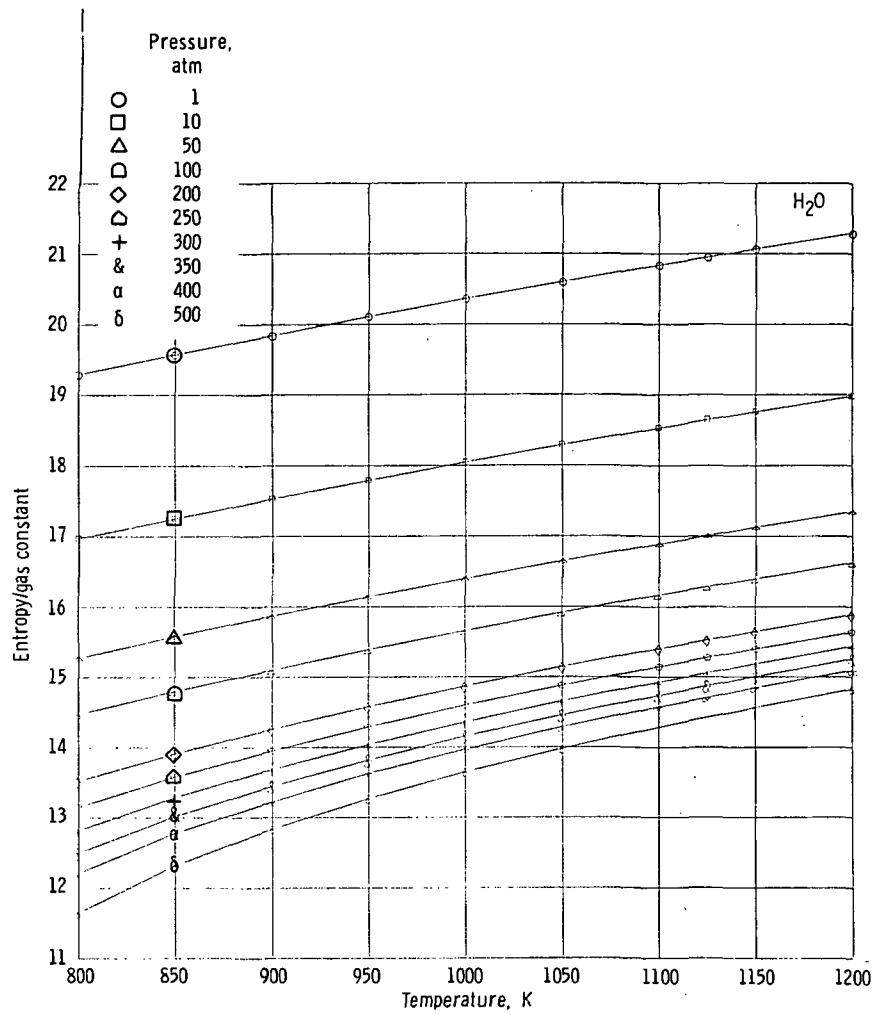
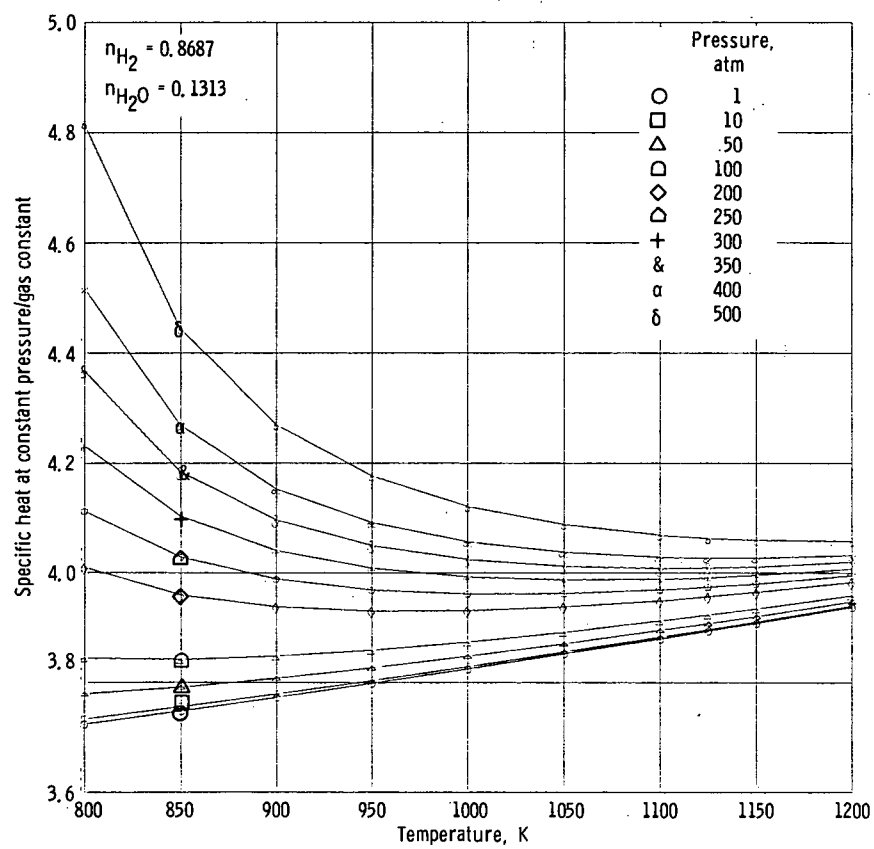Figure 38. – Entropy/gas constant versus temperature.
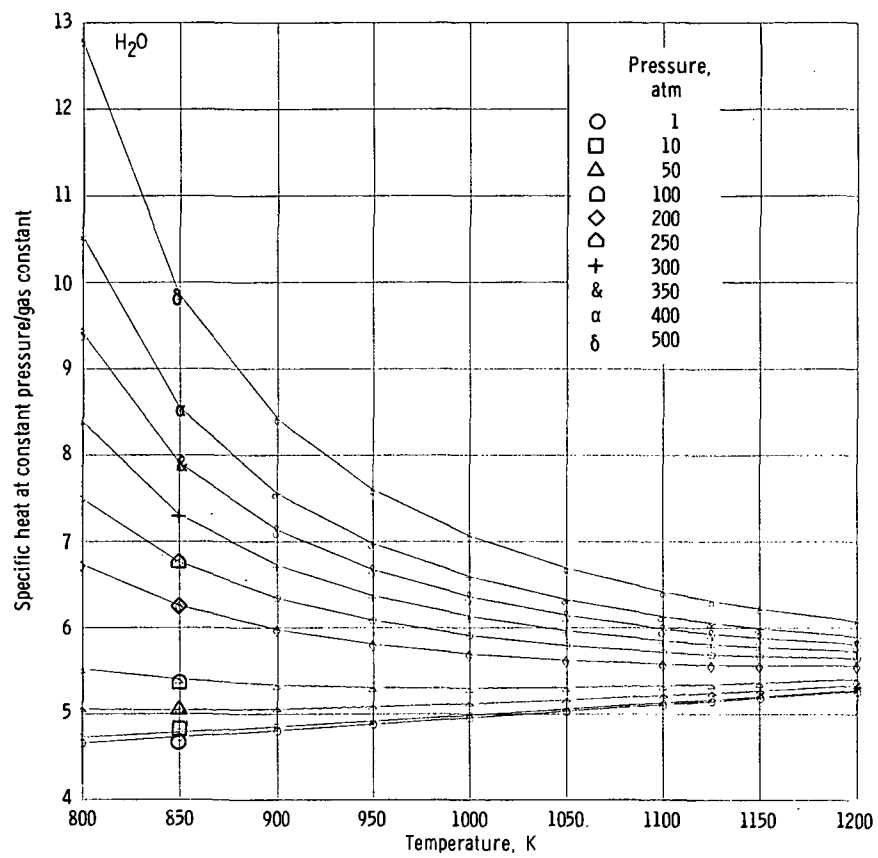
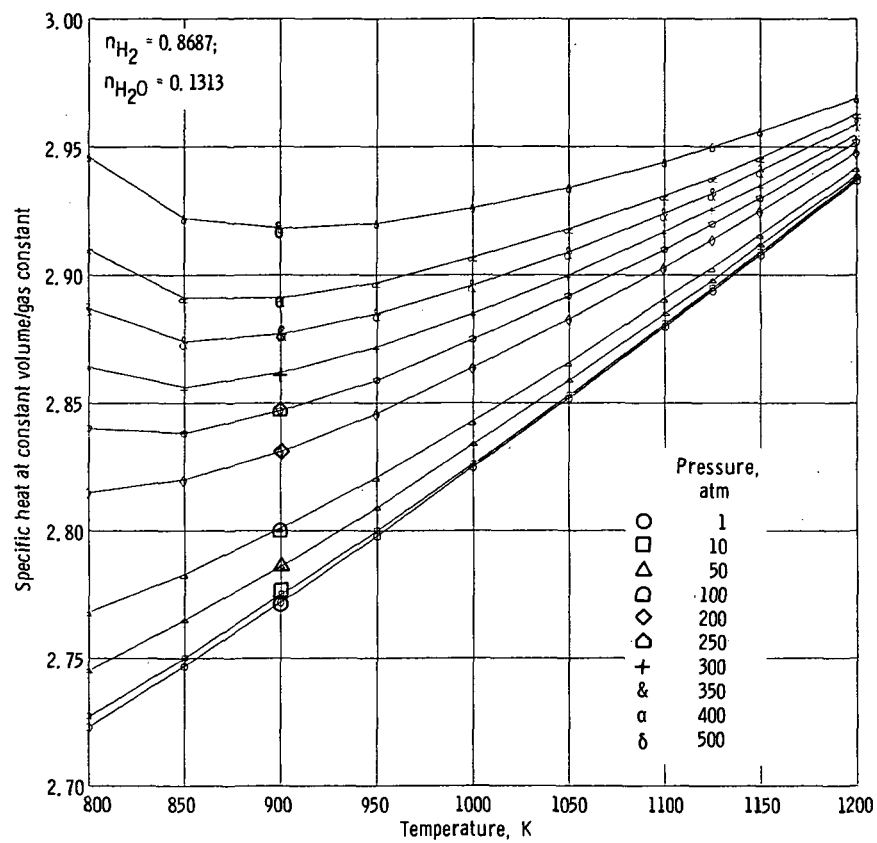Figure 39. – Specific heat at constant pressure/gas constant versus temperature.

Figure 40. – Specific heat at constant volume/gas constant versus temperature.
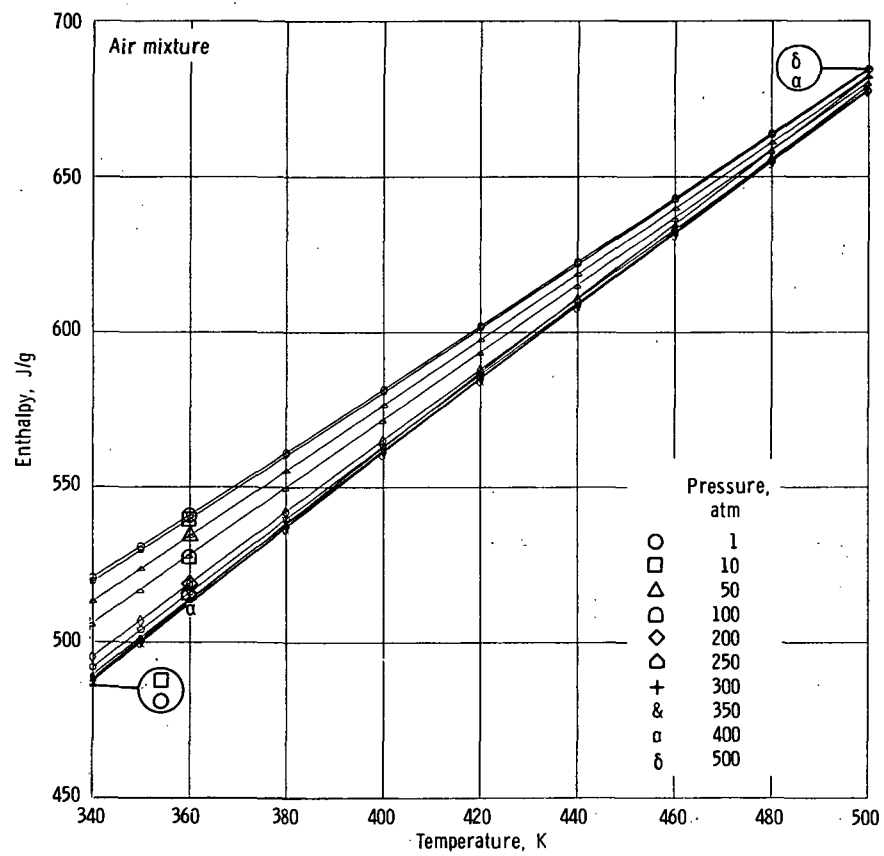
Figure 41. – Enthalpy versus temperature.
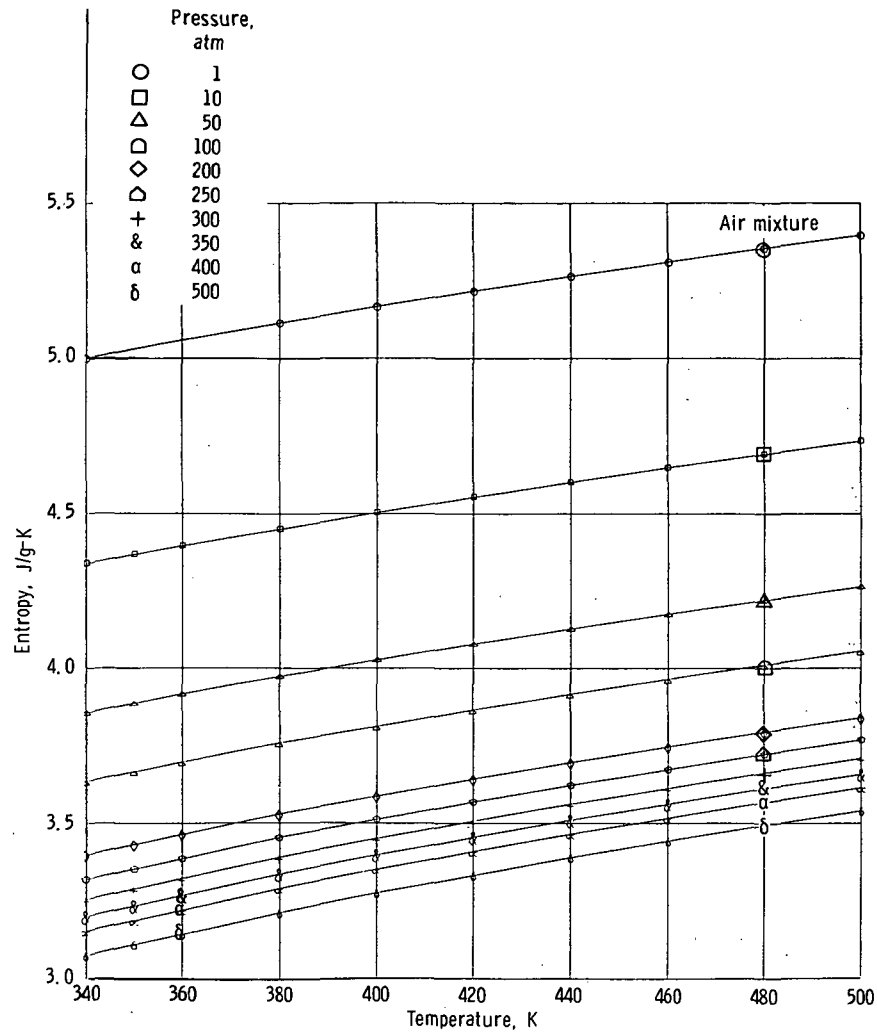
Figure 42. - Entropy versus temperature.

Figure 43. - Specific heat at constant pressure versus temperature.

Figure 44. - Specific heat at constant volume versus temperature.

Figure 45. – Partial derivative of pressure with respect to density at constant temperature versus temperature.

Figure 46. - Molecular viscosity versus temperature.

Figure 47. – Density versus temperature.
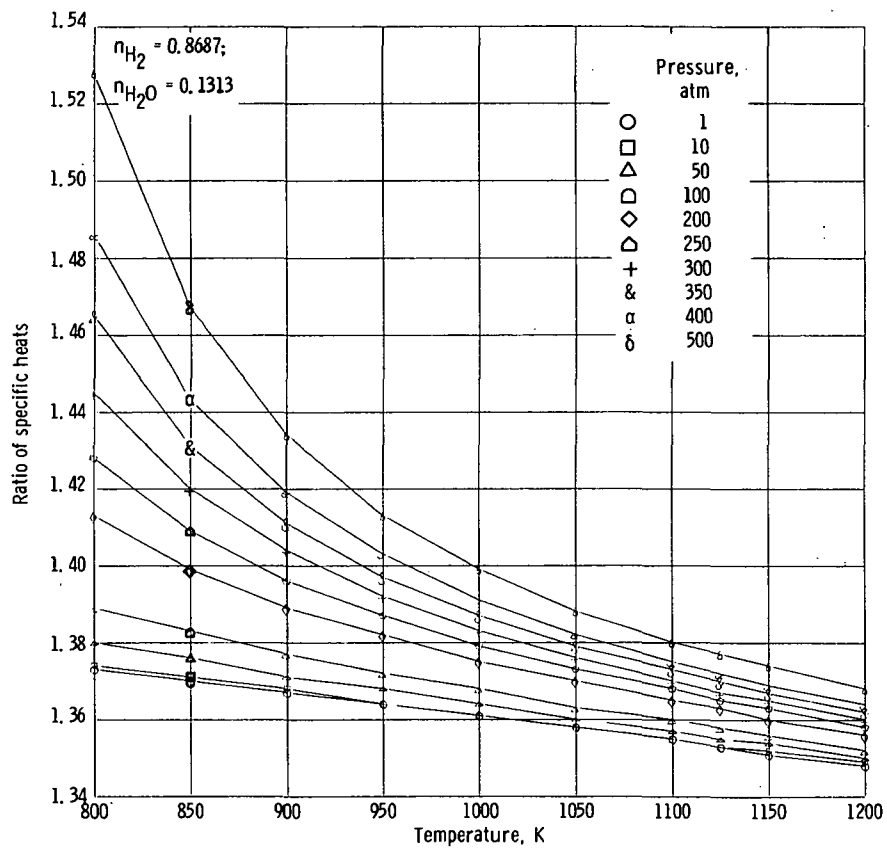
Figure 48. - Ratio of specific heats versus temperature.
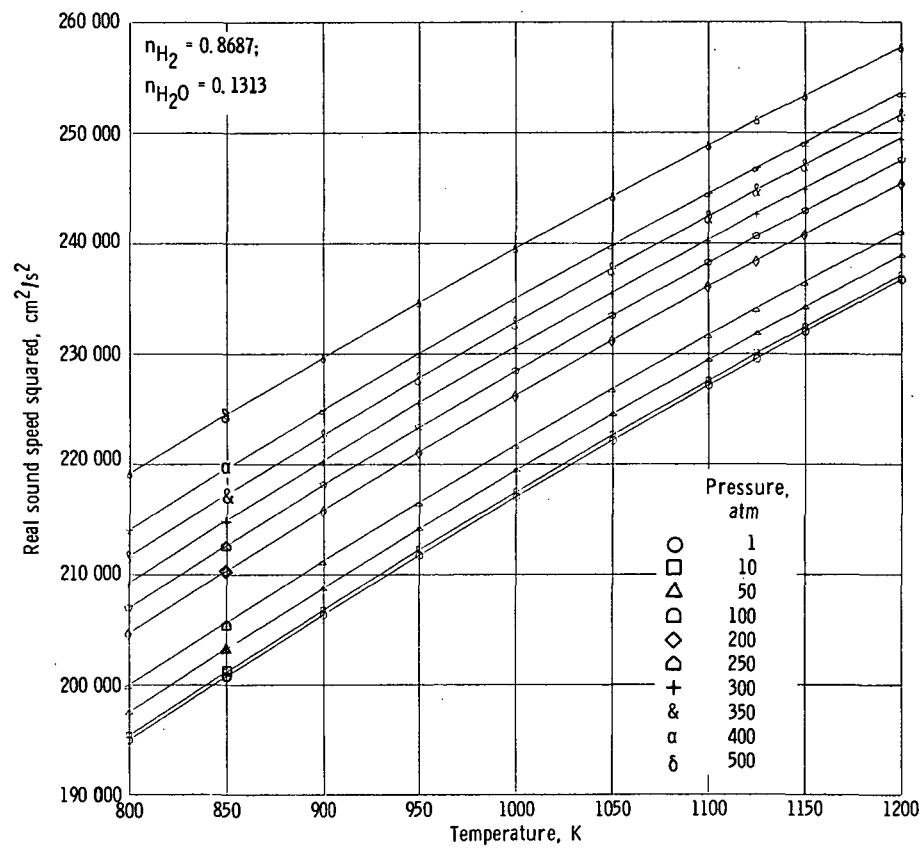
Figure 49. - Real sound speed squared versus temperature.
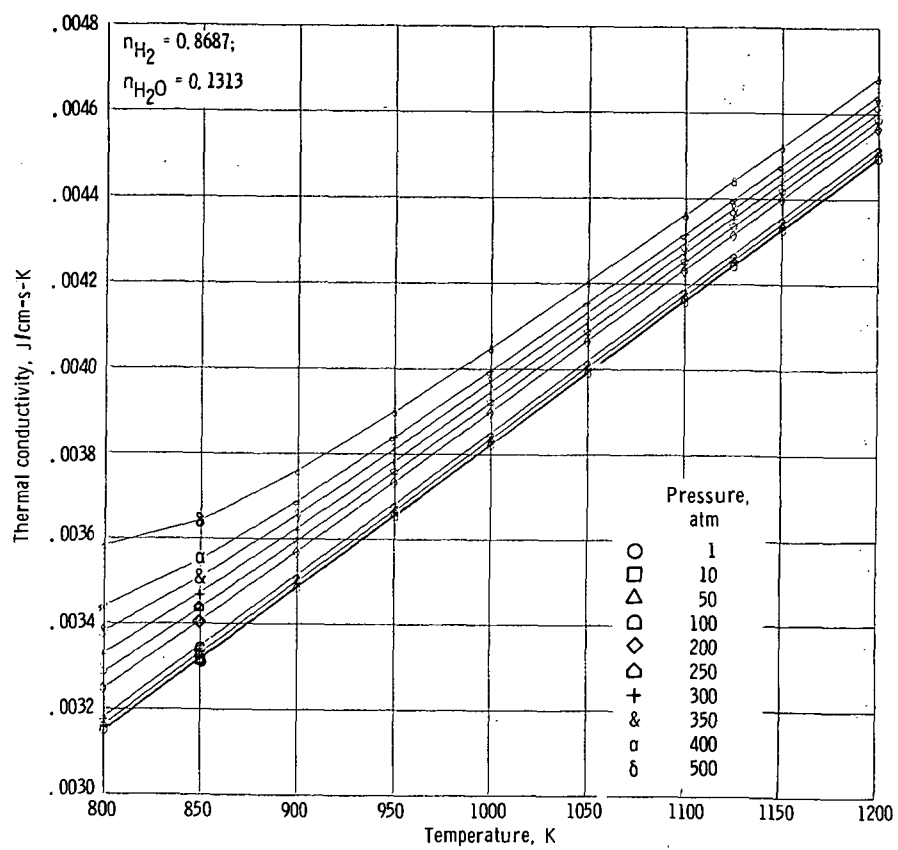
Figure 50. - Thermal conductivity versus temperature.
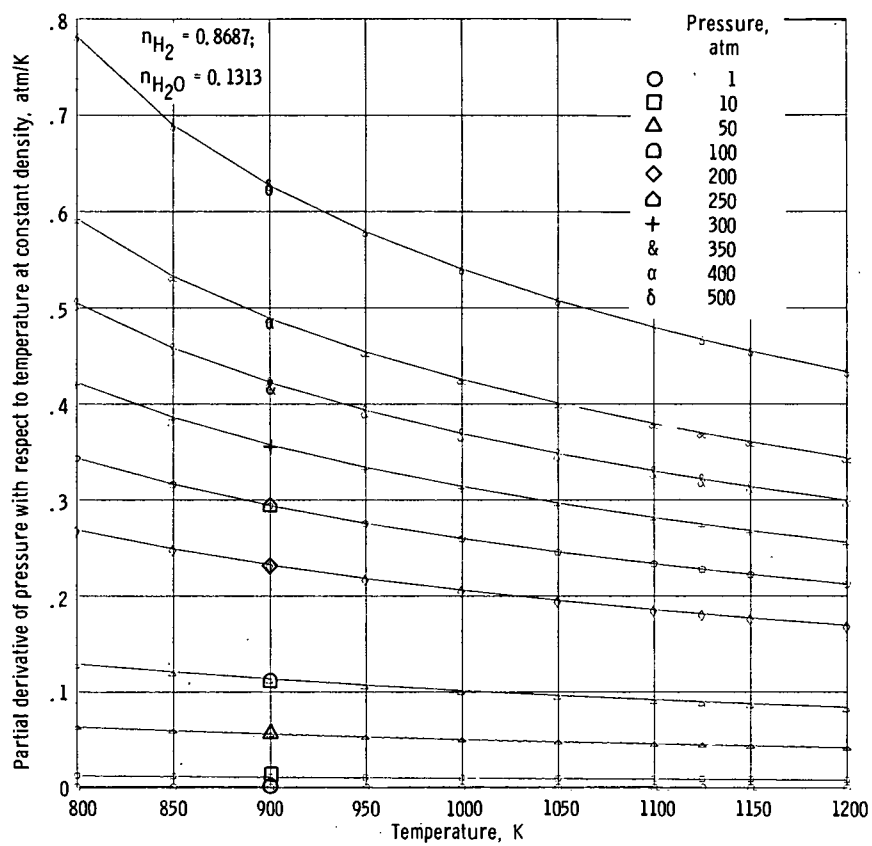
Figure 51. – Partial derivative of pressure with respect to temperature at constant density versus temperature.

Figure 52. - Prandtl number versus temperature.

Figure 53. – Real/perfect sound speed squared versus temperature.

Figure 54. - Perfect/real gas constant versus temperature.

Figure 55. - Compressibility versus temperature.

Figure 56. - Enthalpy/(specific heat at constant pressure x temperature) versus temperature.

Figure 57. - Enthalpy/(gas constant x temperature) versus temperature.

Figure 58. - Entropy/gas constant versus temperature.

Figure 59. – Specific heat at constant pressure/gas constant temperature.

Figure 60. - Specific heat at constant volume/gas constant versus temperature.

Figure 61. - Enthalpy versus temperature.

Figure 62. - Entropy versus temperature.
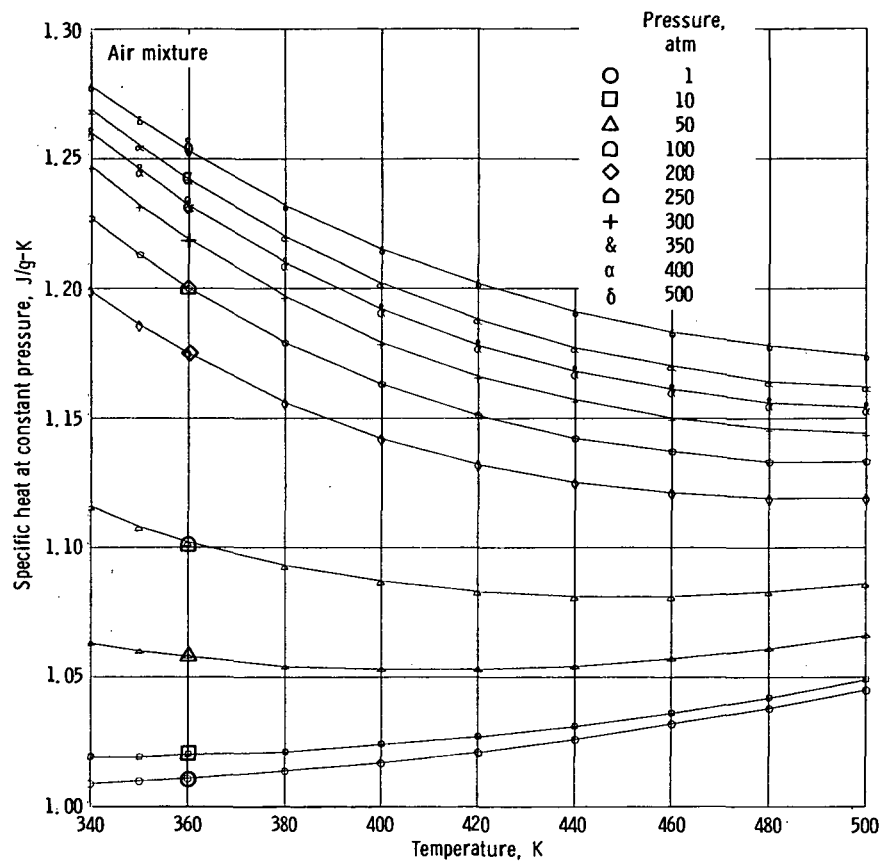
Figure 63. – Specific heat at constant pressure versus temperature.

Specific heat at constant pressure, J/g-K (y-axis)

Temperature, K (x-axis)

Air mixture

Pressure, atm

Symbol	Pressure, atm
○	1
□	10
△	50
◁	100
◇	200
◁	250
+	300
&	350
α	400
δ	500

y-axis values: 1.00, 1.05, 1.10, 1.15, 1.20, 1.25, 1.30

x-axis values: 340, 360, 380, 400, 420, 440, 460, 480, 500

Figure 63. – Specific heat at constant pressure versus temperature.
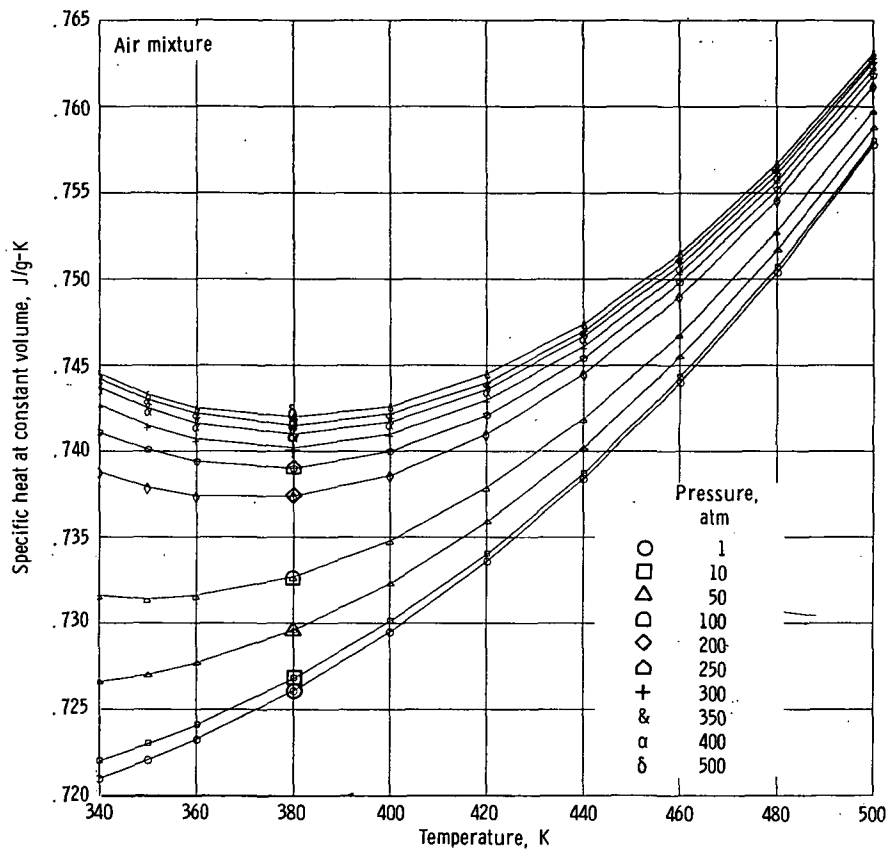
Figure 64. - Specific heat at constant volume versus temperature.
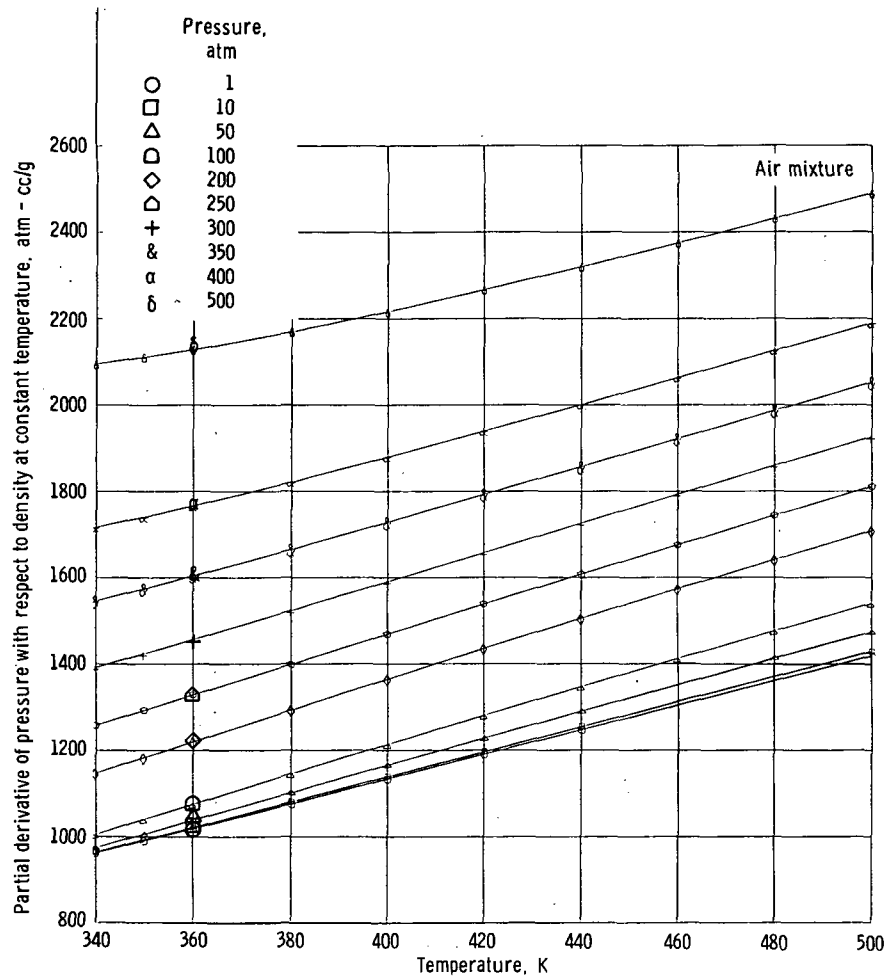
Figure 65. - Partial derivative of pressure with respect to density at constant temperature versus temperature.
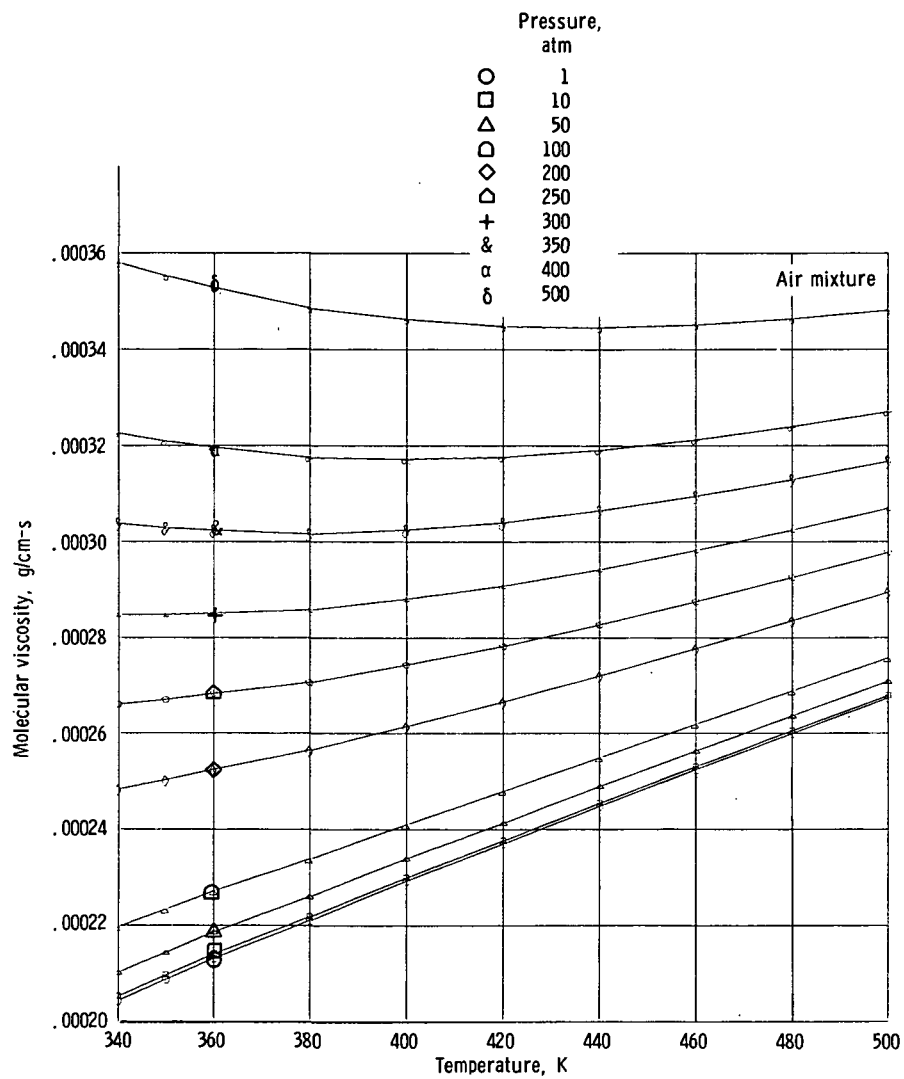
Figure 66. – Molecular viscosity versus temperature.
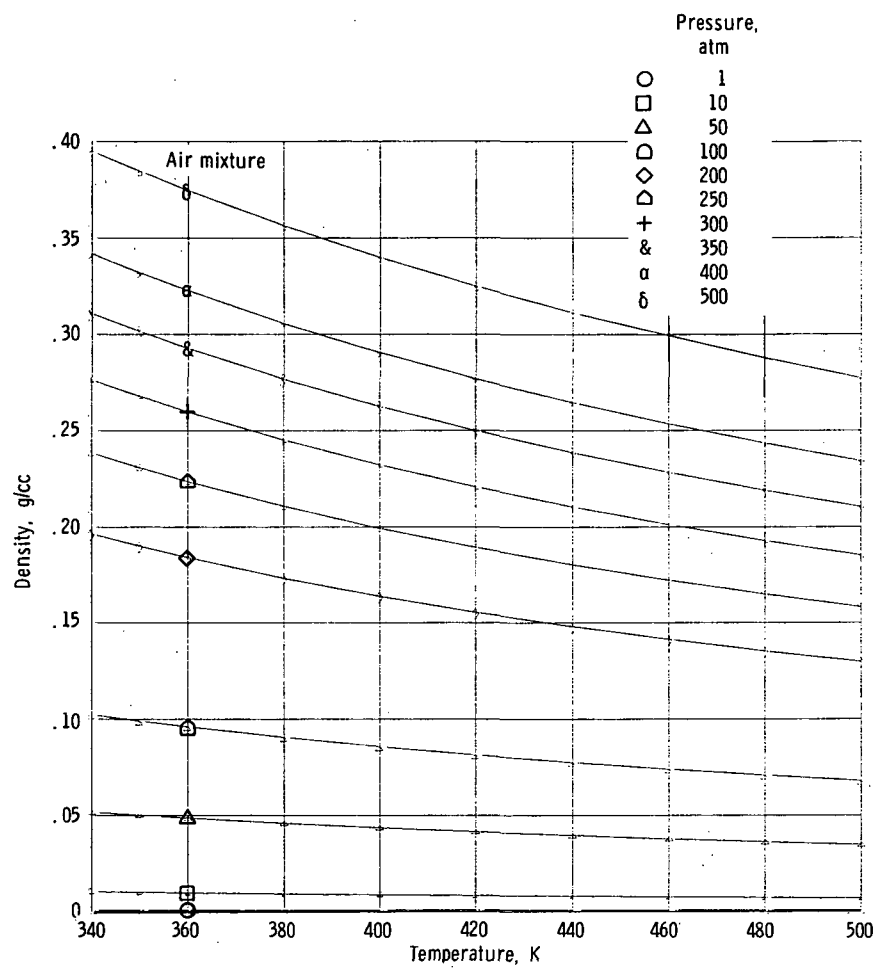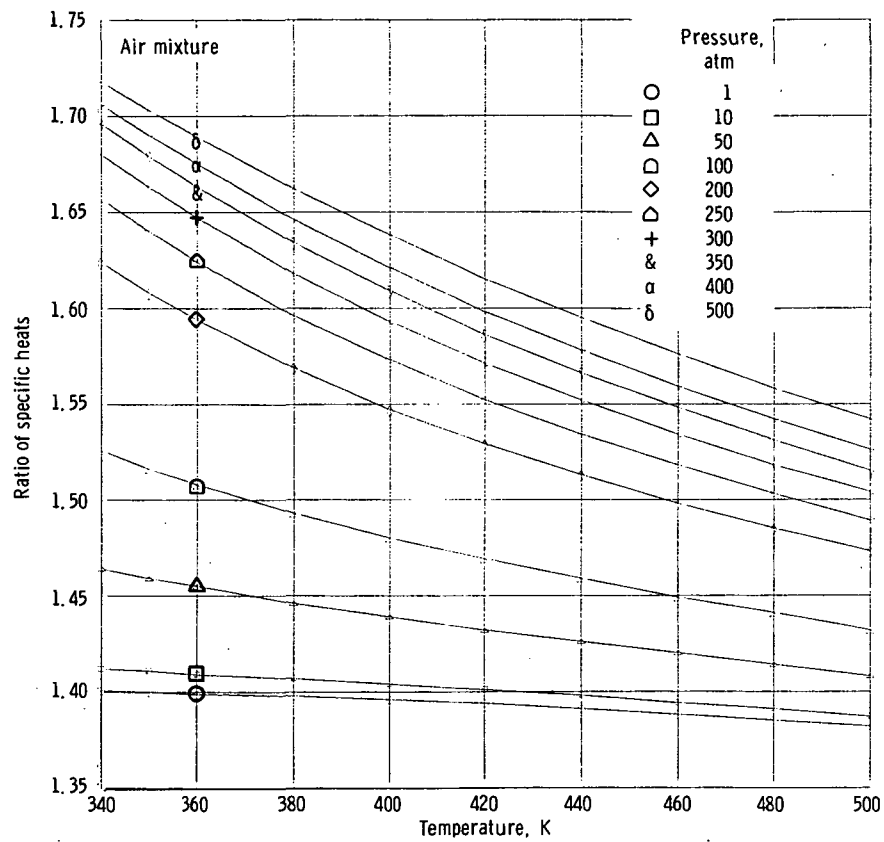
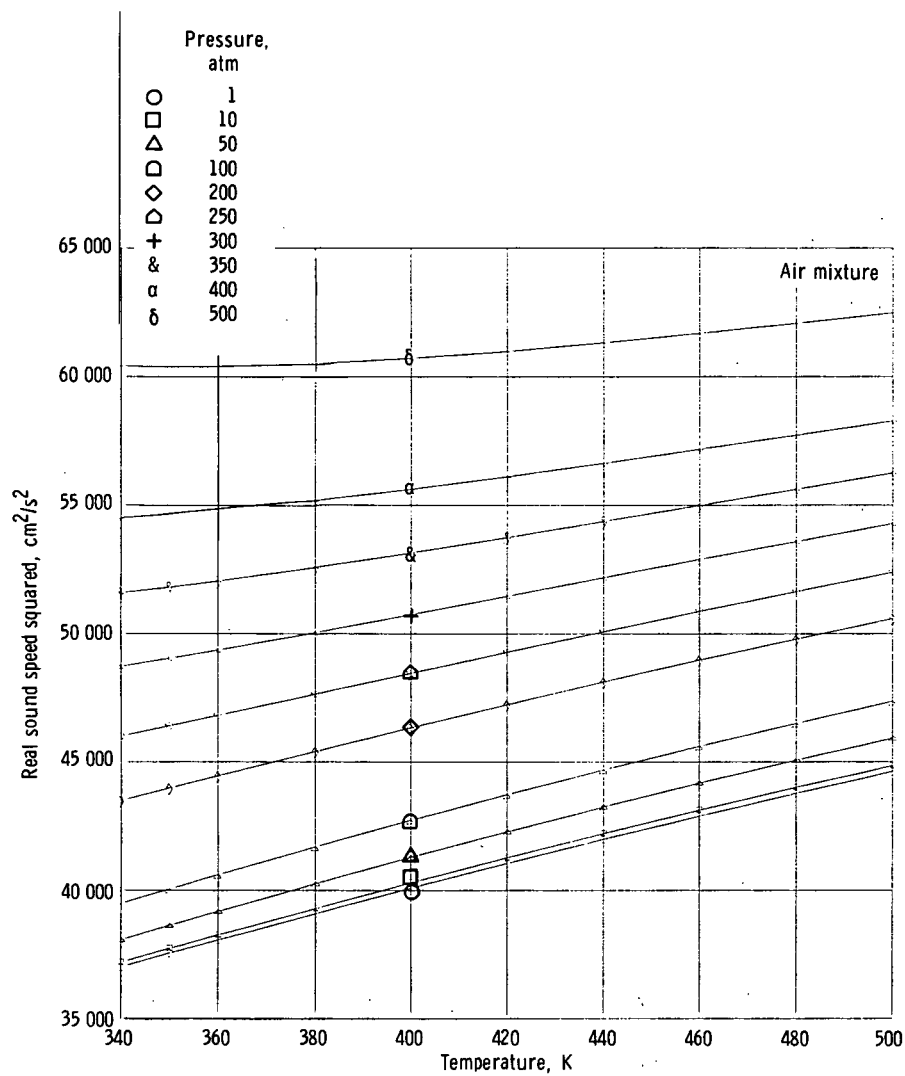Figure 67. – Density versus temperature.

Figure 68. - Ratio of specific heats versus temperature.

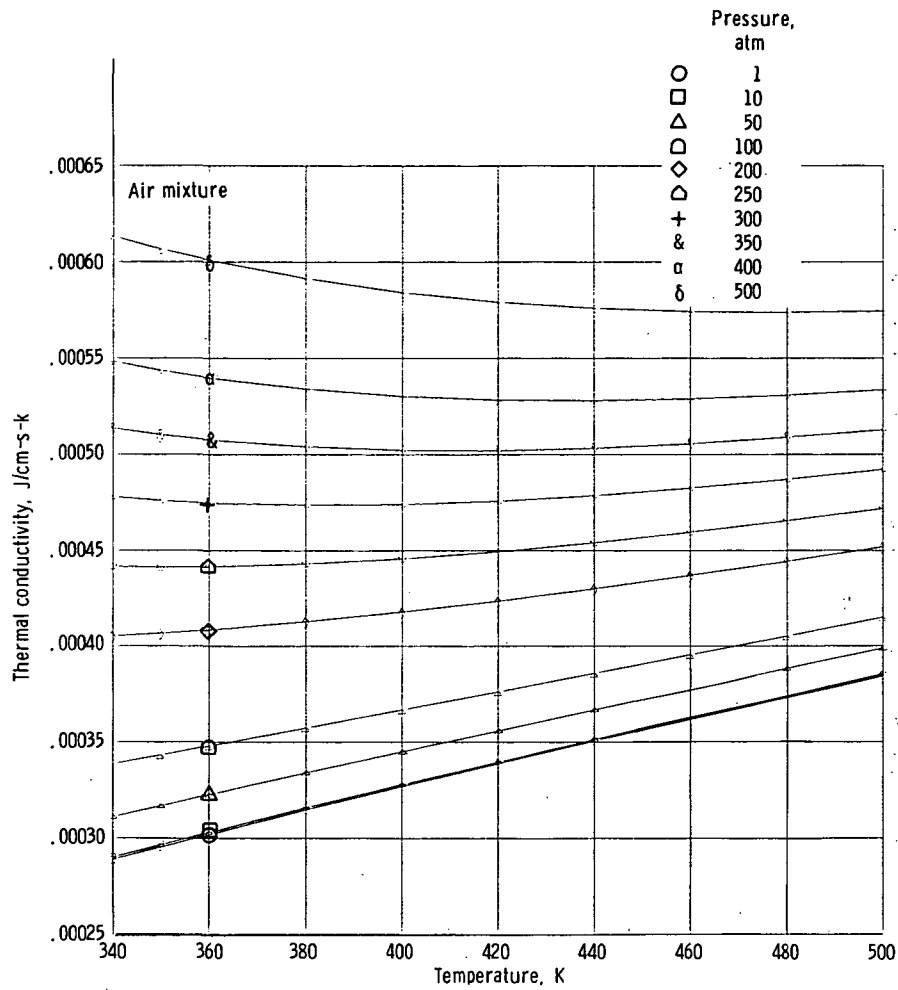Figure 69. – Real sound speed squared versus temperature.

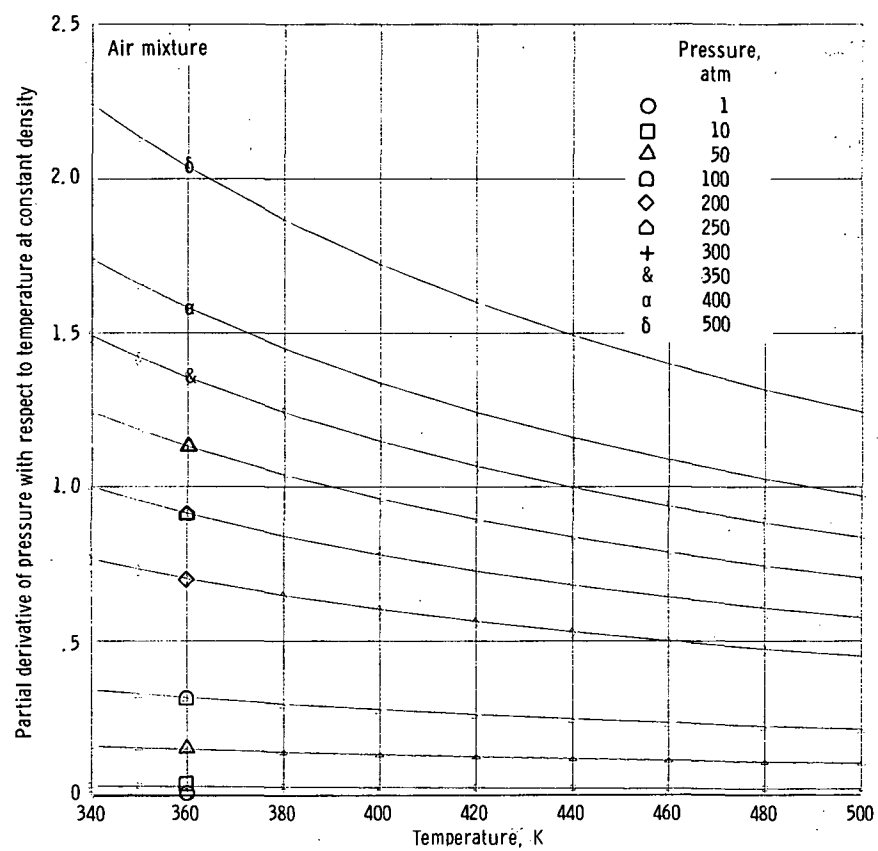Figure 70. - Thermal conductivity versus temperature.

Figure 71. - Partial derivative of pressure with respect to temperature at constant density versus temperature.
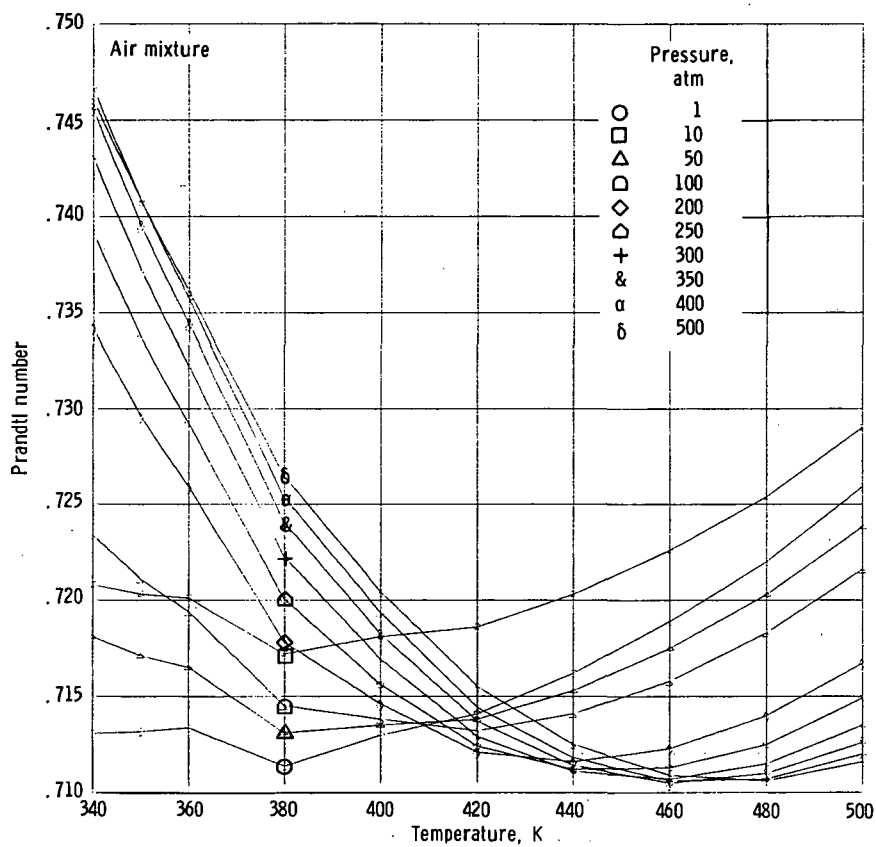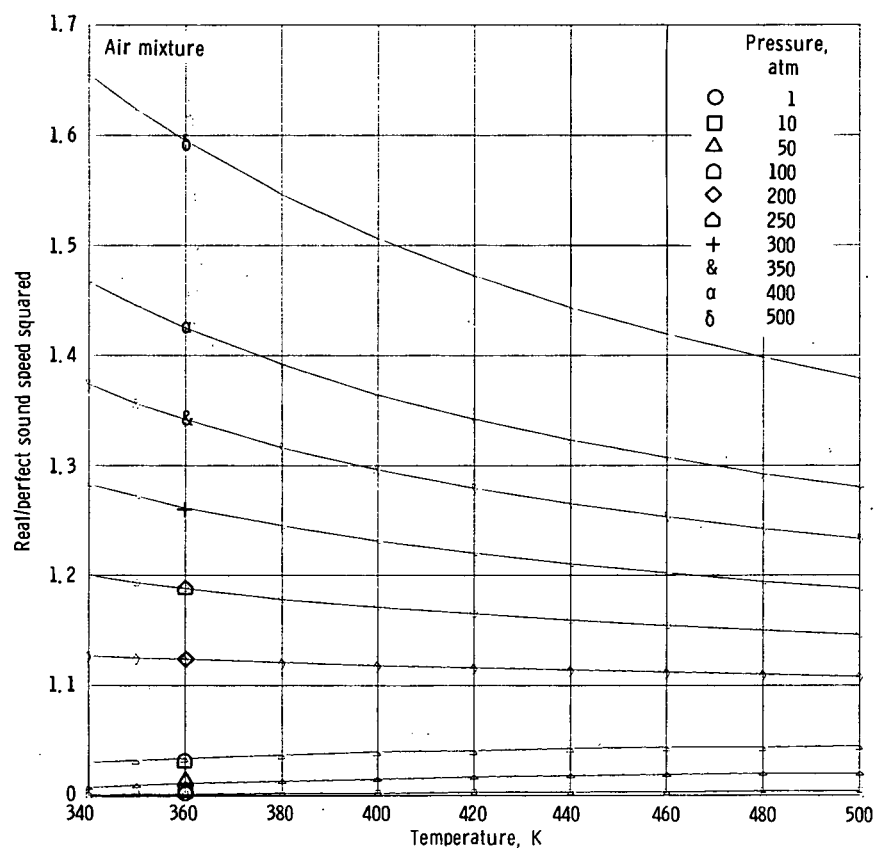
Figure 72. – Prandtl number versus temperature.

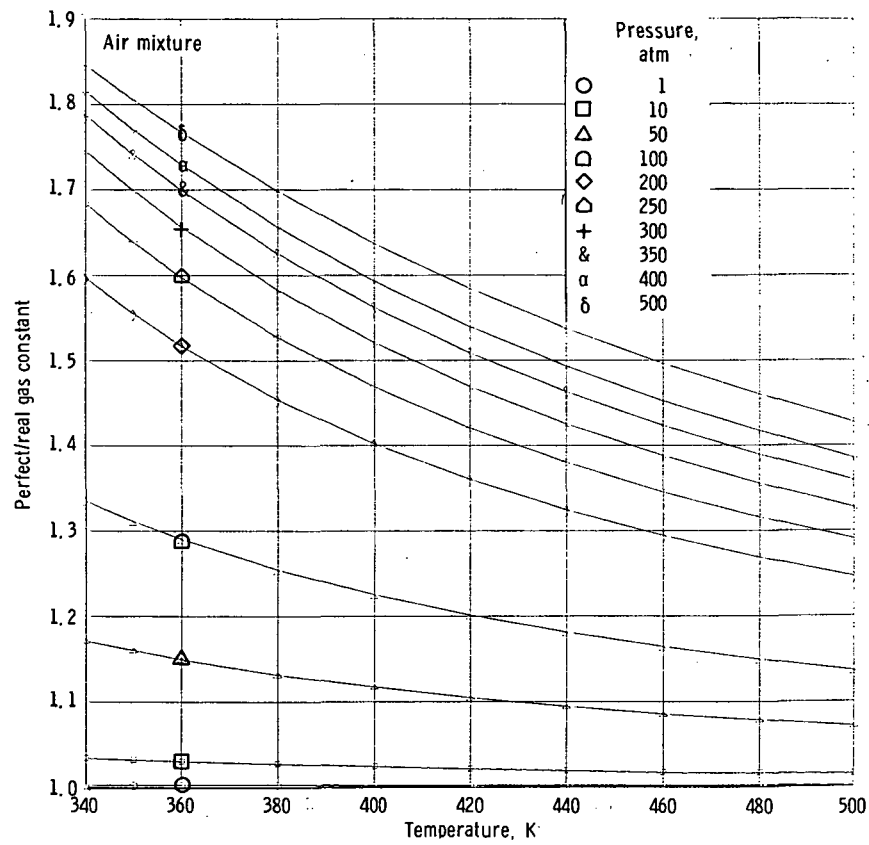Figure 73. - Real/perfect sound speed squared versus temperature.

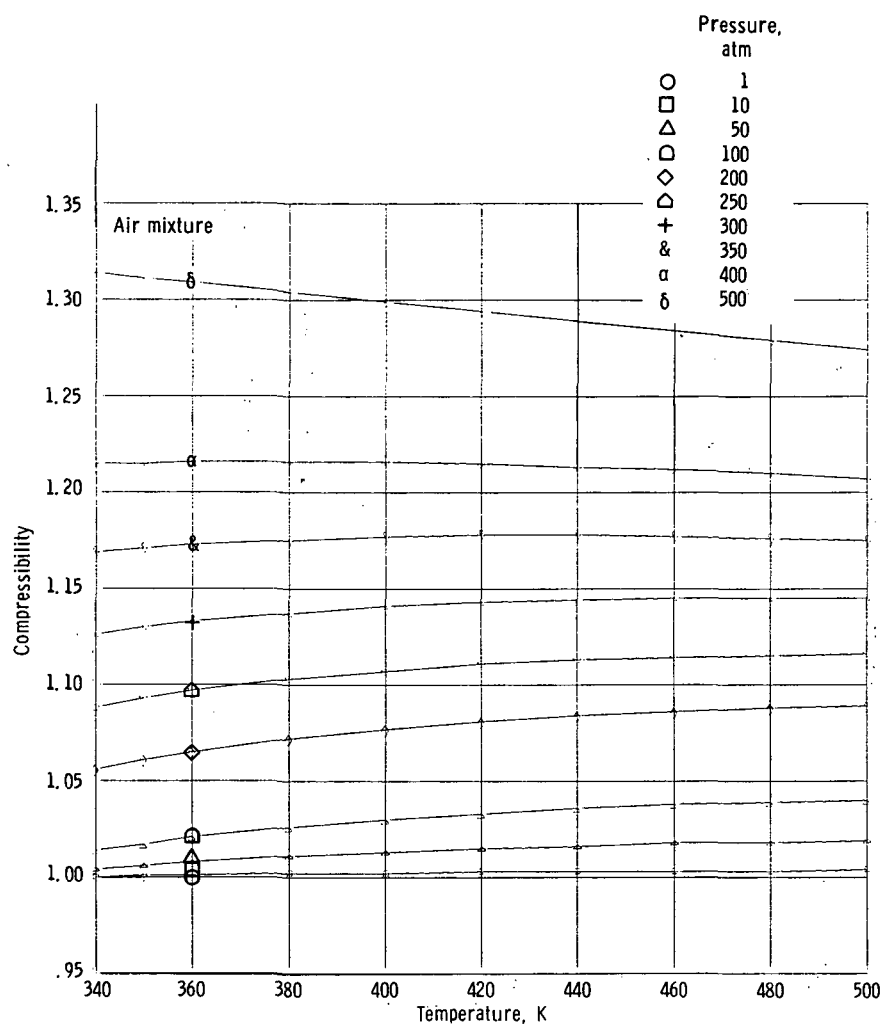Figure 74. - Perfect/real gas constant versus temperature.
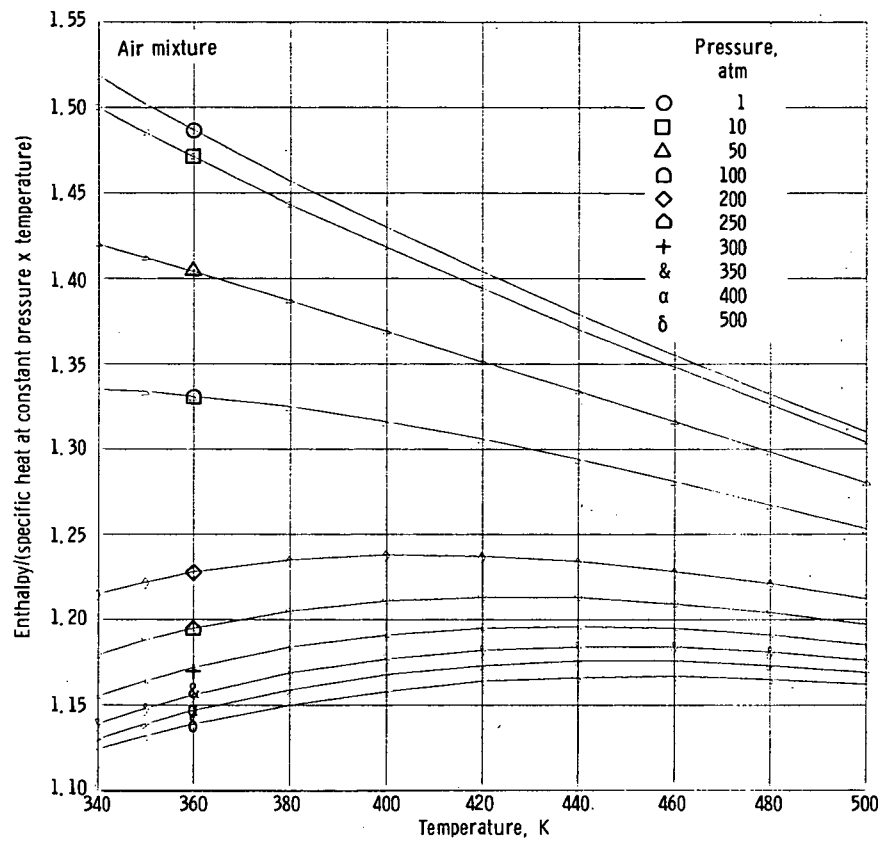
Figure 75. – Compressibility versus temperature.

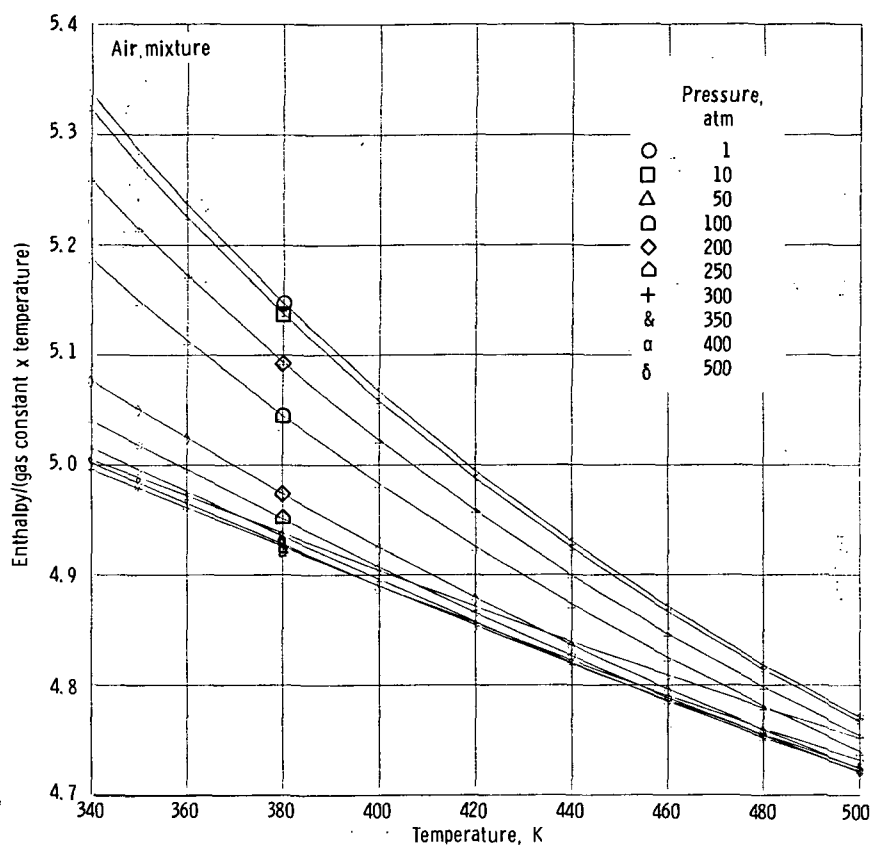Figure 76. – Enthalpy/(specific heat at constant pressure x temperature) versus temperature.

Figure 77. - Enthalpy/(gas constant x temperature) versus temperature.
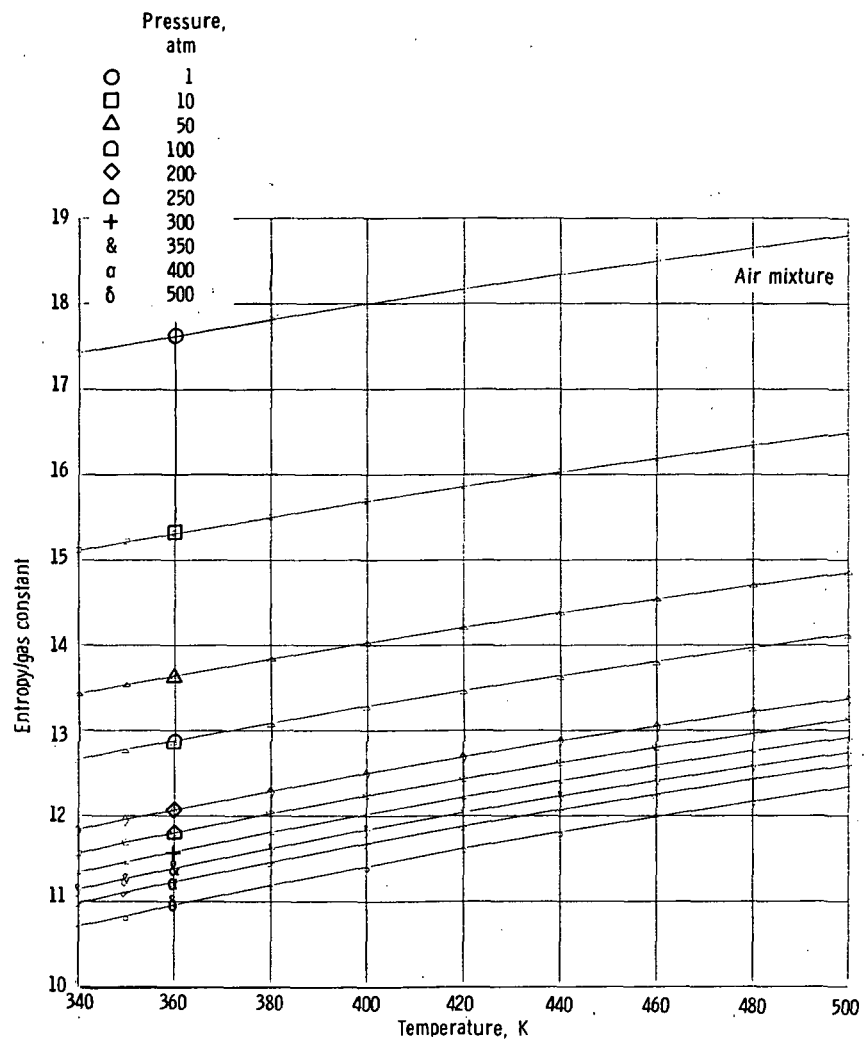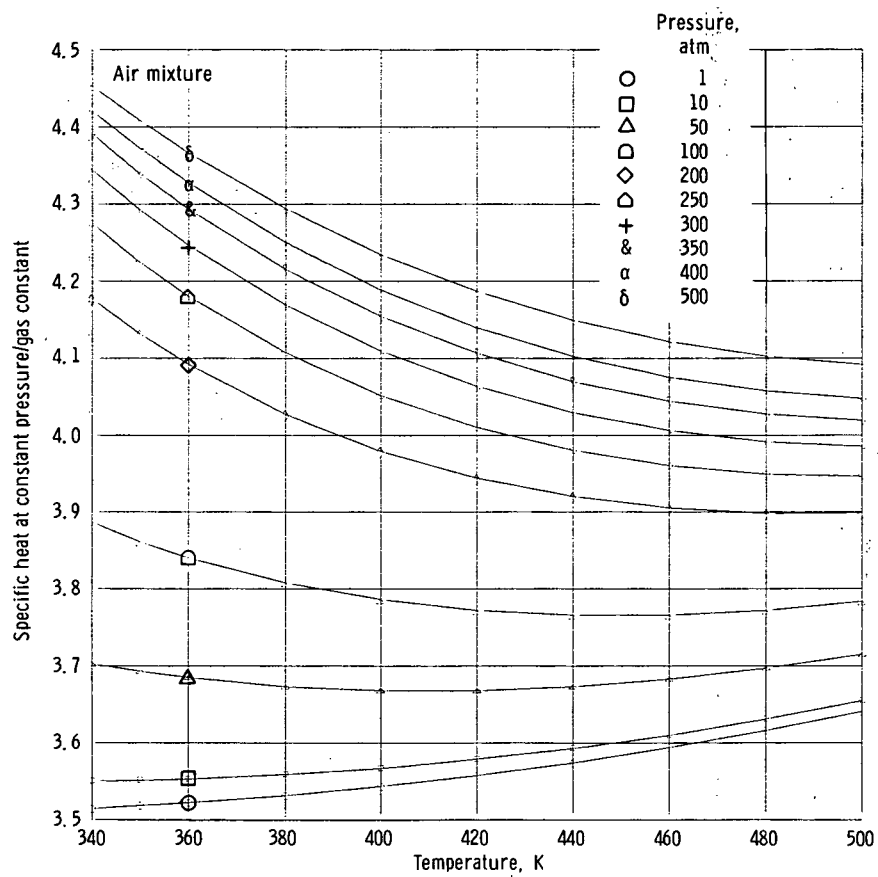
Figure 78. – Entropy/gas constant versus temperature.

Figure 79. - Specific heat at constant pressure/gas constant versus temperature.
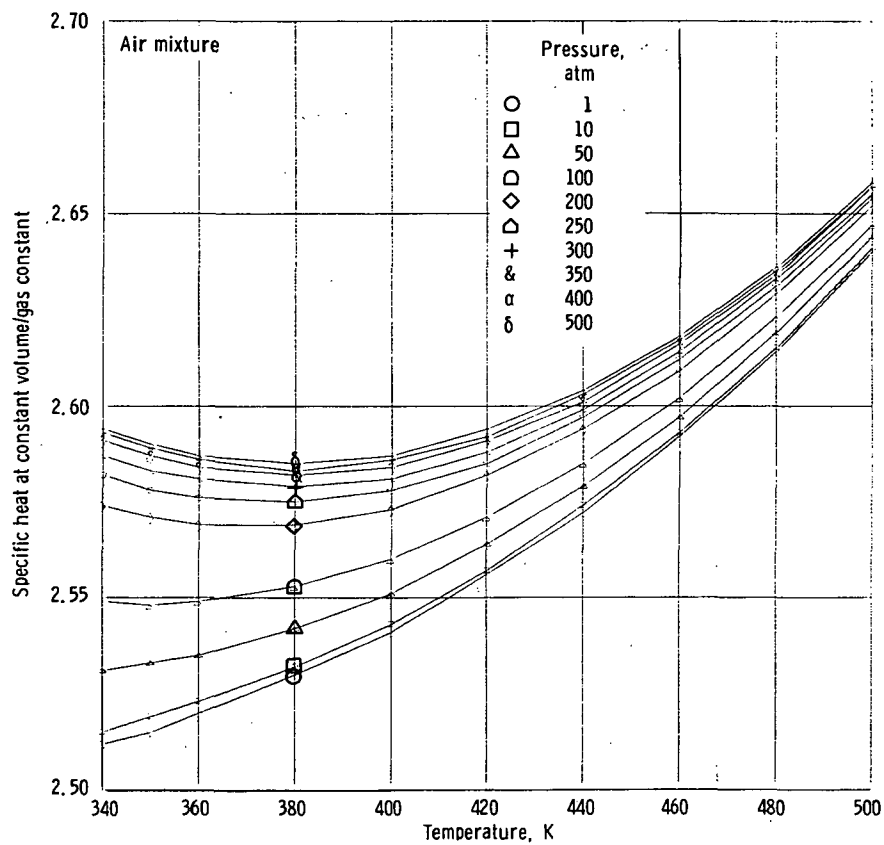
Figure 80. - Specific heat at constant volume/gas constant versus temperature.
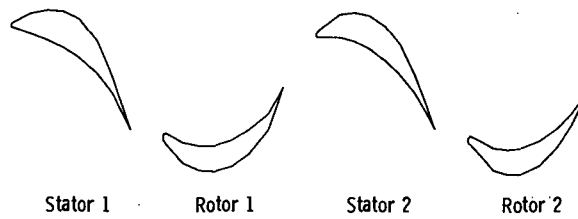
Stator 1   Rotor 1   Stator 2   Rotor 2

Figure 81. - Blade geometry for SSME fuel turbine mid channel.
Positive angles are counterclockwise, see table V.

First-stage stator   First-stage rotor

—— Hub
········· Mean
———— Tip

Second-stage stator   Second-stage rotor
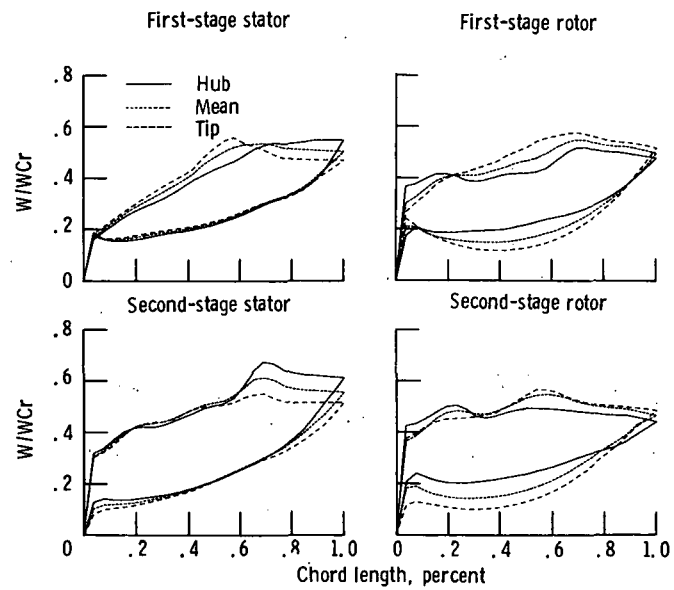
Chord length, percent

Figure 82. - Relative velocity at edge of boundary layer.

1. Report No. NASA CR-175066	2. Government Accession No.	3. Recipient's Catalog No.
4. Title and Subtitle Characterization of Real Gas Properties for Space Shuttle Main Engine Fuel Turbine and Performance Calculations		5. Report Date June 1986
		6. Performing Organization Code
7. Author(s) Gary J. Harloff		8. Performing Organization Report No. None
		10. Work Unit No.
9. Performing Organization Name and Address Sverdrup Technology, Inc. Lewis Research Center Cleveland, Ohio 44135		11. Contract or Grant No. NAS 3-24105
		13. Type of Report and Period Covered Contractor Report
12. Sponsoring Agency Name and Address National Aeronautics and Space Administration Washington, D.C. 20546		14. Sponsoring Agency Code 533-13-00 (E-2938)

15. Supplementary Notes

Final report. Project Manager, Raymond Gaugler, Internal Fluid Mechanics Division, NASA Lewis Research Center, Cleveland, Ohio 44135.

16. Abstract

Real thermodynamic and transport properties of hydrogen, steam, the SSME mixture, and air are developed. The SSME mixture properties are needed for the analysis of the space shuttle main engine fuel turbine. The mixture conditions for the gases, except air, are presented graphically over a temperature range from 800 to 1200 K, and a pressure range from 1 to 500 atm. Air properties are given over a temperature range of 320 to 500 K, which are within the bounds of the thermodynamics programs used, in order to provide mixture data which is more easily checked (than H_2/H_2O). The real gas property variation of the SSME mixture is quantified. Polynomial expressions, needed for future computer analysis, for viscosity, Prandtl number, and thermal conductivity are given for the H_2/H_2O SSME fuel turbine mixture at a pressure of 305 atm over a range of temperatures from 950 to 1140 K. These conditions are representative of the SSME turbine operation. Performance calculations are presented for the space shuttle main engine (SSME) fuel turbine. The calculations use the air equivalent concept. Progress towards obtaining the capability to evaluate the performance of the SSME fuel turbine, with the H_2/H_2O mixture, is described.

END DATE AUG. 25, 1986

17. Key Words (Suggested by Author(s)) Real gas properties Space shuttle fuel turbine	18. Distribution Statement Unclassified - unlimited STAR Category 20	
19. Security Classif. (of this report) Unclassified	20. Security Classif. (of this page) Unclassified	21. No. of pages	22. Price* A

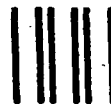*For sale by the National Technical Information Service, Springfield, Virginia 22161

National Aeronautics and
Space Administration

Lewis Research Center
Cleveland. Ohio 44135

Official Business
Penalty for Private Use $300

SECOND CLASS MAIL

ADDRESS CORRECTION REQUESTED

NASA